A role of Alzheimer's disease-associated γ-secretase in lipid metabolism and lipid droplet formation via LXR activation

- DISSERTATION -

zur Erlangung des Doktorgrades (Dr. rer. nat.)

der

Mathematisch-Naturwissenschaftlichen Fakultät

der

Rheinischen Friedrich-Wilhelms-Universität Bonn

vorgelegt von

Esteban Gutierrez

aus Neiva, Kolumbien

Bonn, September 2018

Angefertigt mit Genehmigung der Mathematisch-Naturwissenschaftlichen Fakultät der Rheinischen Friedrich-Wilhelms-Universität Bonn

Gutachter

1. Prof. Dr. rer. nat. Jochen Walter
2. Prof. Dr. rer. nat. Christoph Thiele
1. Prof. Dr. rer. nat. Michael Famulok
2. Prof. Dr. rer. nat. Jochen Dingfelder

Tag der Promotion 01.08.2019

Erscheinungsjahr 2021

An Eides statt versichere ich, dass ich die Dissertation “A role of Alzheimer’s disease-associated γ-secretase in lipid metabolism and lipid droplet formation via LXR activation“ selbst und ohne jede unerlaubte Hilfe angefertigt habe und dass diese oder eine ähnliche Arbeit noch an keiner anderen Stelle als Dissertation eingereicht worden ist.

Auszüge der ausgewiesenen Arbeit wurden beim Journal „Life Science Alliance“ Veröffentlicht, als:

“**Importance of γ-secretase in the regulation of liver X receptor and cellular lipid metabolism**”
Esteban Gutierrez, Dieter Lütjohann, Anja Kerksiek, Marietta Fabiano, Naoto Oikawa, Lars Kuerschner, Christoph Thiele, Jochen Walter

Life Science Alliance
Publication: 2020 April
Print: Volume 3, No. 6, 2020 June
DOI: 10.26508/lsa.201900521

Promotionsordnung vom _____

Esteban Gutierrez Ardila

Things without hands take hands: there is no choice,
Eternity's not easily come by.
When opposites come suddenly in place,
I teach my eyes to hear, my ears to see
How body from spirit slowly does unwind
Until we are pure spirit at the end.

Theodore Roethke – Infirmity.

Abstract

The γ secretase is an intramembrane protease complex, essential for the processing of a wide variety of type-1 membrane proteins. Among these is the amyloid precursor protein (APP), a protein strongly linked to Alzheimer's disease (AD), both for the role of the APP gene in the development of early-onset AD, as well as for being the precursor of the amyloid-β peptide, produced through sequential processing by β and γ-secretases. The primary catalytical proteins of the γ-secretase complex are Presenilins (PS). Interestingly, mutations in the PS genes are associated with the development of autosomal dominant forms of early-onset AD. However, the mechanisms by which APP and PS contribute to the pathogenesis of AD are not fully understood, nor are the cellular roles of APP or its cleavage by γ-secretase. Previous reports have revealed a link between PS and cellular lipid metabolism, with a lack of PS activity leading to dysregulation of cholesterol metabolism and lipoprotein endocytosis. This study revealed how a lack of PS activity leads to an elevation of lipid droplet levels, triglyceride levels, cholesterol metabolite levels and cholesterol secretion, as well as a decrease in cholesterol esterification. These observations are shown to involve an increment of LXR activity. In particular, cells lacking PS activity display a substantial elevation of LXR protein levels, as well as of transcripts of LXR target genes involved in sterol and triglyceride metabolism. Additional experiments showed that the APP C-terminal fragment C99 (C99), a substrate of γ-secretase, accumulate in cholesterol-rich, AP-1 positive vesicles upon pharmacological inhibition of γ-secretase. The cellular levels of C99 positively correlate with an increase in lipid droplet levels, suggesting that C99 accumulation is involved in the alterations of lipid metabolism observed upon inhibition of γ-secretase activity. Together, our findings reveal a mechanism that functionally connects γ-secretase-dependent cleavage of the APP C-terminal fragment to cellular sterol and lipoprotein metabolism, which could potentially contribute to the pathogenesis of AD.

Table of Contents

List of Figures

Abbreviations

ABCA	ABC transporter A
ABCG	ABC transporter G
Aβ	Amyloid-β peptide
ACAT	Acyl-CoA cholesterol acyltransferase
AD	Alzheimer's Disease
AICD	Amyloid precursor protein intracellular domain
ANOVA	Analysis of variance
AP-1	Adaptor protein 1
APOA	Apolipoprotein A
APOE	Apolipoprotein E
APOJ	Apolipoprotein J
APLP1	Amyloid-like protein 1
APLP2	Amyloid-like protein 1
APP	Amyloid precursor protein
APS	Ammonium persulfate
BACE	B-secretase
BCA	Bicinchoninic acid assay
BSA	Bovine serum albumin
C83	Amyloid precursor protein C-terminal fragment C83
C99	Amyloid precursor protein C-terminal fragment C99
CHO	Chinese hamster ovary cells
CTF	C-terminal fragment
CSF	Cerebrospinal fluid
DAPI	4',6-diamidino-2-phenylindole
DAPT	N-[N-(3,5-Difluorophenacetyl)-L-Alanyl]-(S)-Phenylglycin t-Butylester

DMEM	Dulbecco´s modified Eagle´s medium
ECL	Enhanced chemiluminescence
EDTA	Ethylenediaminetetraacetic acid
EEA1	Early Endosome Antigen 1
EGTA	ethylene glycol-bis(β-aminoethyl ether)-N,N,N',N'-tetraacetic acid
EOAD	Early-onset AD
EPR	Electron paramagnetic resonance
FAD	Familial Alzheimer's Disease
FCS	Foetal calf serum
GC-MS	Gas Chromatography-coupled Mass Spectrometry
HDL	High-density lipoprotein
HEPES	4-(2-hydroxyethyl)-1-piperazineethanesulfonic acid
HMG-CoA	3-hydroxy-3-methylglutaryl-coenzyme A
hPS1DA	human Presenilin carrying the catalytically inactive D257A mutation
hPS1WT	Wild-type human Presenilin 1
IGF-1	Insulin-like growth factor 1
IGG	Immunoglobulin G
LCAT	Lecithin–cholesterol acyltransferase
LD	Lipid droplet
LDH	Lactate dehydrogenase
LDL	Low-density lipoprotein
LRP	Lipoprotein receptor-related protein
LXR	Liver-X-Receptor
mTOR	Mechanistic target of Rapamycin
NFTs	Neurofibrillary tangles
NMR	Nuclear magnetic resonance
NPC	Niemann-Pick C protein
NR	Nuclear receptor

PAGE	Polyacrylamide gel electrophoresis
PARP	Poly (ADP-ribose) polymerase
PBS	Phosphate-buffered saline
PCR	Polymerase chain reaction
PHF	Paired helical filaments
PPAR	peroxisome proliferator-activated receptors
PS	Presenilin
q-rtPCR	Quantitative real-time polymerase chain reaction
RIPA	Radioimmunoprecipitation assay buffer
ROS	Reactive oxygen species
RXR	Retinoid-X receptor
SAD	Sporadic Alzheimer's Disease
sAPP	Soluble APP fragments
SDS	Sodium dodecylsulfate
SOAT1	Sterol O-acyltransferase
SREBP	Sterol regulatory element-binding protein
STEN	Sodium Tris EDTA NP40
TEMED	Tetramethyl ethylenediamine
TG	Triglycerides
TGN46	Trans-Golgi network integral membrane protein 2
TLC	Thin-layer chromatography
TMD	Trans-membrane domain
TRIS	Trisaminomethane
WT	Wild-type

1 Introduction

Since the description of the first identified case in 1906, Alzheimer's disease (AD) has been steadily garnering the attention and interest of the scientific community, up to the point where, today, it is perhaps the most studied among all neurological diseases[1] (Figure 1). This comes in great part as a consequence of the tremendous impact AD has on both a personal and a socio-economic level, together with an alarming increase in patient numbers[2]. Yet there is another striking fact, equally fascinating and daunting, which stands out regarding AD: After more than 100 years of research, we have yet to understand how precisely the disease originates[3–5]. Several pathophysiological markers have been identified which allow us to categorize and identify AD, as well as several genetic risk factors which increase the odds of getting the disease or lead to precocious development of the disease, yet the underlying mechanism behind AD has eluded us for more than a century. Throughout my doctoral work I have focused on studying some of the factors believed to be involved in AD and seeking to identify a functional metabolic relation between these factors and AD, in an attempt to assist in uncovering the underlying mechanism behind this disease. Specifically, my studies focused initially on the functional relation of γ-secretase[6–8] and cellular lipid metabolism[9–11], later introducing a third factor, the trans-membrane protein APP[12,13] and its cleavage product C99[14]. On the following pages you will find a detailed description of the different pathological, biochemical and metabolic aspects of

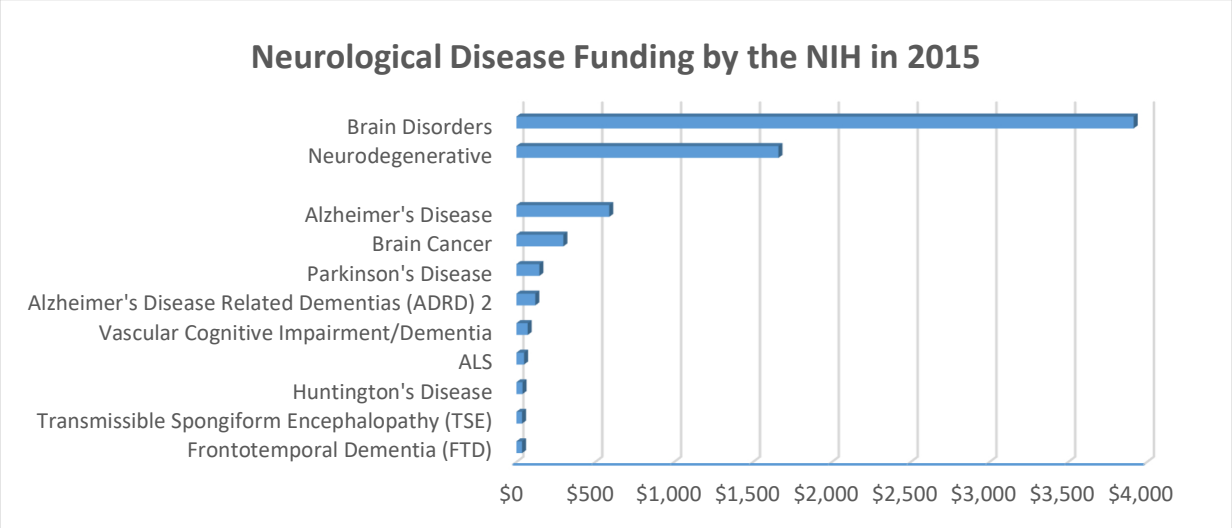

Figure 1: *Most funded neurological diseases by the national institute of health (NIH) in 2015, reported in millions of dollars. Data generated through the NIH Research Portfolio Online Reporting Tools[1].*

Alzheimer's disease necessary to understand the findings and implications of this thesis in a proper context.

1.1 Alzheimer's disease: A short summary of a complicated disease

Alzheimer's disease (AD) is currently one of the most prevalent aging-related diseases and the most prevalent form of dementia, accounting for 60-70% of all dementia cases. This disease is a source of tremendous global financial and medical burden, affecting nearly 44 million people worldwide, a number which is expected to double every 20 years were the disease to be left unchecked. Additionally, annual AD-associated costs correspond to roughly 600 billion dollars, which amounts to 1% of the current worldwide gross domestic product (GDP)[2,15–17].

The main clinical hallmark of the disease is progressive cognitive impairment and substantial neurodegeneration in the central nervous system, ultimately leading to death. The disease can take more than a decade to run its course, initially displaying only mild behavioral symptoms but progressing to affect a diverse range of cognitive functions, from short-term memory and facial recognition, all the way to deglutition and sphincter control. Consequently, the disease places tremendous stress not only on the patient itself, but also on adjacent family members and caretakers, as intense and constant care becomes increasingly necessary with disease progression.

Neuropathologically, AD is primarily characterized by the accumulation of intra- and extra-cellular aggregates within the brain, composed mainly of amyloidogenic peptides[5]. These aggregates are known as amyloid plaques (mostly extracellular) and neurofibrillary tangles (mostly intracellular) (Figure 2). The main component of extracellular plaques is the amyloid β-peptide (Aβ), which derives from proteolytic processing of the β-amyloid precursor protein (APP) by the β- and γ-secretases. The Aβ peptide shows a strong propensity to spontaneously aggregate, and it is these aggregates which make up most of the extracellular AD plaques. Intracellular tangles, on the other hand, are primarily composed of the protein Tau, a neural protein essential for microtubule assembly and stabilization dynamics. Hyperphosphorylated forms of tau assemble into structures known as paired helical filaments (PHF-Tau), which then form the aforementioned neurofibrillary

tangles (NFTs)[18,19]. These plaques and tangles progressively accumulate and spread in the brain of an individual with AD. While AD is routinely diagnosed through neuropsychological testing and functional neuroimaging, the diagnosis can only be confirmed through post-mortem, histopathologic identification of these aggregates in brain tissue[20,21].

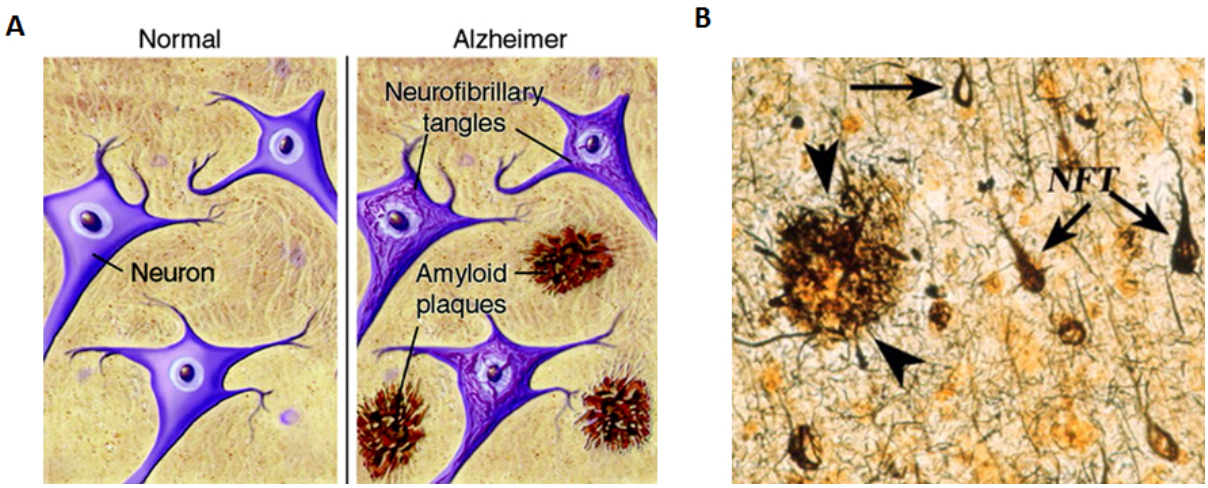

***Figure 2**: Aggregate build-up in Alzheimer's disease. A) Schematic representation of AD amyloid plaque and NFT build up in a neural environment. B) Amyloid plaques (arrowheads) and NFTs (arrows) observed in an AD brain sample by the Bielschowsky silver stain. Images obtained from publications by Silbert[22] and Nixon[23].*

As highlighted above, the etiology and disease progression of AD is not well understood. Still, there are two important sources of information which have allowed us to better understand this disease. The first one can be found in an uncommon set of cases of AD known as familial Alzheimer's disease (FAD) or early-onset Alzheimer's disease (EOAD). While the majority of AD incidences (≈ 95%) arise in individuals over the age of 65 (known as sporadic AD, or SAD), FAD develops earlier in life, and has been linked to a set of mutations in three specific genes: PSEN1, PSEN2 and APP[5]. The proteins corresponding to these genes are central to Aβ generation, but the precise mechanisms of action by which these genes participate in the development of FAD are unclear. However, the fact that the genes, and corresponding proteins, play an essential role in FAD is widely accepted. The second source of information lies in the identification of genetic risk factors for the development of SAD. The principal and most recognized risk factor is APOE4, one of 3 common alleles of the APOE gene. Homozygous carriers of this APOE allele display a 12-time increase on the risk of developing AD, while in heterozygous carriers the risk can be 2-3 times higher than non-carriers[24]. Additionally, the E2 allele has been described as protective against

AD[25,26]. In addition to APOE, several other genetic risk factors for AD have been identified through genome-wide association studies, many of these, such as cholesterol transporter ABCA7, linked to lipid metabolism[27–32]. The genes identified this way have allowed us to find several target proteins to study the pathogenesis and disease progression of AD. In the following section, the main proteins used in the study of AD pathogenesis will be described.

1.2 The main recognized proteins of AD

As highlighted above, this section will focus on the main proteins which have been identified as relevant in AD pathology[5]: the amyloid precursor protein (APP) and its degradation products[33–37], γ-secretase-associated Presenilins (PS)[38–40], the apolipoprotein APOE[9,41,42], and the microtubule-associated protein Tau[43–45]. While the participation of these proteins in the disease is recognized and accepted as a consensus among the scientific community, the mechanism by which they do so, as well as the etiology of the disease itself, remain enigmatic and hotly debated topics. The focus of this work is primarily on PS, lipoproteins and APP, which will now be described in more detail.

1.2.1 Presenilins

PS are trans-membrane proteins of high interest to the AD field, due to their involvement in the etiology of the disease. Two homologues of this protein have been identified in humans, PS1 and PS2. Initially described by the center for research in neurodegenerative diseases in the University of Toronto, the protein class was found through a screen attempting to identify gene mutations involved in the development of early-onset Alzheimer's disease[38]. In this first study, 5 missense mutations were identified which lead to the development of FAD, encouraging the study of the functional role of this protein, as well as its relationship to AD. Up to date, more than 200 PS FAD mutations have been identified[46].

PS proteins function predominantly as the catalytic core of the γ-secretase complex, a multi-protein protease complex responsible for the cleavage of a wide array of type-1 transmembrane

proteins. Cleavage by γ-secretase is an important step in a various of developmental and metabolic pathways[47], including processes such as cell adhesion and apoptosis, with target substrates such as Notch and Cadherins. Furthermore, γ-secretase is responsible for the last step of the sequential cleavage of APP, which leads to the formation of Aβ, the main component of amyloid plaques[48]. In addition to its role in γ-secretase activity, it has been proposed that PS has other metabolic functions which are independent from their enzymatic function, including regulation of lysosomal activity, WNT signaling and insulin signaling[8,49]. While this aspect is still under debate, studies have demonstrated that PS knock-out models display more severe phenotypes than knock-out models of other γ-secretase components, and that reintroduction of a catalytically inactive variant of PS in knock-out models partially alleviates the effects of the knock-out[49].

PS are highly-conserved polytopic transmembrane proteins, that is, they contain multiple membrane-spanning hydrophobic domains. Structural analysis of proteins rich in hydrophobic domains tends to be particularly challenging, and PS is no exception. As such, the structure of PS in biologically relevant conditions has been a matter of considerable debate. The protein is recognized as possessing at least six trans-membrane domains(TMDs) by consensus, but current models predict it to have as many as nine TMDs[50,51] (Figure 3). PS are initially translated as 50kDa catalytically-inactive holoproteins, and require a maturation endoproteolysis step in order to become catalytically active[6]. In this maturation process, PS initially associates with γ-secretase components Nicastrin, Aph-1 and Pen-2. A cleavage event takes place following Pen-2 binding, between TMDs 6 and 7, which makes the catalytical site of the protein accessible to substrate peptides[52] (Figure 3). This protein shares structural similarities with aspartyl proteases, and, indeed, a mutations in aspartic acid residues within the catalytic center (D257 or D385) leads to a loss of γ-secretase activity[53].

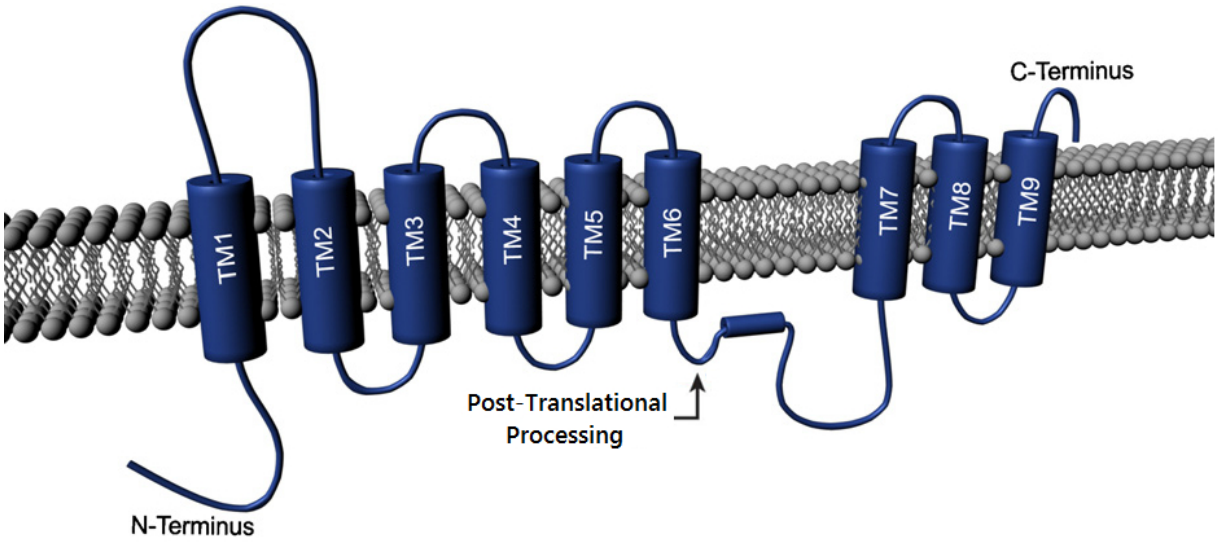

Figure 3: *Proposed 9 TMD membrane topology of Presenilin with transmembrane domains shown as blue columns. The catalytic activity of PS is exerted by two critical aspartyl residues in TM6 and TM7. Access of the corresponding substrates to PS requires endoproteolytic processing on the ICD between TMDs 6 and 7, here highlighted with an arrow. Image modified from Hornanejad and Herms*[54]

As previously indicated, PS is responsible for the cleavage of APP C-terminal fragments leading to the formation of Aβ, one of the main factors linked to AD disease progression. While the involvement of PS in AD is well recognized, as is its role in the cellular production of Aβ, the mechanisms linking PS to the disease are not comprehensively understood. Studies regarding the pathogenic role of PS in AD are made challenging by the fact that γ-secretase has an extensive number of metabolically important substrates besides APP[55]. This makes the analysis and interpretation of observations made in models of altered γ-secretase activity difficult, as observed phenotypes can arise from the impaired processing of one or many of its substrates, not just APP.

The current leading hypothesis on the involvement of PS in AD pathogenesis proposes that an alteration of γ-secretase activity leads to an overall elevation in Aβ production or a decrease in the ratio of Aβ40/Aβ42[56], the latter peptide being assumed to be more pathogenic than the former as it has a higher propensity to aggregate[57]. Controversially, it is speculated that a substantial number of PS mutations associated with FAD are, biochemically, partial loss-of-function mutations with impaired γ-secretase activity[58–61], which is difficult to reconcile with the hypothesis that it is an elevated generation of Aβ which underlies the pathogenic effect of PS in AD. In this regard, it is important to note that FAD mutations have also been reported to alter the processivity of γ-secretase, that is, the shedding of Aβ following cleavage of C99 to produce shorter Aβ species, and that activity and processivity can be independent to each other[62,63].

Contrary to this is the hypothesis that PS FAD mutations are toxic gain-of-function mutations, supported by the fact that these mutations are autosomal-dominant, that is, genetically carrying a single copy of the mutation is sufficient to predispose carriers to FAD[61]. As such, accurately identifying the precise contribution of PS mutations to AD is a challenge which has yet to be achieved, and remains of central importance to the field of AD.

Our working group has previously demonstrated a connection between PS activity, lipoprotein endocytosis, and sterol metabolism[64]. In particular, it was demonstrated that a lack of cellular PS activity leads to an impaired endocytosis of lipoprotein particles, an elevation of cellular cholesterol and desmosterol levels, and an impairment of membrane receptor recycling. These particular observations led us to further explore the impact PS activity has on sterol metabolism, storage and secretion, and it is one of the principal starting points of this thesis.

1.2.2 The Amyloid Precursor Protein

Another unusual aspect of AD research can be found in the research of the amyloid precursor protein, or APP. While this protein was in fact, since its initial cloning in 1987[65], identified as the precursor of the AD-related Aβ peptide, and has been heavily studied since, no consensus as-of-yet has been reached regarding its developmental or metabolic function by the scientific body. All the while, we know the APP protein family is essential for post-natal survival in mice, with double knock-out of APP and APP paralogue APLP2 leading to early post-natal lethality[66].

Structurally, APP and its paralogues are classified as type-I transmembrane proteins, indicating that the proteins only traverse the membrane once, and the N-terminus of the protein is directed extracellularly. APP contains a long N-terminal domain, located extra-cellularly when the protein resides in the cell membrane, and a shorter C-terminal intra-cellular domain. In mammals, this protein has two paralogues, APLP1 and APLP2[67,68].

As previously highlighted, APP is of high interest to the AD field for being the precursor of the Aβ peptide after secretase processing. The processing of APP is primarily a two-step process which can take two different routes, known as the amyloidogenic and non-amyloidogenic pathways (Figure 4). There are three main differences between the two pathways: The cellular localization of the main processing step, the secretase responsible for the first APP cleavage event, and the produced APP cleavage fragments. The amlyoidogenic pathway, notable for leading to the formation of Aβ on its last processing step, starts with the cleavage of APP by the β-secretase (BACE1). BACE1 cleavage of APP is believed to take place primarily endosomal compartments, and leads to the formation of soluble sAPP-β and the APP-CTF C99, so called due to its length of 99 amino acids. C99 is subsequently cleaved by γ-secretase, and leads to the formation of Aβ and the APP intracellular domain (AICD). The non-amyloidogenic pathway, on the other hand, begins with the cleavage of APP by the α-secretase. This cleavage takes place adjacent to the cell membrane, and leads to the generation of the slightly longer sAPP-α, and of the shorter C83. Following this, C83 is cleaved by γ-secretase, producing the peptides P3 and AICD (Figure 4).

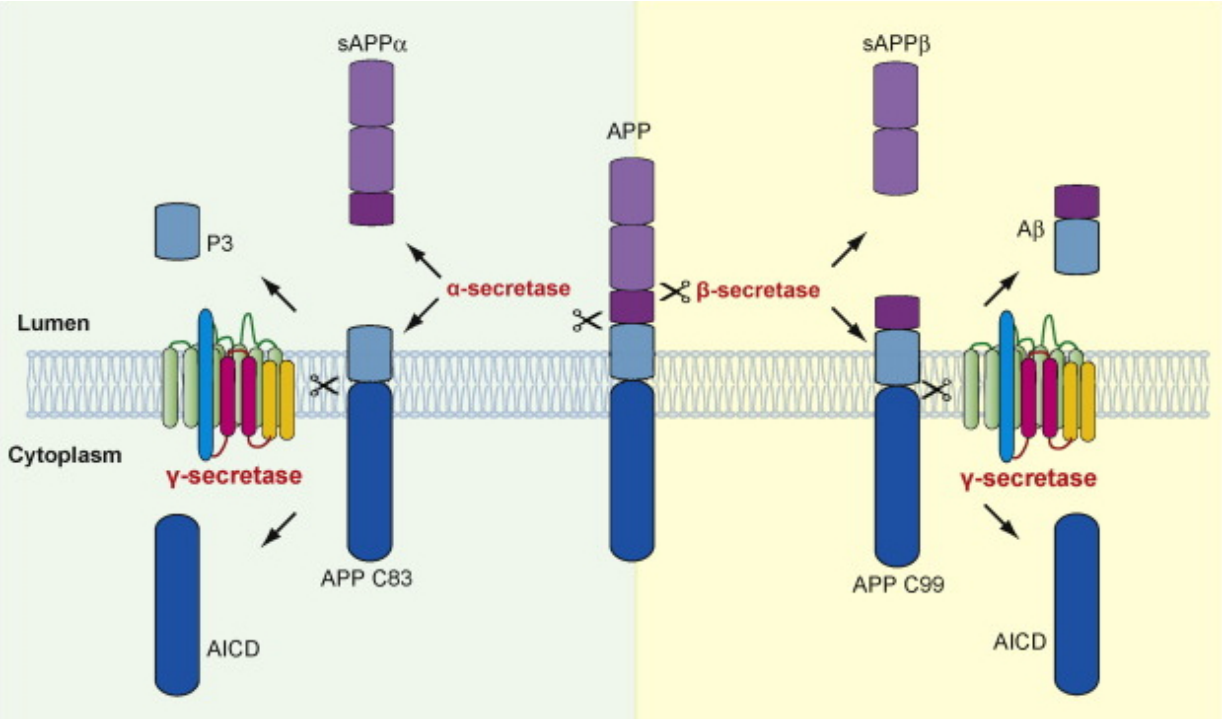

Figure 4: *Amyloidogenic (yellow background) and non-amyloidogenic (blue background) processing of APP by secretases. The amyloidogenic pathway is initiated by β-secretase, producing sAPPβ and the APP CTF C99, and followed by γ-secretase cleavage of C99 by γ-secretase, which generates the Aβ peptide and the APP ICD. The non-amyloidogenic pathway, on the other hand, begins with α-secretase cleavage of APP, releasing sAPPα and APP C83, with subsequent C83 cleavage by γ-secretase, producing the P3 peptide and the APP ICD (AICD). A color scheme is used to identify the different components of the γ-secretase: PS (red), Nicastrin (blue), Pen-2 (yellow), Aph-1 (green).*[69]*. Image obtained from Duggan and Mcarthy*[49]*.*

The potential roles of APP are vast, which can be attested by the large number of reported interaction partners, including heparin, collagen type I, LRP1, notch2, and Reelin, among many others[70]. The metabolic relevance of many of these interactions has yet to be identified, however, and remains an open question. Importantly, APP has been found to carry a YENPTY clathrin-binding motif, which mediates the protein's cell surface recycling and trafficking. This motif has been reported to both mediate its processing and subsequent Aβ production, as well as confer potential roles in cell signaling, as it is essential for the binding of several interacting proteins, including adaptor proteins and kinases[71–73]. APP expression is ubiquitous, but substantially elevated expression levels can be observed in the nervous system, and the primary functions of APP are speculated to take place in a neural environment[74,75]. However, other more ubiquitous functions for APP are speculated as well, given that neural APP is primarily composed by one of eight identified splicing isoforms[12,76]. The proposed roles of APP are remarkably broad, and hinge on an important question, whether APP functions as a receptor, by binding its putative ligands,

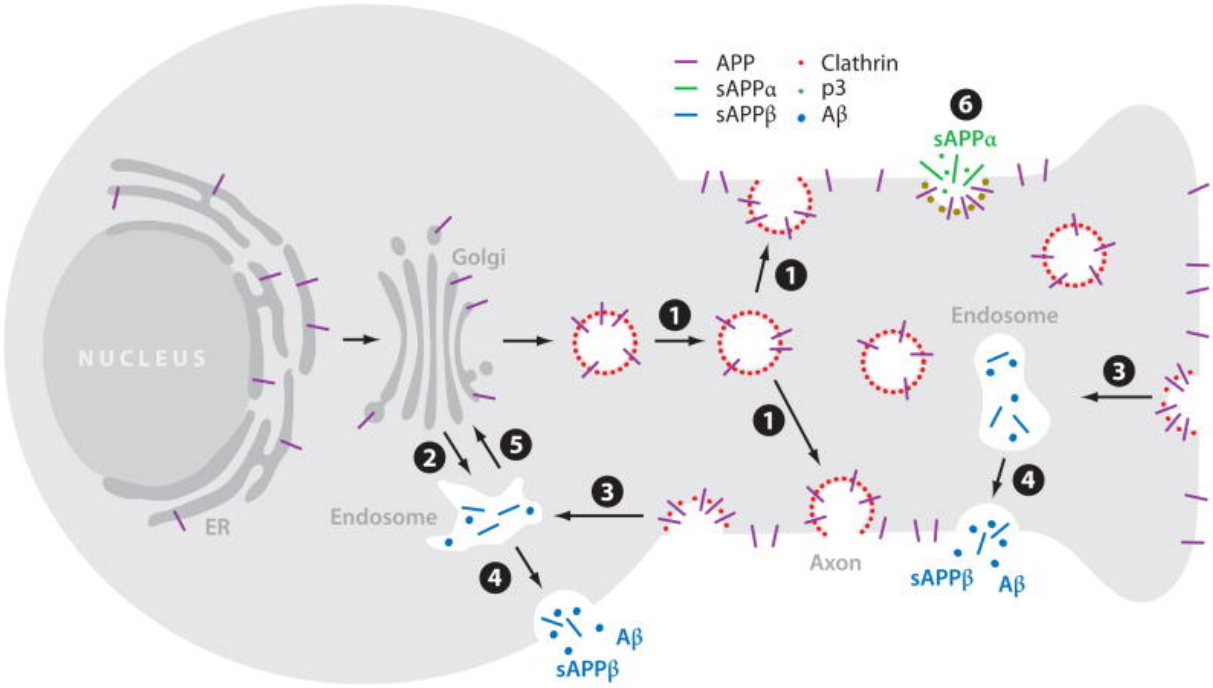

Figure 5: *Cellular localization of amyloidogenic and non-amyloidogenic APP processing steps. Following APP translation in the ER, APP is transported to the Golgi apparatus. Subsequently, APP can be transported to the cell membrane by clathrin-coated vesicles (**1**), or to an endosomal compartment (**2**). Membrane-bound APP ca be either cleaved by the α secretase on the non-amylodiogenic pathway, which produces sAPP α and P3 (**6**), or be recycled back to endosomal compartments (**3**). Endosomal APP is cleaved by β-secretase on the amyloidogenic pathway, leading to the production of sAPPβ and Aβ (**4**). APP retrograde transport from endosomes to the Golgi is also reported to take place (**5**). Image obtained from O'brien and Wong[12].*

or as a signaling ligand, through its processing and production of sAPP and AICD[70]. These proposed roles range from neurotrophic function and synaptic adhesion in a neural context, all the way to apoptosis, calcium homeostasis and intracellular signaling[70]. Until now, however, the findings on the precise function of APP remain remarkably ambiguous, frequently controversial, and lacking a clear mechanism[70]. Nonetheless, the fact that APP does indeed play an important role in neural metabolism is strongly supported by a wide range of *in-vivo* observations, such as the reduced neuronal viability and brain mass which can be observed in APP knockout models, as well as the reduced synaptic activity observed in siRNA knockdown models[77–79].

The mechanisms by which APP participates in the AD pathogenic process is a subject of ongoing debate, although it is frequently assumed that it is primarily associated to Aβ production and subsequent toxicity. Several APP mutations leading to FAD have been identified, most of these clustering around the γ-secretase cleavage site, but with some also within or neighboring the BACE1 cleavage site. These mutations have been reported to affect APP processing primarily by increasing the production of Aβ[80,81], or by elevating the Aβ42/Aβ40 ratio[82]. It should be noted, however, that mouse models carrying single FAD APP mutations can develop abundant plaque load, but generally fail to display significant neurodegeneration or cognitive defects[83], which further complicate the interpretation of how APP and Aβ contribute to AD. A few FAD APP mutations have also been reported to alter the production of AICD, which has been suggested to act as a signaling ligand following cleavage by γ-secretase, but these findings have been reported to be inconsistent and therefore controversial[84]. An interesting and seldom discussed aspect linking APP metabolism to AD is the APP-CTF C99. This C-terminal fragment is an intermediate fragment of the amyloidogenic processing of APP, produced by the cleavage of β-secretase and further cleaved by γ-secretase to produce Aβ. C99 was shown to be potentially relevant in the disease progression, originally by Neve et al. in 1996[85]. Mice overexpressing C99 under a neural promoter were reported to show drastic neuronal loss, reduced axonal myelination, and accumulation of irregularly shaped secondary lysosomes, without amyolidogenesis[86–88], indicating a potential role of the c-terminal fragment in neurotoxicity, independent of amyloidogenic peptide toxicity. Interestingly, the observed lysosomal aberrations recapitulate pathophysiological changes described on FAD cell models[89]. This model saw little follow through, in the advent of more recent amyloidosis-relevant models wherein neuropathology can be

observed in conjunction with amyloidogenesis, such as the 3x-FAD[90], and, more recently, the 5x-FAD mouse models[91], which carry multiple FAD mutations on PS and APP simultaneously. The C99 APP-CTF was additionally shown to be potentially involved in cholesterol metabolism, as recent findings by Barret et al.[92], demonstrated by nuclear magnetic resonance (NMR) and electron paramagnetic resonance (EPR) spectroscopy, an *in-vitro* binding of cholesterol to C99.

1.2.3 Apolipoproteins, lipoproteins and the AD risk factor APOE4

Apolipoproteins constitute a highly conserved protein family across mammalian species, which play an essential role in the transport of cholesterol and other lipids through the circulatory system. These proteins associate in protein-lipid complexes known as lipoproteins, which function as soluble shuttles for otherwise insoluble or poorly soluble lipids. Apolipoproteins can perform their task because they are amphipathic, that is, they possess both hydrophilic and hydrophobic domains, which simultaneously permit water solubility and interaction with hydrophobic lipids. Lipoproteins adopt a spheroid form, with insoluble lipids in the core, and a protein-phospholipid-cholesterol shell (Figure 6). Several classes of apolipoproteins are present in mammals, and their relative distribution in different types of lipoproteins affects their density and size, by influencing the relative amounts of triglycerides (TG) and cholesterol esters. As the main cargo of lipoprotein consists of TG and esterified cholesterol, changes in their relative amounts in lipoproteins is primarily what leads to differences in lipoprotein density. Consequently, there are several types of lipoproteins, classed by density, from high-density lipoproteins (HDL) to ultra-low-density lipoproteins, also known as chylomicrons. One of the primary functions of lipoproteins is the distribution of cholesterol and lipids synthesized in the liver, the primary organ responsible for cholesterol synthesis in the body.

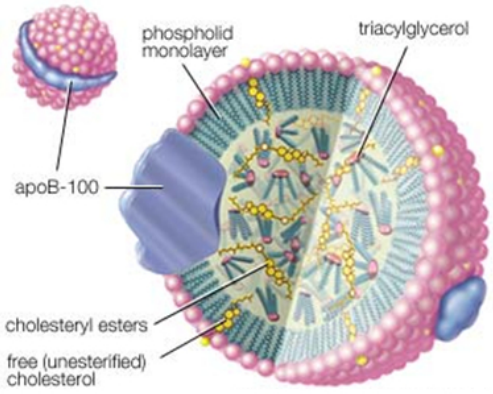

Figure 6: *Schematic representation of the structure and components of a lipoprotein[298].*

It is important to note, however, that while most organic tissue greatly depends on circulating cholesterol, an important exception can be found in the brain, where lipoproteins access is

hindered by the blood-brain barrier. Therefore, brain cholesterol is synthesized within the brain, and is also internally transported by lipoproteins. In the brain, three primary apolipoproteins have been observed - APOE, APOEJ and APOA-1 – all present in lipoproteins of similar density to the peripheral high-density lipoprotein[93,94]. Of these apolipoproteins, APOE is the predominant brain lipoprotein[94]. Indeed, APOE expression in the brain is notably high, second only to expression in the liver[95]. Neurally, this protein is primarily expressed by astrocytes and microglia[96], the former of which produce most of the neuronal cholesterol[97], delivered via lipoprotein transport. Nonetheless, low amounts of APOE expression can also be observed in neurons[98].

Among apolipoproteins, apolipoprotein E (APOE) is of great interest in the study of AD pathology. This protein has 3 common alleles in humans, APOE2, 3 and 4, and APOE4 was identified as a strong genetic risk factor for SAD by chromosomal linkage and association analysis. Through one of these studies, it was reported that APOE4 carriers show a higher risk of developing AD than non-carriers, from 20% to 90%, and the median age of onset of carriers was reported to sink from 84 to 68 years[42]. This link between APOE4 and AD has been confirmed by multiple independent studies[9]. Additionally, the allele APOE2 has been reported to have the opposite effect, reducing AD risk by as much as 50%[25,99]. The molecular mechanisms by which APOE influences APOE pathogenesis are not clear, but an interaction between this protein and Aβ has been described[41,100]. It is proposed that APOE may facilitate the clearance of amyloid plaques in the brain by directly binding Aβ and thereby enhancing glial clearance, and APOE4 has been reported to be less efficient at promoting this[101–103]. However, it has also been suggested that the role APOE plays in amyloid clearance may not be due to direct binding to Aβ, but rather by competing with Aβ for the same neural clearance pathways[104,105]. APOE plays, as indicated above, a crucial role in lipid metabolism, and an increasing number of publications have reported a connection between AD and the metabolism of various lipids and sterols[11,106–110]. As this last aspect plays an essential part in this work, it will be covered in more detail in the following section.

1.3 The theories of AD pathology and pathogenesis

With a lack of clear consensus on the etiology of AD, several concurrent hypotheses on the matter have been developed and refined through the years since its discovery. The oldest proposed hypothesis is known as the cholinergic hypothesis, which proposes that AD is caused due to an impaired synthesis of the neurotransmitter acetylcholine[111]. Therapeutic approaches were developed on the basis of this hypothesis, intended to enhance or recover neural acetylcholine levels, primarily in the form of cholinesterase inhibitors. Unfortunately, while these approaches did show mild cognitive benefits in AD patients, they failed to show any signs of slowing or curing the disease[112,113], and the theory was abandoned by most of the scientific body. A second, more accepted hypothesis is the tau hypothesis, which proposes that the microtubule-associated protein tau is at the heart of AD etiology. This hypothesis suggests that the abnormally elevated phosphorylation and aggregation of tau, which culminates in the formation of NFTs, leads to a destabilization of microtubule structure and dynamics, and that it is this event which initially triggers the disease cascade ultimately leading to neurodegeneration and dementia[114,115]. It is important to mention, however, that tau dysfunction is not unique to AD. Diseases where tau aggregation and tangle formation take place are known as tauopathies, and include conditions such as frontotemporal dementia, Parkinsonism and Picks disease. In addition, from more than 200 familial forms of AD and a substantial number of reported risk factors, few, if any, have been directly linked to effects on tau. This suggests that while tau dysfunction and aggregation are important components of AD disease progression, these lie downstream in the disease cascade and are not directly involved in AD etiology. The third, and perhaps most widely accepted hypothesis is the amyloid hypothesis, which proposes that irregularities in the production and aggregation of Aβ is the main cause for the development of the disease. The amyloid hypothesis has evolved significantly since its conception, as initially it was based on the assumption that fibrillar amyloid plaques formed by Aβ aggregation are neurotoxic. Initial studies in cultured neurons supplemented with fibrillar Aβ reported changes in action potential frequency and membrane depolarization, together with reduced cell viability[116]. The neurotoxicity of amyloid plaques, however, proved to be neglectable in mice, as several mouse models were generated which displayed significant amyloid plaque formation in the absence of neurodegeneration[83,117].

This development led to the idea that it is not amyloid plaques which are directly neurotoxic[118,119], but smaller intermediate Aβ aggregate species, known as Aβ oligomers. Several studies have shown neurotoxic effects of Aβ oligomers[120–123], as well as elevated levels in AD patients' brain[124,125] and CSF[126,127], and oligomeric Aβ has been shown to have a strong binding affinity to synapses[128] and inhibit long-term potentiation[129]. A challenge in the Aβ oligomer hypothesis lies in the interpretation of different findings, as both the size and conformation of oligomers used, as well as the conditions in which they are prepared and used, vary strongly between studies[130]. Currently, both the tau and amyloid hypotheses are hotly debated, and a difficulty in both is to fully account for all observed effects, that is, plaque theories have difficulties comprehensively accounting for tangle formation, and vice versa[115].

Autophagic and endolysosomal dysfunction have been proposed to possibly underlie the Aβ and tau pathology of AD[131–133], as such dysfunction would impair the efficient degradation of aggregation-prone peptides and proteins, leading to their progressive accumulation[134,135]. Dysfunction of the endolysosomal–autophagic system has, in fact, been reported to take place in AD, wherein endosomal compartment enlargement, autophagic vacuole accumulation and lysosomal deficits can be observed[133], together with altered levels of essential components of the endolysosomal–autophagic system, such as PI3P, Vps34, Beclin 1 and Sorl1[131,136–139]. In addition, PS has been reported to be essential for lysosomal proteolysis and calcium homeostasis[89,140], and Aβ42 has been suggested to negatively impact endosomal sorting and cholesterol efflux from endosomes[141,142]. Several lysosomal storage disorders are known to lead to neurodegeneration[143], and one in particular, Niemann–Picks disease type-C (NPC), displays notable biochemical similarities to AD. NPC is caused by mutations of the NPC1 or NPC2 proteins, and is characterized by an impairment of cholesterol shuttling within lysosomal compartments, leading to an accumulation of unesterified cholesterol in these compartments[144]. In addition to cholesterol accumulation, NPC displays tau NFT formation[145], intracellular Aβ42 deposition[146] and altered trafficking of APP and β-secretase[147], features reminiscent of AD. This would suggest that NPC and AD may share common pathogenic processes, in particular regarding endolysosomal dysfunction. An important remaining question, however, regarding endolysosomal–autophagic disfunction in AD, is whether this dysfunction is an underlying cause or a consequence of AD. An additional theory which attempts to account for both abnormal tau phosphorylation and Aβ

aggregation proposes impaired WNT signaling as the precursor to both, as this signaling pathway can affect both APP processing and tau metabolism[115].

While the hypotheses presented above attempt to answer the question of what the main pathogenic entity in AD is, in all these, two essential question remain unanswered: What triggers the disease cascade which leads to the formation and accumulation of these neurotoxic entities in SAD? And how is APOE involved in the SAD pathogenic process? A hypothesis which attempts to comprehensively explain the systemic changes which trigger SAD during aging is that of the mitochondrial dysfunction cascade[148,149]. Mitochondrial dysfunction is a common and well described occurrence in aging[150], and its effects include an impairment of the electron transport chain function, an elevated formation of noxious reactive oxygen species (ROS), neuroinflammation, alterations in lipid homeostasis, and impairment of essential signaling pathways[151–155]. Concerning SAD, the mitochondrial dysfunction cascade hypothesis proposes that it is primarily the production and accumulation of ROS during aging, combined with elevated neuroinflammation, which leads neural cells to increase the production of Aβ, cause neurotoxicity and lead to the hyperphosphorylation of tau[148,150]. While this hypothesis could comprehensively explain most of the features of AD pathophysiology, it is currently by no means accepted as consensus by the scientific community, as several aspects of it have yet to be thoroughly verified, and there are no available in-vivo models which show a direct causative link between mitochondrial dysfunction and AD. As for the role of APOE in SAD, this lipoprotein component has been associated with both Aβ clearance and mitochondrial dysfunction, but again, the lack of data clearly associating any of these observations with AD pathogenesis or disease progression underlies the lack of clear consensus, and the need to further study the question. All in all, the lack of a clear consensus on hypothesis regarding AD pathogenesis and disease progression highlight the need to explore alternative hypotheses. A particularly promising alternative hypothesis lies in the described connection between AD and lipid metabolism.

1.3.1 The link between AD and lipid metabolism

While a great deal of academic research on Alzheimer's disease currently focuses on the formation, metabolism and accumulation of amyloidogenic peptides, such as APP-derived Aβ, and hyperphosphorylated Tau, a substantial amount of evidence has been accumulated in the past years suggesting a potential role of lipids in the pathogenesis and disease progression of this disease. A recent publication, by Tamboli et al.[64], showed clear evidence associating γ-secretase activity to lipoprotein endocytosis and de-novo cholesterol synthesis[64]. A loss of the Presenilin genes, as well as pharmacological inhibition of γ-secretase activity correlated with an impaired endocytosis of lipoprotein particles, and a significant increase in cellular cholesterol and desmosterol. This accumulation was shown to be mediated by an increase in SREBP-2 expression, which likely mediates the observed increase in the expression of CYP51 and HMG-CoA reductase. Additionally, it was shown that an accumulation of C99 leads to an impaired endocytosis of LDLR, likely explaining the impaired lipoprotein endocytosis observed in PS deficient models. Overall, the results highlighted sterol metabolism as a potential link connecting γ-secretase activity and APP processing, both factors associated with FAD, to the main risk factor for late-onset AD, the lipoprotein APOE. A second recent publication reported a substantial increase of cholesteryl-ester content in brain samples from human AD patients and mouse AD models[156]. In addition, two publications, focusing on cell-based AD models and AD mouse models respectively, have reported a strong effect of the pharmacological inhibition of ACAT (ACAT is also known as SOAT1, an intracellular cholesterol acyltransferase) on Alzheimer pathology, reporting an 88-99% reduction in amyloid plaque load and an 83%-96% reduction in insoluble Aβ after treatment with the ACAT inhibitor[157,158]. Together, the presented data suggest that an involvement of sterol metabolism, potentially involving sterol storage mechanisms, such as lipid droplet formation and dynamics, could be relevant in the pathogenesis of AD. Indeed, the research articles highlighted above are but a small sample of a wealth of publications[10,11,106–110,159–162] showing effects, in cases of altered metabolism, of virtually every major lipid class on markers for Alzheimer's disease, not only in regards to amyloidogenesis, but also affecting cognitive impairment and neuronal loss. While few publications claim to have found an etiological role of lipid metabolism in AD, the fact that it plays a role in the development of the disease is unmistakably clear. Unfortunately, several of these

findings have apparently not seen thorough follow through. One of the primary goals of this thesis is to further study and elucidate the observed link between PS activity, APP processing and lipid metabolism, in particular regarding sterol metabolism.

1.4 Cholesterol metabolism

Cholesterol is a remarkably important lipid in mammals, which plays essential roles both as a structural component of membranes and as a metabolite[163,164]. In the membranes, it contributes not only to overall membrane rigidity, but also as a lipid raft microdomain component. As a metabolite, it is the common precursor of steroid hormones, as well as vitamin D and bile acids. Body cholesterol is acquired both by nutrition and *de-novo* synthesis, the latter taking place primarily in the liver and then distributed to other tissues by the circulatory system. An exception to this is the brain, where cholesterol is produced and distributed locally[165].

Physiological regulation of cholesterol metabolism is mediated by a rich and complex set of intra - and-extra cellular processes, which mediate intracellular sterol content, storage and dynamics[163,166] (Figure 7). Lipoprotein particle endocytosis and *de-novo* cholesterol synthesis are two of the main mechanisms which determine the amount of

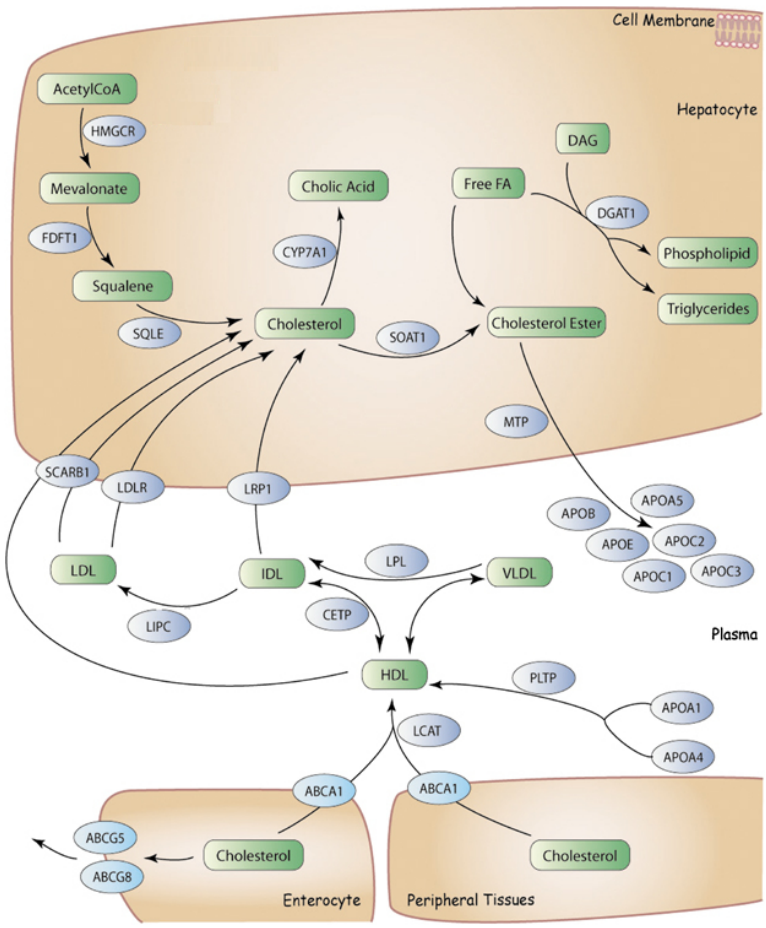

***Figure 7**: Simplified schematical representation of cholesterol de-novo synthesis, esterification and transport. Relevant enzymes are displayed as blue ovals. Cholesterol precursors, lipoproteins and associated lipids are shown as green rectangles. Image obtained fom Mangavite et al.[299].*

cholesterol available in different peripheral cells. Excess cellular cholesterol is stored in the form of cholesteryl-esters, with cholesterol acyltransferases (such as LCAT and ACAT) and cholesteryl-ester esterases (such as steryl-ester acylhydrolase) playing important roles in intracellular sterol storage and dynamics. Cholesteryl-esters, together with triglycerides, are stored in lipid droplets, cellular storage organelles for hydrophobic molecules[167]. The formation, and dynamics, of these organelles is closely related to the synthesis and available pools of free cholesterol, as both synthesis and storage of cholesterol is tightly regulated to maintain free cholesterol levels within a stable range[166]. De-novo cholesterol synthesis is a multi-step process mediated by several enzymes, such as HMG-CoA reductase and CYP51, and the expression of most of these enzymes is regulated by transcription factors known as sterol regulatory element-binding proteins (SREBPs)[168]. Cholesterol secretion is mediated by membrane transporters known as ABC transporters, primarily ABCA and ABCG. These proteins secrete cholesterol, either before or after esterification, to be loaded into lipoproteins extracellularly[169].

Cholesterol in the brain is isolated from peripheral cholesterol and synthesized locally, by astrocytes and oligodendrocytes, with dietary cholesterol being virtually absent[165]. This isolated system is achieved by means of the blood-brain barrier, which restricts the access of peripheral lipoproteins to the brain environment. While the general mechanisms by which cholesterol is synthesized and transported in the brain are believed to be comparable to those in the periphery, the specific neural mechanisms are not understood in depth[170], and there are notable differences, such as is the case with brain lipoproteins, as has been covered in the corresponding section above.

A more recently identified participant in the regulation of sterol metabolism is the liver-x receptor (LXR), essential in both peripheral and brain cholesterol homeostasis.

1.4.1 The Liver-X receptor

The liver-x receptor (LXR) is an essential transcription factor in cholesterol and lipid homeostasis. LXR is one of many nuclear receptors (NR), which exert transcriptional regulation following nuclear translocation when binding a specific ligand. This transcription factor belongs to the type II NR family, a family of NRs which necessitate the formation of heterodimers with the retinoid-x receptor (RXR) for nuclear internalizations and gene regulation. As most type II NRs, LXR can act both as a gene repressor and gene activator, this function depending on its binding to a putative ligand (Figure 8A). Initially identified as an orphan receptor, LXR was later found to respond to cellular sterol levels, with oxysterols and cholestenoic acids as its natural ligands. This transcription factor promotes *de-novo* cholesterol synthesis, as well as cholesterol secretion and uptake. This is accomplished by regulating the expression of key enzymes in both pathways, such as SREBPs in *de-novo* synthesis[171], as well as ABCA1, APOE and LRP in cholesterol distribution and uptake[172]. LXR has been found to act, additionally, as a regulator of triglyceride metabolism[171], as well as inflammation[173] (Figure 8B).

LXR has two paralogues in humans, termed LXR-α and LXR-β. While LXR-α expression is primarily restricted to peripheral environments essential to lipid homeostasis, such as the liver and adipose tissue, LXR-β is more ubiquitously expressed, with notably high expression in the liver and the brain[170]. Indeed, in conjunction with peroxisome proliferator-activated receptors (PPARs), LXRs are the main regulators of lipid homeostasis in the brain[176].

LXR has, in previous years, been found as an interesting candidate in the study of AD pathology due to its regulatory effect in APOE expression[176]. Indeed, LXR inactivation was initially found to enhance Aβ load, potentially due to an impairment of glial phagocytosis, an important process for Aβ clearance in the brain, caused by a decrease in LXR-mediated inhibition of microglial inflammatory response[177]. Studies involving the use of synthetic LXR agonists were, however,

more complicated to interpret. Reports regarding the clearance of Aβ load following agonist treatment were conflicting, with some reporting positive changes while some revealed no

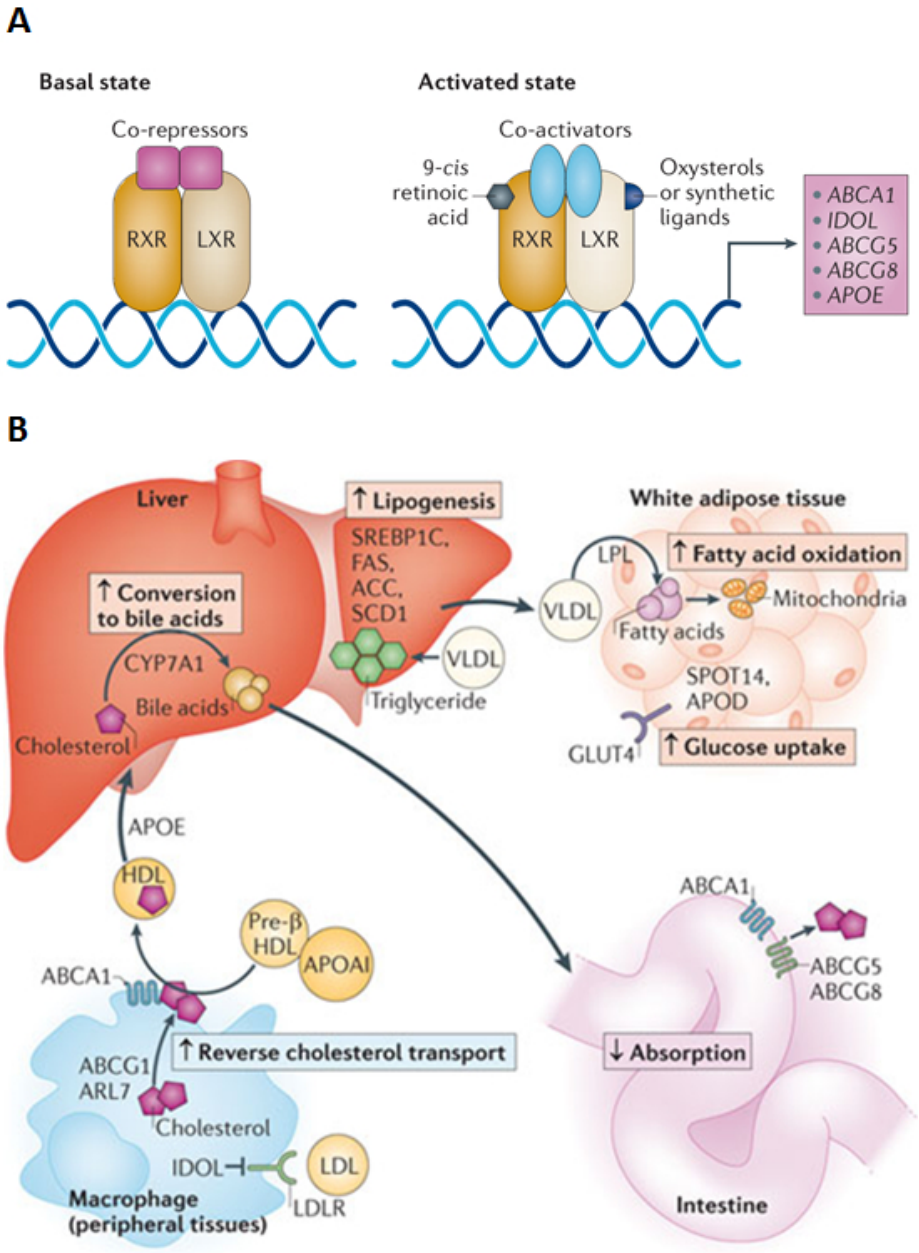

Figure 8: *LXR gene regulation and metabolic functions.* ***A)*** *Regulation of gene expression by LXR. In absence of activating ligands, LXR can function as a transcriptional repressor. In such instances, the LXR-RXR heterodimer is bound to co-repressors which hinder gene transcription and subsequent protein expression. Upon association to activating ligands, the LXR-RXR heterodimer undergoes conformational changes which displace bound co-repressors, and promote the binding of co-activators, thereby leading to an enhanced gene transcription.* ***B)*** *Metabolic effects of LXR activation in different tissues[175]. Broad metabolic effects of LXR activation in different tissues are highlighted with rectangles and arrows, and named proteins are those under transcriptional regulation by LXR which are relevant to the corresponding mechanisms. Image obtained from Hong and Tontonoz[174].*

significant change[176,178,179]. Notwithstanding, most studies on mouse models reported an enhancement of cognitive performance following agonist treatment[180,181]. These studies highlighted the potential LXR has both as a candidate for improving our understanding of AD pathogenesis, and as a target for therapeutic approaches against AD.

1.4.2 Lipid droplets

Our understanding of lipid homeostasis has vastly improved in the last decades, including the understanding of the lipid droplet (LD). This intracellular organelle functions primarily as a storage compartment for poorly soluble lipids, in particular cholesterols and fatty acids, in the form of cholesterol esters and triglycerides. The organelle takes the form of a large, complex micellar structure, with a membrane monolayer composed of phospholipids, cholesterol and proteins, and a lipophilic core containing neutral lipids (figure 9). In addition to serving as a reserve for excess lipids, the LD also serve as a regulator of cellular lipid homeostasis, as LD formation, size, and dynamics responds rapidly to changes in cellular fatty acid and cholesterol levels[166,182]. While this organelle is currently not fully understood, it is an essential target in the study of sterol and lipid metabolism, in particular regarding the cellular regulation of excess cholesterol[167].

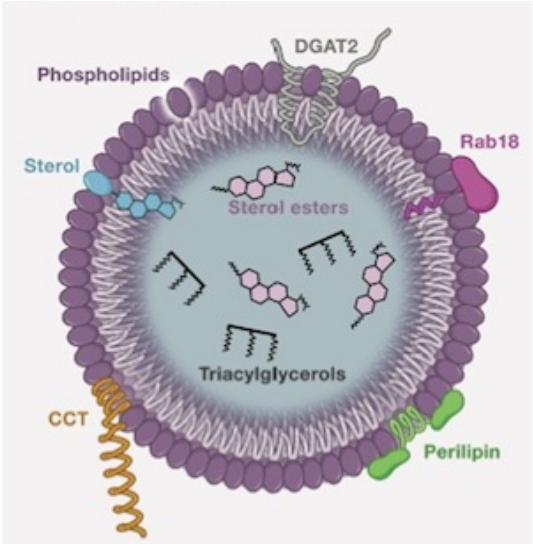

***Figure 9**: Schematic representation of the structure, components and content of the lipid droplet[300].*

1.5 Aim of this study

The purpose of this body of work, as a whole, is to uncover the underlying mechanisms which link AD pathology with lipid metabolism, PS activity, lipoprotein metabolism and APP processing. Previous reports by Tamboli et al.[64] already suggested a metabolic relation between PS activity,

APP processing and lipoprotein metabolism could be found in sterol metabolism, and we intended to pursue that lead.

Our point of departure was PS, the catalytic proteins of the γ-secretase protease complex[6]. This complex is responsible for the cleavage of a large number of type I membrane proteins, including the APP CTF C99[48]. The initial focus of this work was to further our understanding of the role of PS activity in lipid metabolism within the frame of AD pathology. Specifically, this study initially focused on uncovering the potential effects of PS activity on cholesterol esterification, storage, and secretion, as well as lipid droplet metabolism. Having identified a specific set of effects, we intended to uncover a molecular mechanism responsible for the observed effects. Finally, we intended to explore the possibility of a link between the uncovered effects, lipoprotein metabolism and APP processing.

By this, we hoped to examine the potential relevance of lipid metabolism in AD, as well as to facilitate a more unified understanding of several different facets known to play a role in AD pathology, which have been extensively described as individually linked to AD pathology, but which have yet to be comprehensively linked between each other in either a metabolic or pathogenic level.

2 Materials and Methods

2.1 Chemical reagents

Unless otherwise noted, the chemical reagents employed in the frame of this work were acquired in purity grade "*per analisi*" from the following suppliers: Sigma-Aldrich (Steinheim, Germany), Thermo Fisher Scientific (Waltham, Massachusetts, United States), Roth (Karlsruhe, Germany), or Applichem (Darmstadt, Germany). Cell culture media and buffers were acquired from Life Technologies (Frankfurt, Germany).

LD540 lipid droplet-specific dye, alkyne cholesterol ((25*R*)-25-ethinyl-26-nor-3β-hydroxycholest-5-en), alkyne cholesterol ester ((25*R*)-25-ethinyl-26-nor-3β-Hydroxycholest-5-en 3-oleate), and reagents for the labeling of alkyne derivates by click reaction (3-azido-7-hydroxycoumarin, $[acetonitrile]_4CuBF_4$ in acetonitrile) were graciously provided by Dr. Lars Kuerschner, from the laboratory of Prof. Christoph Thiele (Biochemistry & Cell Biology of Lipids, LIMES institute, Bonn, Germany).

2.2 Instruments and software

Instrument	*Manufacturer*
AxioVert 200 Fluorescence Microscope	Zeiss
Colibri.2 Microscope light source	Zeiss
7300 Real-Time PCR System	Applied Biosystems
Mastercycler personal PCR cycler	Eppendorf
Multiskan RC plate reader	Thermo Scientific
SpectraMAX Gemini plate reader	Molecular Devices
P-class Nanospectrophotometer	Implen
Cell culture CO_2 incubator	Binder

Temperature-controlled water bath	Medigen
Laminar flow cell culture clean bench	Thermo Scientific
-80°C Freezer	Thermo Scientific
5804R Centrifuge	Eppendorf
E100 Cooling system	Lauda
Protein-electrophoresis chamber	Höfer
XCell SureLock Mini-Cell electrophoresis system	Thermo Scientific
Western-blotting chamber	Höfer
ChemiDoc XRS chemiluminescence Imager	Bio-Rad
DNA-electrophoresis chamber	Amersham
GVM 20 trans-UV illuminator	Syngene
Sonopuls, UW 2070 Sonifier	Bandelin
Genesis photometer	Thermo Scientific
MP 225 pH meter	Mettler Toledo
Magnetic stirrer	Velp Scientifica
SBH 130 D Heating Block	Stuart Scientific
5415D microcentrifuge	Eppendorf
5804R refrigerated Centrifuge	Eppendorf
5415R refrigerated microcentrifuge	Eppendorf
Incubator	Binder
Thermomixer Compact	Eppendorf
Labstyle 204 analytical balance	Mettler Toledo
PL 202-S Balance	Mettler Toledo
Autoclave	H+P
MS 2 Minishaker	IKA

Software	*Supplier*
ZEN microscopy software	Zeiss
Quantity One 1-D Analysis Software	Bio-Rad
ImageJ image processing software with FIJI image processing package	Public domain/NIH
Graphpad PRISM	Graphpad software
Microsoft Excel	Microsoft

2.3 Methods

2.3.1 Cell culture

Mouse embryonic fibroblasts (Wild-type (WT), PS1/PS2 double-knockout (PSdKO)[183], and PSdKO overexpressing human PS1 wild-type (hPS1WT) and catalytically inactive PS1 D257A (hPS1DA)[184]) and H4 astroglioma cells (WT and WT overexpressing APP CTF C99-GFP (H4 C99-GFP)[185]) were cultured in Dulbecco´s modified Eagle´s medium (DMEM) supplemented with 10% fetal calf serum (PAN) and 1% penicillin and streptomycin (v/v) (Life Technologies). Cell cultures were maintained in incubation at 37°C, 95% humidity, with 5% CO_2 atmosphere until confluence of 80-90%. For passaging, cells were washed with Phosphate-buffered Saline (PBS; 140 mM NaCl, 10 mM Na_2HPO_4, 1.75 mM KH_2PO_4, dH_2O, pH 7.4), enzymatically detached with the aid of a Trypsin-EDTA solution (0.05 % (w/v) trypsin (Invitrogen), 0.53 mM EDTA, dH_2O), and re-seeded on culture media at the desired concentration. Cell harvesting for analysis was done by washing cells thrice with PBS, manual scraping and collection in Eppendorf tubes, and centrifugation of collected cells. Collected cell pellets were either immediately used or shock-frozen in liquid nitrogen and stored at -80°C for future use.

Primary human astrocytes were a generous gift of Dr. Constantin Glebov, and were cultured in similar conditions to MEFs and H4 cells.

WT and NPC1-null Chinese hamster ovary (CHO) cells were obtained from Dr. Daniel S. Ory, from the Washington University School of Medicine, USA. NPC1-null cells are CHO cells in which the NPC1 gene has been deleted. CHO cells were cultured in DMEM/F12 medium (1:1) + 10% FCS + 2mM L-Glutamate.

Pharmacological inhibition of PS activity with N-[N-(3,5-Difluorophenacetyl)-L-Alanyl]-(S)-Phenylglycin t-Butylester (DAPT) (Sigma Aldrich) was achieved by incubating the cells in culture medium supplemented with 5-10µM DAPT, for either five or seven days prior to analysis, to ensure proper inhibition of Presenilin, disappearance of Presenilin cleavage products, and observable accumulation of Presenilin substrates. DAPT was stored at a 10mM stock solution in DMSO.

Pharmacological activation of LXR was achieved with the LXR agonist GW3965 (Sigma Aldrich), reported to act as a full agonist for both hLXRα and hLXRβ[186]. The agonist was stored as a stock solution of 5mM in DMSO, and used in cell culture at a concentration of 5µM overnight.

Low-density lipoprotein (LDL) supplementation of MEFs was done by supplementing the standard cell culture media with 10µg/ml LDL (Human LDL, Sigma-Aldrich) for 18h, followed by harvesting and analysis by Western-blotting and q-rtPCR.

2.3.1.1 Determination of cholesterol in cell culture media

To analyze cholesterol secretion in cell media of the different analyzed MEF cultures, the standard culture media was removed from the cultures, cells were washed thrice with PBS, the media was replaced with FCS-free culture media (DMEM +1% penicillin and streptomycin (v/v)), and the media was collected after 36 hours of incubation. The collected media was centrifuged 3x at 3000 RPM to remove cellular debris, and the recovered media was shock-frozen in liquid nitrogen and stored on -80°C prior to analysis by GC-MS (described below).

2.3.2 Cell Fractionation

Fractionation of harvested cell samples into cytoplasmic, membrane and nuclear fractions was performed as follows: The harvested cell pellets were washed 3x in PBS, followed by dissolving and re-suspending the harvested cell pellet in 0.3 ml hypotonic buffer D (10 mM Tris.Cl pH7.5, 10 mM NaCl, 0.1 mM EGTA, 25 mM β-Glycerophosphate, 1 mM DTT, 1x cOmplete proteinase Inhibitor (Roche)). Samples were then incubated on ice for 15 min, followed by 10-15 times homogenization with 1ml syringe and a 0.6-mm cannula. Cells were then centrifuged 3800rpm for 5 min. at 4°C, and the supernatant (S1) and the pellet (P1) separated. The pellet (P1) was resuspended in 100 µl Buffer C (25 % Glycerol, 20 mM HEPES pH7.9, 0.4 M NaCl, 1 mM EDTA pH8.0, 1 mM EGTA, 25 mM β-Glycerophosphate, 1 mM DTT, 1x cOmplete proteinase Inhibitor (Roche)) rocked for 20 min. on ice, and centrifuged at 13200rpm for 15 min. at 4°C, with the remaining supernatant of this fraction being the nuclear fraction. The previous supernatant (S1) was centrifuged at 13200 rpm for 60 min. at 4 °C, and the pellet (P2) and the supernatant (S2) were separated. The supernatant (S2) was the cytoplasmic fraction. The pellet (P2) was resuspended in 50 µl STEN lysis buffer (50mM Tris HCL pH 7,6 , 150mM NaCl , 2mM EDTA, 1% Igepal , 1% Triton X – 100, 1x cOmplete proteinase Inhibitor (Roche)) incubated on ice for 10 min and centrifuged at 13200rpm and 4°C for 15 min. The recovered supernatant was the membrane fraction. Following fractionation, the protein concentration of each sample was determined by BCA protein estimation. Analysis of the samples was done by sodium dodecyl sulfate polyacrylamide gel electrophoresis (SDS-PAGE) and detection by Western-blotting and ECL imaging (Bio-Rad).

2.3.3 Sodium dodecyl sulfate polyacrylamide gel electrophoresis

For the separation of proteins based on their molecular weight, the SDS-PAGE method was used. For this purpose, two-phase discontinuous SDS-PAGE gels were cast, with an upper protein stacking phase, and a lower protein separation phase. Both gel phases are prepared with a TRIS-buffered solution of acrylamide/bisacrylamide in H_2O. The separation phase gel has an

acrylamide/bisacrylamide solution (30 % (v/v) Acrylamide/Bisacrylamide in the ratio of 37.5:1) concentration ranging from 7 -12% depending on the molecular weight of the proteins of interest, and a high pH buffer (1.5 M Tris, 0.4 % (w/v) SDS, dH2O, pH 8.8; Lower Tris). The stacking phase gel has an acrylamide/bisacrylamide solution concentration of 4% and a low pH Buffer (500 mM Tris, 0.4 % (w/v) SDS, dH2O, pH 6.8; Upper Tris). To trigger the acrylamide polymerization reaction, 0.25% ammonium persulfate (APS, Roth) and 0.25% tetramethyl ethylenediamine (TEMED, Sigma-Aldrich) are added to the solution prior to casting. The separation phase solution is initially cast on a PAGE gel cassette, and 0.5 ml of isopropanol is added on top of the solution immediately after casting to prevent dehydration and ensure the formation of a homogeneous surface. After the separation gel is formed, the isopropanol is removed, and the stacking gel solution is prepared and cast on top. A plastic comb is inserted into the stacking gel solution immediately after casting, to form sample loading wells. The plastic comb is removed when the stacking gel has formed, the gel cassette is inserted into an SDS-PAGE chamber, and PAGE running buffer (25 mM Tris, 200 mM Glycine, 0.1 % SDS, dH2O) is then added to the chamber. The protein samples to be analyzed are prepared by the addition of an SDS loading buffer (25 % Upper Tris, 0.34 M SDS, 0.1 M dTT, 50% glycerol, bromphenol blue in H_2O) and incubation of this mixture at 95°C (80°C for Presenilin blots) for 5 minutes, or to ensure protein denaturation. The respective samples, and a molecular weight protein standard (PageRuler; Thermo Scientific) are then loaded in different sample loading wells, and electrophoresis is performed at 30 mA and a maximum of 180 Volts.

2.3.4 Western immunoblotting

In order to detect specific proteins by Western blotting, after SDS-PAGE separation, the proteins are initially transferred from the PAGE gel to a nitrocellulose membrane. This is done by laying the separated protein gel onto a nitrocellulose sheet (0.2 µM pore size) of corresponding size and covering both sides with Whatmann blotting papers (Sigma Aldrich) and plastic sponges. The assembly is clamped together and placed on a blotting chamber. The blotting chamber is then filled with transfer buffer (5 mM Tris, 200 mM Glycine, 10 % methanol, in H_2O), and the proteins

are transferred onto the membrane with a current of 400 mA for 1.5h. The membrane is then washed with TBS-T (10 mM Tris, 150 mM NaCl, 0.1 % Tween20, pH 7.5, in H_2O), and successful protein transfer is verified by dousing the membrane in a Ponceau red solution (3 % (w/v) Ponceau S, 3 % trichloroacetic acid, in H_2O) and washing the excess dye with H_2O. Following, the membrane is washed thrice with TBS-T for 5 min, and incubated with blocking solution (5 %, BSA (Roth) in TBS-T) for 1 h. The membrane is then incubated in a primary antibody solution (2.5 % BSA, antibody solution in the respective concentration (see table below) in TBS-T) overnight at 4°C, or 2h at RT. This is followed by washing the membrane 4 times with TBS-T, and incubation with the respective HRP-coupled secondary antibody solution (2.5 % BSA, antibody solution in the respective concentration (see table below) in TBS-T) for 1h at RT. Finally, membrane is washed 4 times with TBS-T, excess liquid is removed from the membrane, and then the membrane is shortly incubated in an electrochemiluminescence (ECL) solution (1:1 mix of W1 and W2 ; W1: 0.1 M Tris pH 8.5, 0.4 mM cumaric acid, 0.25 mM luminol, dH2O ; W2: 0.1 M Tris pH 8.5, 0.018 % H2O2, dH2O). Luminescence produced by the product of the HRP-ECL reaction is detected with the aid of an ECL imager (Biorad). In case signal intensity is deemed insufficient, the membranes are incubated in a solution of ECL Advanced (GE healthcare). Signal intensity was measured with the ImageJ/FIJI software.

Antibody	*Protein target*	*Species*	*Source*	*Dilution*
C1/6.1	APP C-terminal domain	Mouse	Biolegend	1:1000
3109	Presenilin-1 C-loop	Rabbit	Eurogentec	1:1000
A1978	B-Actin	Mouse	Sigma-Aldrich	1:5000
N-20	PARP-1	Goat	Santa Cruz	1:1000
H144	LXR α/β	Rabbit	Santa Cruz	1:1000
α-ms-HRP	Mouse IgG	Rabbit	Sigma-Aldrich	1:25000
α-rb-HRP	Rabbit IgG	Goat	Sigma-Aldrich	1:25000
α-gt-HRP	Goat IgG	Rabbit	Sigma-Aldrich	1:25000

2.3.5 Amplex red cholesterol assay

To determine cholesterol levels, the Amplex Red cholesterol assay kit (Molecular Probes) was employed as indicated by the manufacturer. Samples were obtained by culturing MEFs until 90% confluence, followed by scraping of the cells for harvesting, centrifugation, washing of the cell pellet with cold PBS, removing of the remaining liquid from the pellet, and shock-freezing in liquid nitrogen for storage of the samples until use. Cell lysates were produced by incubating cell pellets in RIPA buffer (1% NP-40, 0.1% SDS, 50 mM Tris-HCl pH 7.4, 150 mM NaCl, 0.5% Sodium Deoxycholate, 1 mM EDTA) for 10 minutes on ice. Quantified cholesterol was standardized to the protein concentration of the samples, previously determined by the BCA assay. An excitation wavelength of 530 ± 10 nm and emission wavelength of 590 ± 10 nm were used for detection. RIPA lysis buffer, accordingly diluted, was used as a negative control, and H_20_2 (Molecular probes) was used as a positive control. The cholesterol standard curve was done with the cholesterol/cholesterol ester mixture supplied in the kit for such purpose.

2.3.6 Triglyceride assays

In order to determine the triglyceride content of cell lysates, an enzymatic lipase-based kit (Triglyceride Quantification Colorimetric/Fluorometric Kit, Biovision) was used, according to the instructions of the manufacturer. Briefly, cell culture samples are diluted in the provided triglyceride assay buffer on a 96-well plate, followed by the addition of the provided lipase solution. After a 20 minute incubation, the provided triglyceride reaction mix is added to the samples, incubated for one hour, and the samples are measured by colorimetry with absorbance at a 570nm wavelength. Samples were obtained by culturing MEFs until 90% confluence, followed by scraping of the cells for harvesting, centrifugation, washing of the cell pellet with cold PBS, removing of the remaining liquid from the pellet, and shock-freezing in liquid nitrogen for storage of the samples until use.

2.3.7 Fluorescence microscopy

For analysis by fluorescence microscopy, cells were seeded on uncoated glass coverslips by adding 0.6 -1.2 x 10^4 cells (depending on cell type) on 3-cm cell culture dishes containing three glass coverslips, and fixed for staining and analysis after 24 or 48h. Cells were fixed with 4% Paraformaldehyde in phosphate buffered saline (PBS) for 10 min. Prior to antibody stainings, cells were permeabilized with a Triton X-100 solution (0.25 % (v/v) Triton X-100 (Sigma-Aldrich) in PBS) for 10 min, and incubated in blocking solution (10 % (w/v) BSA in PBS) to prevent non-specific protein interaction with the respective antibodies. Cells were not permeabilized for lipid droplet and cholesterol stainings, as both the lipid droplet dye LD540 and the cholesterol dye Filipin-III are lipophilic and passively traverse the cell membrane. Coverslips were washed 3x with PBS (+ 0.125% (v/v) Triton-X 100 for antibody stainings) before and after incubation with the respective dye or antibody in order to remove excess dye or unbound antibodies. Primary and secondary antibody labeling was done for 1 hour in PBS + 2% (w/v) BSA, and chemical stainings were done by incubating samples with the respective dye, diluted in PBS, as indicated in the tables below. Following stainings, coverslips were washed once with water, quickly dried, and mounted on microscopy slides with the aid of ImmuMount (Thermo Scientific). Following mounting, microscopy slides were allowed to dry overnight at 4°C (36h for LD540), and the slides were analyzed with the aid of the AxioVert 200 Fluorescence Microscope (Zeiss).

Chemical dye	*Dye affinity*	*Stock*	*Dilution*	*Incubation time*
LD540[187]	Lipid droplets	0.5mg/mL in ethanol	1/20000	10-15 min.
Filipin-III	Cholesterol	10mg/ml in DMSO	1/180	20 min.
DAPI	Nucleus	3mM/ml dH_2O	1/1000	5 min.

Antibody	*Antibody Target*	*Species*	*Dilution*	*Source*
Anti-Giantin	Giantin	Mouse	1:300	Dr Hauri, Basel
T7576	TGN46	Rabbit	1:200	Sigma-Aldrich
PM062	EEA1	Rabbit	1:300	MBL
A4200	AP-1 G1	Mouse	1:200	Sigma-Aldrich
Anti-Rabbit Alexa 647	Rabbit IGG	Goat	1:500	Thermo Scientific
Anti-mouse Alexa 546	Mouse IGG	Goat	1:1000	Thermo Scientific

2.3.8 Gas Chromatography-Mass Spectrometry

Cellular levels of cholesterol precursor (lathosterol, lanesterol and desmosterol), plant sterols (sitosterol, sigmasterol and campesterol), cholestanol and cholesterol concentrations were analyzed, by Anja Kerksiek, in the frame of a collaboration with Prof. Dieter Lütjohann (institute for clinical chemistry and clinical pharmacology, laboratory for special lipid diagnostics, Bonn university clinic, Bonn, Germany) by gas chromatography–mass spectrometry (GC-MS) as described in their corresponding publication[188]. Cell samples were produced by culturing mouse embryonic fibroblasts until 90% confluence, followed by scraping of the cells for harvesting, centrifugation, washing of the cell pellet with cold PBS, removing of the remaining liquid from the pellet, and shock-freezing in liquid nitrogen for storage and delivery of the samples. Four biological replicates were used for each condition tested.

2.3.9 Spectroscopic protein estimation assay by the BCA protein assay

Analysis of protein concentration was conducted by the use of the Pierce® BCA Protein Assay Kit (ThermoScientific; Waltham, USA) that combines the biuret reaction with specific colorimetric enhancer reactions. The assay was performed following the provided indications by the manufacturer.

2.3.10 Alkyne cholesterol tracing

For the detection of free and esterified alkyne cholesterol metabolized after feeding, cells were initially fed the alkyne cholesterol for 24h at a concentration of 10µM in full media. The cells were then harvested, and the lipids extracted. The lipids of harvested cells were isolated by a biphasic extraction. Briefly, The harvested cell suspension (900 µl) is added to 4 ml of 2:1 methanol:chloroform, and sonicated for 5 minutes on a water sonication bath. The samples are then centrifuged (5 min, 4000 g), and the supernatants are recovered. 7 ml of 6:1 H2O:chloroform are added to the recovered supernatants, followed by vigorous mixing and centrifugation (5 min, 4000 g). Two fractions are obtained from the mixture following centrifugation, with remaining proteins visibly accumulating in the interface of the two fractions. The lower (organic, chloroform) fraction is recovered, and the chloroform is evaporated with a centrifugal evaporator. If storage is required, the pellets were redisolved in 500µl $ChCL_3$, and re-evaporated as needed. The alkyne sterols were then fluorescently labeled with 3-azido-7-hydroxycoumarin by click-reaction. To do this, the extracted lipid pellet was initially redisolved in 10µl CHCl3, bath-sonicated, shortly centrifuged and 30 µl of $[acetonitrile]_4CuBF_4$ of acetonitrile together with 5 µl of 44.5 mM 3-azido-7-hydroxycoumarin was added, followed by vortexing and short centrifugation. The reaction takes place at 43°C, with no agitation, for 4h, in a closed Eppendorf tube. The sample lipids are then separated on a glass silica gel TLC plate by running initially in CHCl3/MeOH/water/AcOH 65/25/4/1 for 10 cm, followed by drying and running in hexane/ethyl acetate 1/1. The plate is then dried and quickly rinsed in 4% Hunig's base/hexane, which drastically enhances the fluorescent signal. The fluorescent imaging of the labeled sterols is performed by excitation with 420 nm, and detection on 482–502 nm.

2.3.11 Quantitative real-time PCR (q-rtPCR)

Q-rtPCR was employed to analyze cellular gene expression. Briefly, RNA was initially isolated from MEFs via the RNeasy mini kit (Qiagen), and cDNA of the isolated RNA was produced with the RevertAid First Strand cDNA Synthesis Kit (Thermo Scientific), as indicated by the respective manufacturer's instructions. Following, the 7300 Real-Time PCR System (Applied Biosystems) was

employed to detect the relative abundance of cDNA. For this purpose, master mixes for primers corresponding to the genes of interest (primer + Sybr Green PCR Master Mix (Applied Biosystems)) and for cDNA templates (cDNA in DNase-free water) were produced, and subsequently plated in triplicates on a 96-well plate for analysis with the instrument. Volume fluctuations between wells were controlled with the ROX reference dye. The levels of DNA generated through the reaction were analyzed by an automatically-set cycle threshold (Ct), in which fluorescence is found to be above baseline levels and below exponential growth. This Ct was then used to calculate relative gene expression (2 -ΔΔCt), by normalizing to two reference housekeeping genes (lactate dehydrogenase A and actin β). The employed primer pairs were Quantitect primers, obtained from Qiagen. The primer sequence is not disclosed by the manufacturer. The used primers are indicated in the table below.

Primer	*Target mRNA*	*Provider*
NR1h2_1 SG	LXR-β	QIAGEN
ABCA1_1 SG	ABCA1	QIAGEN
SREBF1_1 SG	SREBF1	QIAGEN
LDHA_1 SG	LDH	QIAGEN
ACTB_2	ACTb	QIAGEN

2.3.12 Statistical analysis and quantification of microscopy metadata

Numerical results are shown as bar graphs, displaying average +/- SEM. Statistical significance was analyzed by unpaired t-test with Welch's correction when comparing two conditions, and by one-way ANOVA and Holms-Sidak multiple comparison test when comparing more than two conditions, unless indicated otherwise. P-Values are indicated as following: * ≤ 0.05 , ** ≤ 0.01 , *** ≤ 0.001

C99-GFP fluorescent intensity and LD levels were analyzed with the aid of the ZEN microscopy software (ZEISS).

3 Results

3.1 γ-secretase activity and lipid metabolism

The primary findings of this thesis expand on those of Tamboli et al.[64], which reported alterations on lipoprotein particle endocytosis and the *de-novo* cholesterol synthesis pathway within cells

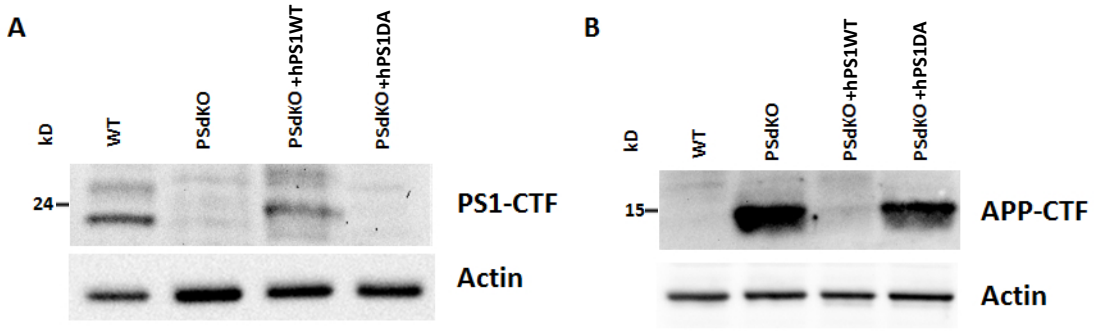

Figure 10: PS1-CTF levels and APP-CTF levels in MEFs lacking PS activity by Western immunoblotting. A) *PS1-CTF levels in MEF with different PS expression, detected by Western Immunoblot probed with a C-terminal Presenilin antibody. The PS1-CTFs produced by endoproteolysis of PS are necessary for γ -secretase activity[6], and the absence of PS1-CTFs can be observed in MEFs lacking PS or expressing a catalytically inactive variant of PS.* ***B)*** *APP-CTF levels in MEF with different PS expression (wild-type (WT), Presenilin double-knockout (PsdKO), and PSdKO stably expressing human WT Presenilin (+hPS1WT) or a catalytically inactive variant of human Presenilin (+hPS1DA)) detected by Western Immunoblot probed with an APP CTF antibody. Substantial accumulation of APP-CTFs can be observed in cells lacking PS activity.*

lacking functional Presenilin (PS). Our interest was focused in understanding the metabolic consequences and the mechanism of the described link between PS and sterol metabolism, as well as understanding the role that other proteins involved in AD pathology may play therein. Consequently, our initial goal was to uncover the effects of PS expression and γ-secretase activity on the storage and homeostasis of cholesterol. For this purpose, we elected to analyze, in cell models lacking PS activity and wild-type controls, four main factors involved in sterol storage and homeostasis: lipid droplet levels, sterol precursor levels, sterol esterification and cholesterol secretion. Additionally, triglyceride levels where studied, as they relate to lipid droplet levels, and the influence of APP-CTF accumulation on lipid droplet levels.

The principal cell models used in the following experiments were mouse embryonic fibroblasts (MEF), with MEFs carrying a knock-out mutation of both Presenilin-1 (PS1) and Presenilin-2 (PS2) (PSdKO)[183] compared to wild-type MEFs (WT). Two additional rescue models, with re-expression of either human wild-type PS1 (PSdKO +hPS1WT) or catalytically inactive variant of human

Presenilin PS1, carrying the loss-of-function D257A point mutation (PSdKO +hPS1DA)[6], were used as controls. The efficient retransfection of MEFs with the respective Presenilin variants was verified by Western blot analysis of both PS1-CTF levels, observed to be absent in cells lacking functional PS, and an enzymatic substrate of PS (APP-CTF) observed to accumulate in cells lacking functional PS (Figure 10).

3.1.1 Lipid droplet levels in cells lacking PS activity

Lipid droplets (LD) are the primary cellular organelles responsible for the storage of cellular cholesterol and triglycerides. In order to study these organelles in the frame of PS function and AD pathology, the recently developed fluorescent dye LD540, shown to selectively stain lipid droplets[187], was used for the observation of LDs by fluorescence microscopy.

3.1.1.1 Elevated lipid droplet levels in MEFs lacking PS activity

With the aid of the lipophilic dye LD540, cellular LD levels were studied in MEFs lacking PS expression by fluorescence microscopy. Initial observations with the lipid droplet-specific dye suggested that MEFs lacking PS activity had an increased amount of lipid droplets, as opposed to the WT MEFs (Figure 11). While the differences appeared to be substantial, several characteristics of the PS knock-out cells are fundamentally different from WT cells, such as morphology and size, which makes it difficult to adequately asses the significance and relevance of the comparison between the WT and PSdKO MEFs. With this in mind, we opted to study the LD phenotype in the two MEF PSdKO rescue models, PSdKO +hPS1WT and PSdKO +hPS1DA, described in the previous section (Figure 10). PSdKO MEFS with re-expression of functional WT PS1 show partial rescue of the wild-type phenotype, with lipid droplet accumulation being dramatically reduced. In contrast,

re-expression of the inactive PSDA variant had no notable effect on lipid droplet levels, further validating the functional recovery effect of WT PS1 retransfection.

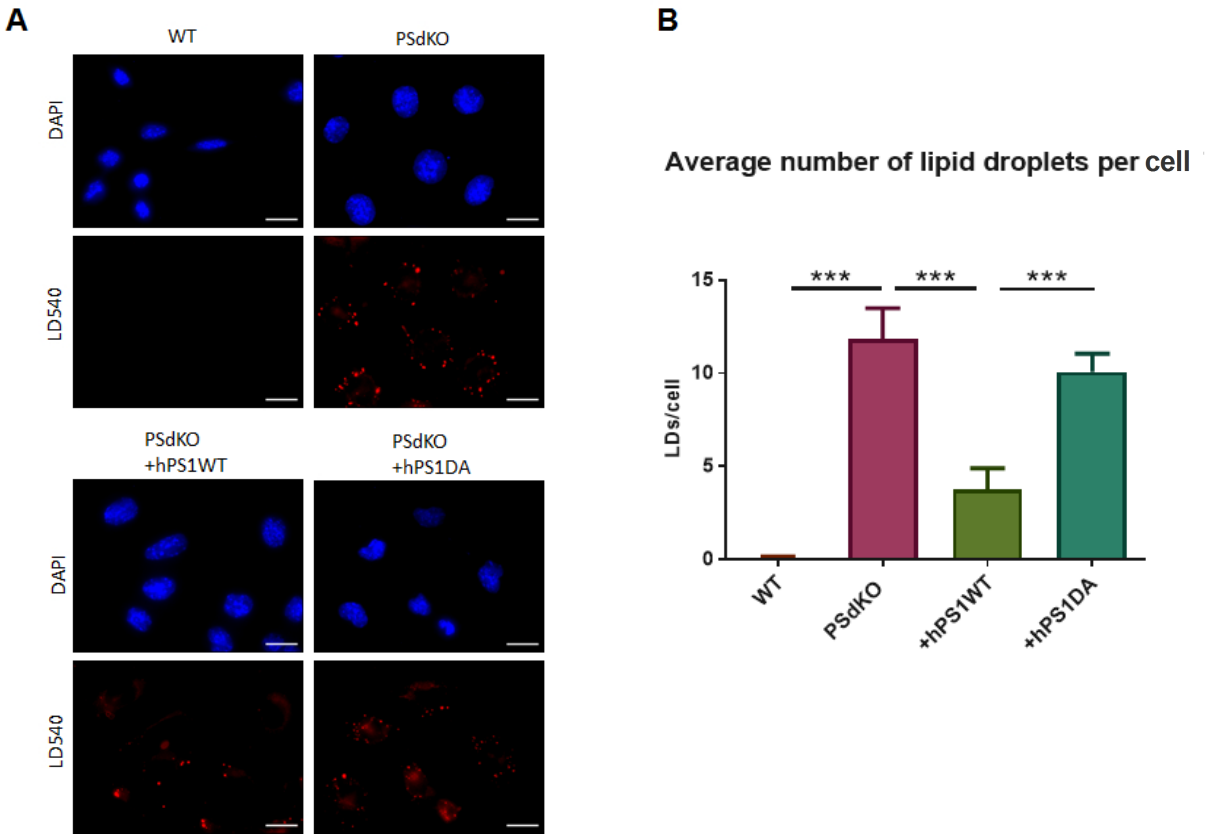

Figure 11 : Lipid droplet staining of MEFs cells with different PS expression. A) *Representative fluorescence microscopy images of MEFs stained with the LD540 dye, specific for lipid droplets, and the nuclear dye DAPI. An increase in the number of lipid droplets was observed in the models lacking functional Presenilin expression. Scalebar = 20µm* ***B)*** *Quantification of the average amount of lipid droplets per cell on the different genotypes. Data shown is average +/- SEM. N=10. Significance was analyzed by one-way Anova and Holms-Sidak multiple comparison test. Significance of compared groups shown with ***: P≤0.001.*

3.1.1.2 Cellular lipid droplet levels are increased after pharmacological inhibition of γ-secretase in different cell models

In order to further test the effect of γ-secretase activity on lipid droplet formation and accumulation, rule out cell type-specific effects, and approach more brain relevant cell models, other cell types were used for fluorescence microscopy analysis, together with pharmacological inhibition of γ-secretase activity through the use of the dipeptidic small molecule DAPT, a well-described γ-secretase inhibitor[189]. Initially, WT MEFs were assayed, in order to establish whether

the effect of purely pharmacological inhibition of γ-secretase by DAPT would lead to similar observations as those made through the previously described genetic approach (Figure 12).

Treatment with DAPT (10µM, 5 days) led to a concomitant increase in LD levels, further supporting the initial observations made by the PS knock-out approach.

In addition to MEFs, it was of interest to test if such an effect could be observed in different cell models, in particular with regards to more neurally-relevant models. The DAPT pharmacological inhibition strategy was therefore employed with two astrocyte cell models, given that these are the main cells involved in the production of neuronal cholesterol and lipids[97]. The models were

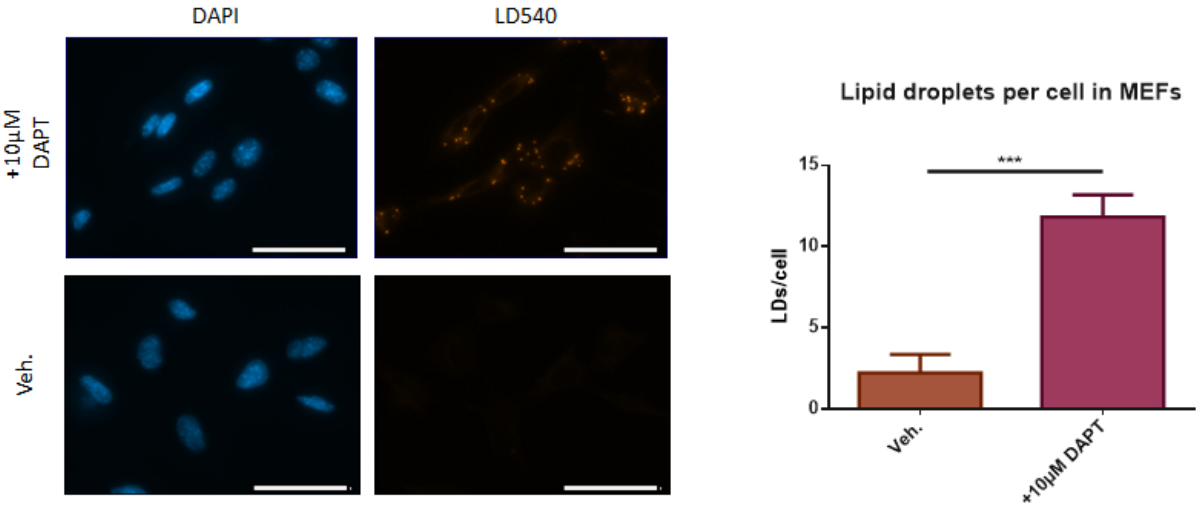

Figure 12: Lipid droplet staining of MEFs following treatment with PS inhibitor DAPT. *Representative fluorescence microscopy images of MEFs stained with the LD540 dye, specific for lipid droplets, and DAPI nuclear staining. A substantial increase in the number of lipid droplets can be observed with DAPT treatment (10µM). Scale bar = 20 µm. Quantification of the average amount of lipid droplets per cell is shown on the right. Data shown is average +/- SEM. Significance was analyzed by unpaired t-test with Welch's correction, N=6. ***: P≤0.001.*

the H4 astroglioma cell line, and primary human astrocytes. The observed phenotypes were similar to those obtained with the knock-out MEF models in both analyzed cell types, where treatment with DAPT led to a significant and substantial increase in lipid droplet content, thereby

confirming the role of the γ-secretase activity on lipid droplet accumulation (Figure 13). These observations strongly suggested that γ-secretase plays an important role in intracellular lipid metabolism, but the biochemical characteristics and the mechanism behind these observations were still under question.

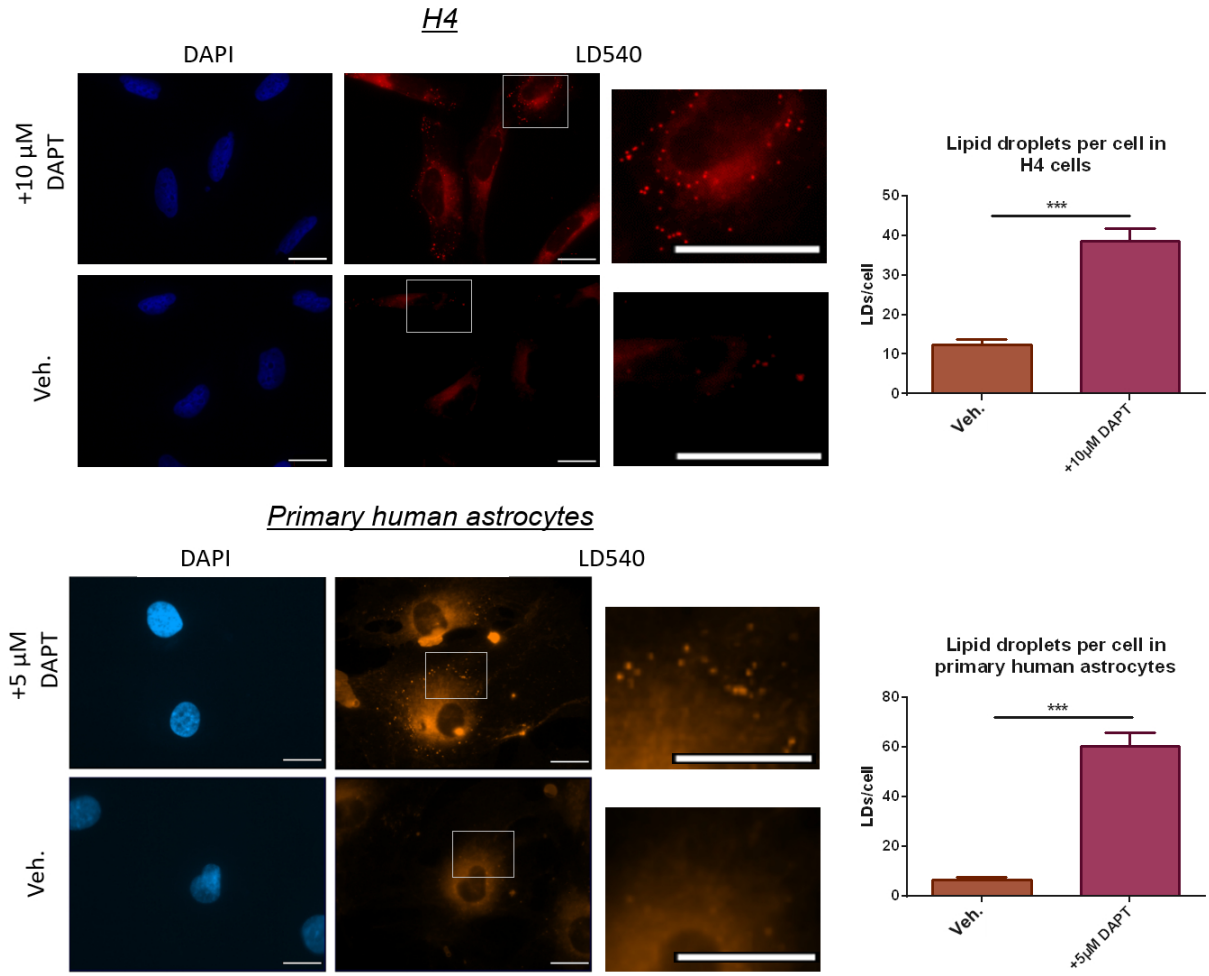

Figure 13: Lipid droplet staining of H4 cells and primary human astrocytes cells following treatment with γ-secretase inhibitor DAPT. *Representative fluorescence microscopy images of H4 astroglioma cells (above) and primary human astrocytes (below) stained with the LD540 dye, specific for lipid droplets, and DAPI nuclear stain. A substantial increase in the number of lipid droplets can be observed with DAPT treatment in both cell types. Scale bar = 20 µm. Quantification of the average amount of lipid droplets per cell for both cell types is shown below the respective microscopy images. Data shown is average +/- SEM. Significance was analyzed by unpaired t-test with Welch's correction, N=35 for H4 cells, N=11 for primary human astrocytes. ***: P≤0.001.*

3.1.2 Sterol and triglyceride levels are altered in cells lacking γ-secretase activity

Given our findings on LD levels upon loss of γ-secretase activity, we found it likely that there would be notable alterations in cellular levels of cholesterol metabolites, cholesterol esters and possibly triglycerides, as the primary role of the LD is the storage of excess lipids. Our initial findings concerning decreased sterol esterification on cells lacking functional PS were found to be discrepant with previous reports in the literature, namely those of Area-Gomez et al[190], and we therefore employed three approaches for the analysis of cholesterol metabolites and cholesterol ester levels, in order to ensure the validity of our findings. The approaches used were gas chromatography-coupled mass spectrometry (GC-MS), the Amplex red cholesterol assay, and feeding of a "click-able" alkyne-cholesterol probe, for Coumarine labeling and fluorescent detection of the labeled cholesterol.

3.1.2.1 Sterol levels and cholesterol esterification in MEFs by gas-chromatography-coupled mass spectrometry

The MEFs models described above were cultured, harvested, the different lipids extracted, and then separated by gas chromatography, followed by analysis of the isolated sterol fractions by mass spectrometry. A panel of different sterol metabolites were analyzed, namely desmosterol, lathosterol, lanosterol, cholestanol, sitosterol, sigmasterol and campesterol, as well as total cholesterol and cholesterol esterification. Of the analyzed panel, three sterols were found to be substantially and consistently different in cells lacking γ-secretase activity: Desmosterol, lathosterol, and cholesterol esters. Our observations with this method revealed that cells lacking the expression of functional Presenilin (PSdKO and PSdKO +hPS1DA) show significantly increased levels of lathosterol and desmosterol, as well as a significantly decreased esterification of cholesterol, as compared with WT and PSdKO +hPS1WT (Figure 14). The elevated levels of cholesterol precursors demosterol and lathosterol confirmed previous findings[64] reporting elevated cholesterol metabolism on cells lacking PS activity. However, our findings revealed the levels of total cholesterol to be barely different at all, only slightly lower – but not significantly so - with a lack of PS activity. It was therefore expected, given these findings and the elevated levels

of LDs, that cholesterol esterification levels would be higher in cells lacking PS activity, but, against expectations, cholesterol esterification was found to be substantially lower (Figure 14). Given the counter-intuitive nature of our findings, we opted to verify the validity of these findings with an alternative method.

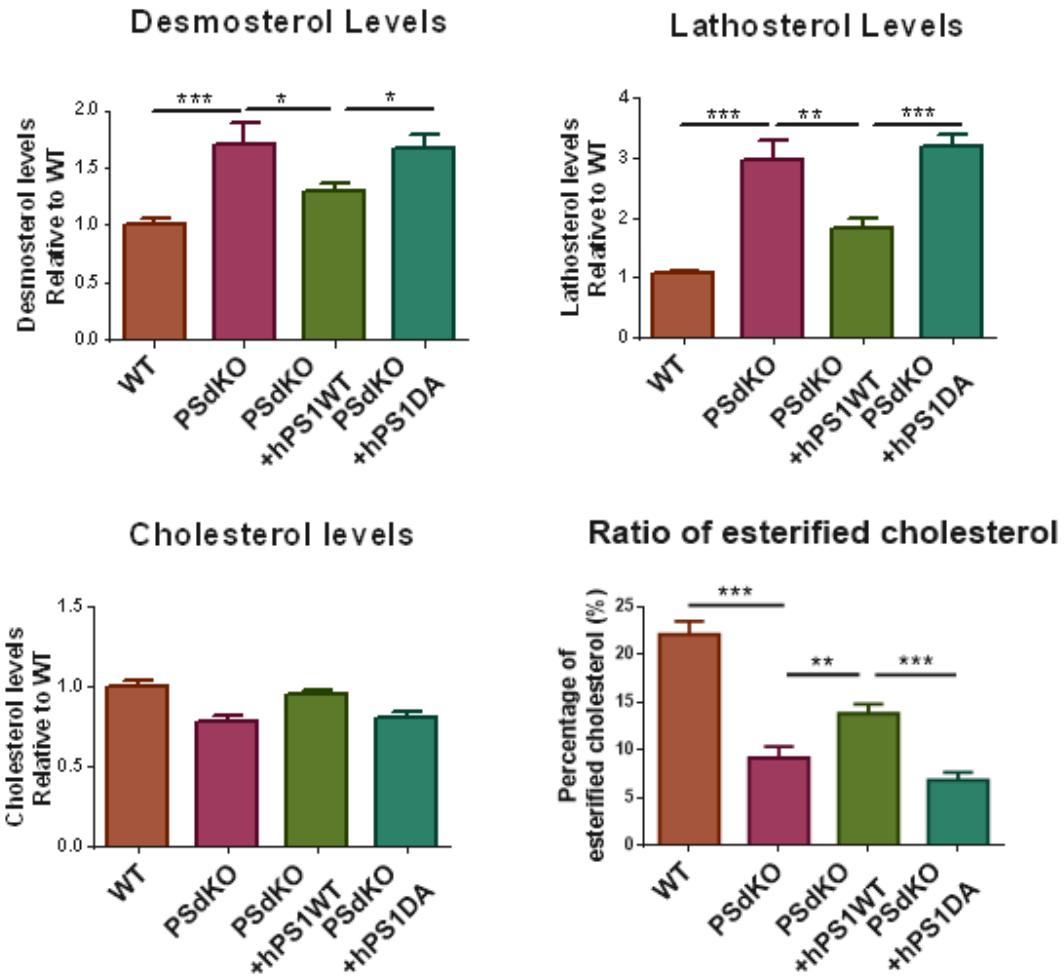

***Figure 14**: **Content analysis of a panel of sterols in MEFs with different PS expression, determined by GC-LC-MS.** Shown sterols are cholesterol precursors (lathosterol and desmosterol), as well as cholesterol and esterified cholesterol. Significantly increased levels of lathosterol and desmosterol can be observed in MEFs lacking functional PS expression, together with a significantly decreased cholesterol esterification ratio. Data shown is average +/- SEM. N=9 for lathosterol, desmosterol, and cholesterol levels, and N=7 for esterification ratio. Significance was analyzed by one-way Anova and Holms-Sidak multiple comparison test. Significance of compared groups shown with *: P≤0.05, **: P≤0.01, ***: P≤0.001.*

3.1.2.2 Sterol levels and esterification in MEFs and H4 cells by the Amplex red method

The second method used for this purpose was the Amplex red cholesterol assay, a fluorogenic assay coupling the enzymatic activity of cholesterol esterase and cholesterol oxidase, with the production of the fluorescent dye resofurin upon oxidation of the Amplex red molecule. In this

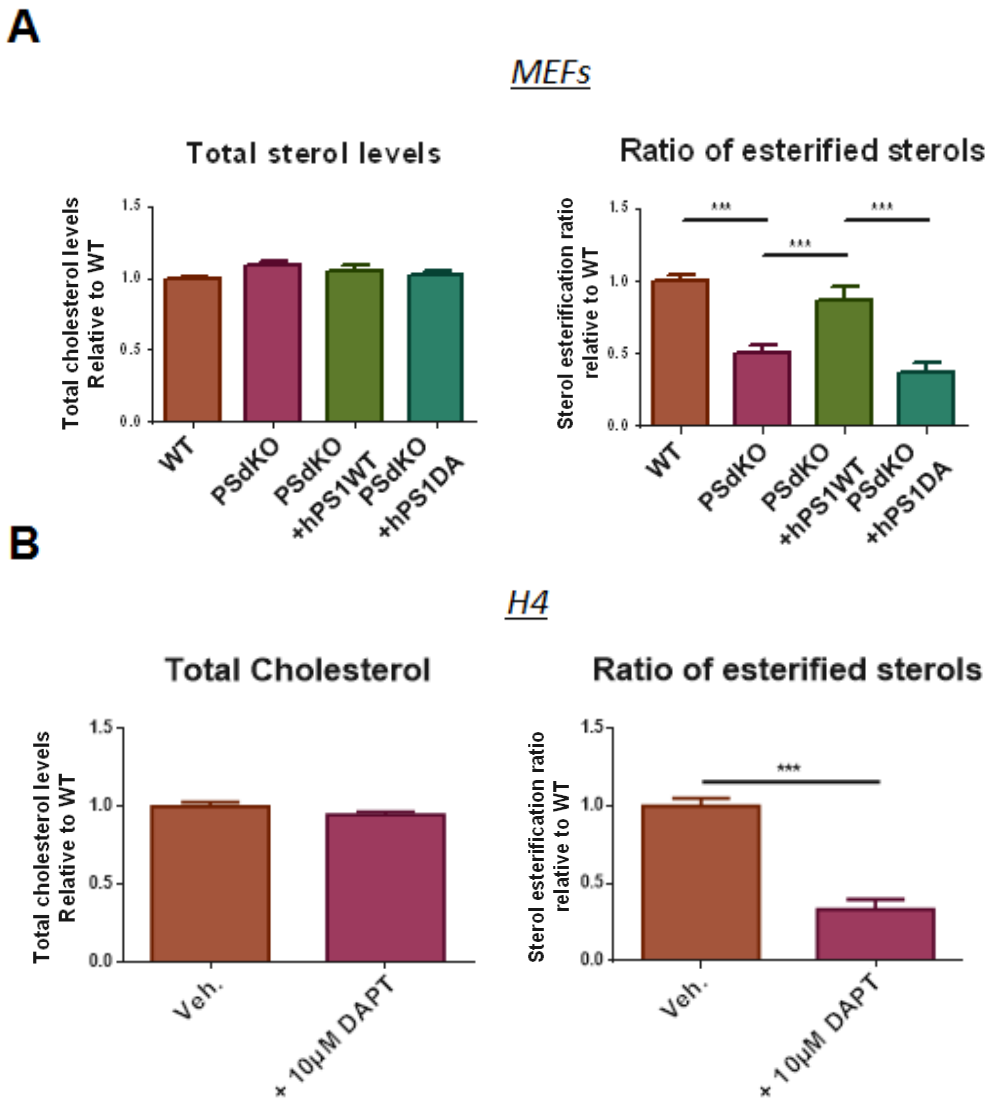

Figure 15: Sterol and sterol esterification levels of MEFs and H4 cells with different PS expression by Amplex red. *MEFs with different PS expression* ***(A)*** *and H4 cells following DAPT treatment* ***(B)****, analyzed for total cholesterol and cholesterol esterification by the Amplex red cholesterol assay. Significantly reduced levels of cholesterol esterification can be observed in cells lacking functional PS expression or activity. No significant differences can be observed on total sterol levels. Data shown is average +/- SEM. N=12 for MEFs and N=8 for H4 cells. In MEF experiments, significance was analyzed by one-way Anova and Holms-Sidak multiple comparison test. In H4 Amplex red experiments, significance was analyzed by unpaired t-test with Welch's correction. Significance of compared groups shown with ***: P≤0.001.*

assay we employed the MEF PSdKO cell model, as well as DAPT-treated H4 cells. Results acquired with this method were concurrent with those made by GC-MS (Figure 15A), with cells lacking functional PS displaying significantly lower sterol esterification levels as compared to those expressing functional PS, and no notable changes in absolute sterol levels. Results obtained with H4 cells after pharmacological inhibition of γ-secretase revealed comparable results, with DAPT inhibition (Figure 15B) leading to decreased sterol esterification and similar levels of sterols. It should be noted that a caveat of this method is that cholesterol oxidase does not fully discriminate cholesterol from other sterols[191,192], and therefore observations with this method cannot be attributed exclusively to cholesterol, but to sterols in general, and we therefore refer to sterol and sterol esterification instead of specifically mentioning cholesterol.

3.1.2.3 Cholesterol esterification in MEFs monitored by alkyne-cholesterol tracing

A third independent method was used for the analysis of cholesterol esterification on the MEF cell models, making use of a modified cholesterol carrying a clickable alkyne group on C26 (clickable cholesterol)[193]. In this assay, MEFs were cultured in medium containing clickable cholesterol for 24 hours, and cellular lipids were isolated. Following, isolated lipids were labeled with an azido-modified Coumarin compound and separated by thin-layer chromatography (TLC). Detection of labeled cholesterol derivates was carried out by fluorescence imaging. The experimental outcome was in line with the previous results and revealed significantly decreased levels of cholesterol esterification upon loss of functional PS expression on our MEF models (Figure 16). In summary, these experiments consistently showed a substantial decrease in cholesterol esterification upon loss of γ-secretase activity, which could not properly explain the observed increase in LD levels.

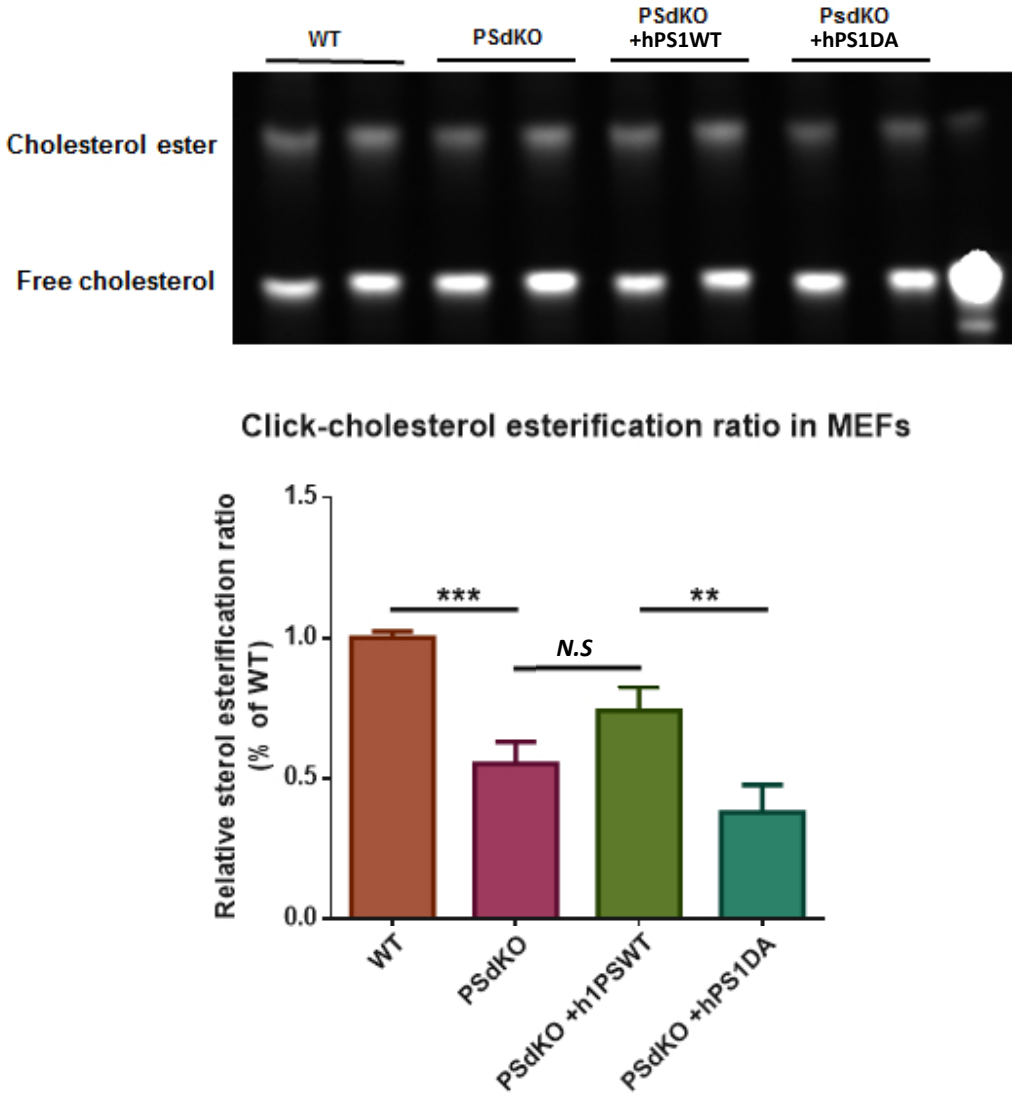

Figure 16: Analysis of sterol esterification in MEFs with different PS expression backgrounds by alkyne-cholesterol feeding and detection*. MEF cell cultures of different PS backgrounds were supplemented with alkyne cholesterol and harvested. The lipid fractions of the harvested cells were isolated, and alkyne cholesterol was labeled with Coumarine by the click-reaction. Isolated and labeled lipids were separated by thin-layer chromatography (TLC). Coumarine fluorescence imaging of separated lipid samples was performed on the TLC plate (above) and the ratio of esterified to total cholesterol quantified (below). Significantly decreased cholesterol esterification can be observed in MEFs lacking functional PS. Data shown is average +/- SEM. N=6. Significance was analyzed by one-way Anova and Holms-Sidak multiple comparison test. Significance of compared groups shown with **: P≤0.01, ***: P≤0.001, N.S: P>0.05.*

3.1.2.4 *An NPC cell model displays increased lipid droplet levels together with decreased cholesterol esterification*

These observations, taken together, revealed a simultaneous increase in LD levels and cholesterol precursors together with a decreased sterol esterification rate. As this seemed initially counterintuitive, we intended to analyze if a different model, displaying a comparably altered sterol metabolism with an entirely different background, would also show elevated LD levels together with a proportionally lower ratio of esterified cholesterol. For this purpose, we chose to study a well-known and well described disease model which canonically involves altered cholesterol metabolism, the Niemann-Pick C disease model (NPC)[194]. In this disease, a mutation in the gene of the NPC1 or NPC2 protein leads to a dramatic lysosomal accumulation of cholesterol in parallel to progressive neurodegeneration. Interestingly, the impairment of lysosomal cholesterol transport in NPC has been associated with decreased cholesterol esterification[195]. The NPC model employed was a Chinese hamster ovary cell (CHO) model lacking expression of the NPC1 protein, which displays the characteristic accumulation of cholesterol in lysosomal compartments. In order to assay the LD phenotype in these models and to verify the expected cholesterol accumulation phenotype, cells were fixed and stained in parallel with LD540 and Filipin-III (a polyene macrolide dye commonly used for cholesterol staining[196]), for analysis by

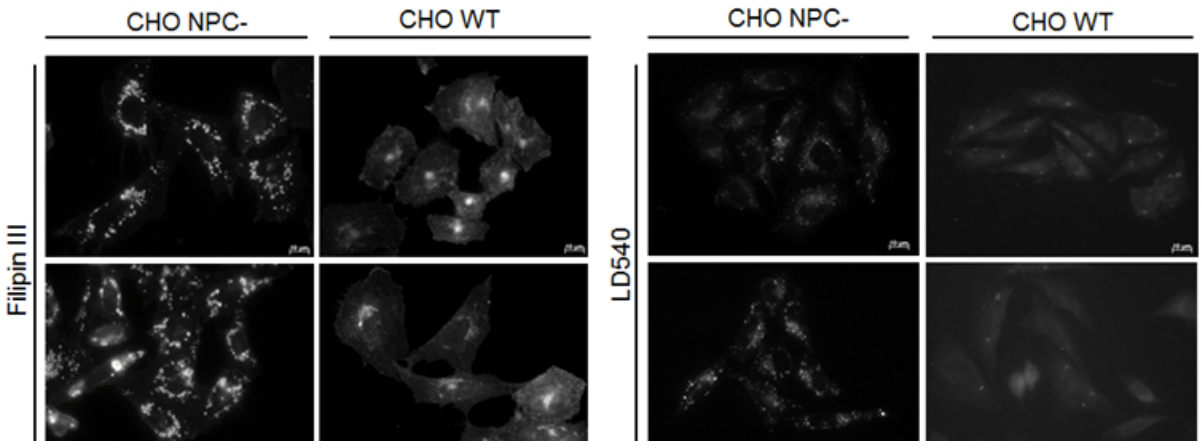

Figure 17: Cholesterol and lipid droplet staining of CHO cells with different NPC1 expression. *Representative fluorescence microscopy images of CHO wild-type (WT) and carrying an NPC1 knock-out mutation (-NPC) stained with either the Filipin III dye, targeting cholesterol-rich environments, or LD540, targeting lipid droplets. Together with a notable vesicular accumulation of cholesterol, a substantial increase in lipid droplet levels can be observed in cells lacking NPC expression.*

fluorescence microscopy (Figure 17). It should be noted, however, that double staining with both Filipin-III and LD540 could not be properly performed on the same samples successfully (likely due to an interaction between the two lipophilic dyes), and stainings were therefore done simultaneously, but in different samples of the same model. In addition to the expected lysosomal cholesterol accumulation, the CHO NPC models displayed comparably elevated levels of cellular LDs as those observed in the PSdKO models. In order to measure cholesterol esterification in the CHO NPC model, the Amplex red method was used (Figure 18). As with the MEF PSdKO model, we could observe a significant reduction in cholesterol esterification in this model.

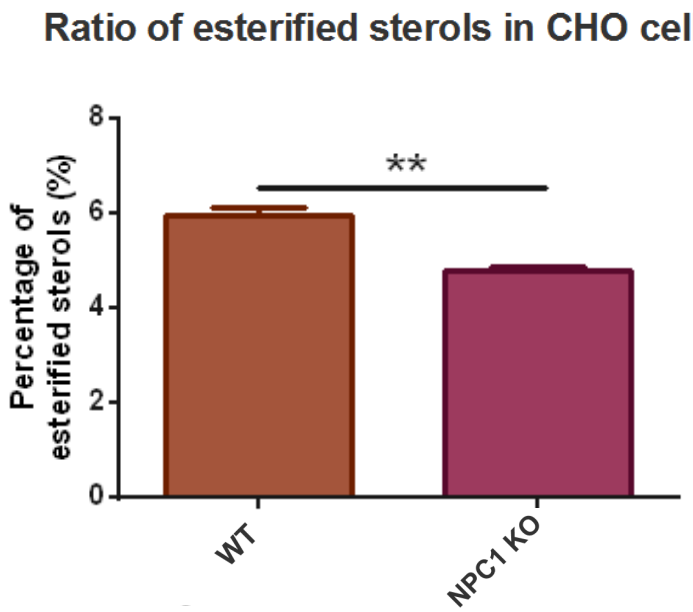

Figure 18: Sterol esterification levels of CHO WT and NPC1 KO cells by Amplex red. *CHO WT cells, and lacking NPC expression (NPC1 KO), analyzed for total cholesterol and cholesterol esterification by the Amplex red cholesterol assay. Significantly reduced levels of cholesterol esterification can be observed in cells lacking the NPC protein. Data shown is average +/- SEM. N=3. Significance was analyzed by unpaired t-test with Welch's correction. **: P≤0.01.*

3.1.2.5 Triglyceride levels are increased in cells lacking γ-secretase activity

While our observations regarding increased lipid droplet levels together with decreased sterol ester levels upon loss of γ-secretase activity may appear conflicting at first, LDs are not exclusively reserved for the storage of cholesterol ester, they are also the main storage reservoir for cellular triglycerides[167]. The next logical step was therefore to evaluate triglyceride levels in our MEF models. This was accomplished by the analysis of cell-derived triglyceride levels of cultured MEFs via a glycerol oxidation-coupled fluorogenic assay employing enzymatic hydrolysis of triglycerides by lipase, followed by fluorogenic detection of the oxidized glycerol by a fluorescent probe. Thereby, MEF cells displayed a significant increase in triglyceride levels upon loss of functional PS expression (Figure 19), which coherently explained the described increase in LD levels on these models.

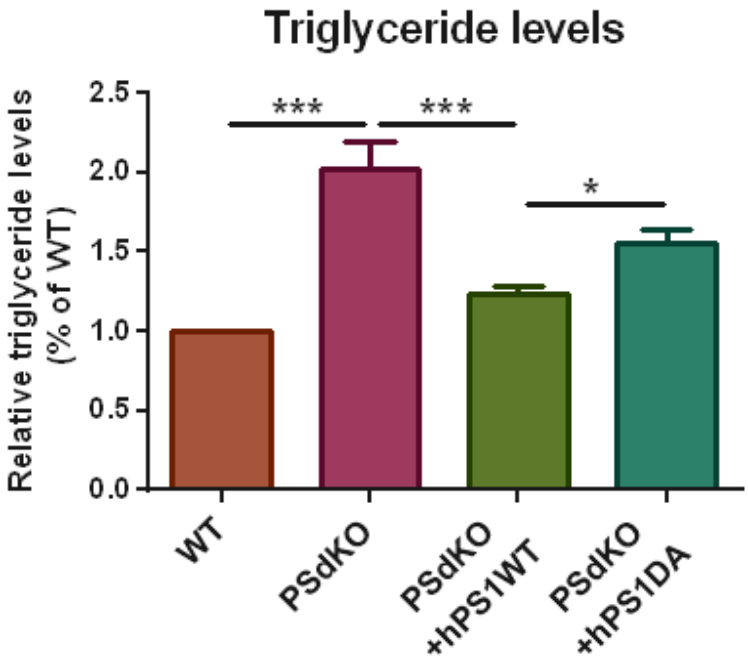

Figure 19: Total triglyceride levels in MEFs with different PS expression*. Triglyceride levels were analyzed an enzymatic assay based on lipase activity and detection of free glycerol. Significantly increased triglyceride levels can be observed in MEFs lacking functional PS expression or activity. Data shown is average +/- SEM. N=6. Significance was analyzed by one-way Anova and Holms-Sidak multiple comparison test. Significance of compared groups shown with *: P≤0.05, ***: P≤0.001.*

3.1.2.6 Elevated cholesterol secretion in cells lacking PS activity

Our observations, revealing an elevation of sterol metabolism in absence of notable intracellular accumulation of cholesterol, suggested a potentially significant role of cellular cholesterol efflux in the observed alterations of sterol metabolism by impaired γ-secretase activity. To verify if this was indeed the case, we quantified secreted levels of cholesterol in cells lacking functional PS expression, by culturing MEFs in culture media lacking foetal calf serum (FCS) for 18 hours, and analyzing the cholesterol levels in the media by GC-LC-MS. Our findings confirmed our hypothesis, with PSdKO and PSdKO +hPS1DA showing significantly elevated levels of cholesterol in the culture media, as compared to WT and PSdKO +hPS1WT MEFs respectively (Figure 20). These findings, together with the elevated triglyceride levels, could explain our finding on the effect of γ-secretase activity on sterol and LD metabolism, and suggest that the elevated cholesterol efflux could contribute to the observed decrease in intracellular cholesterol esterification.

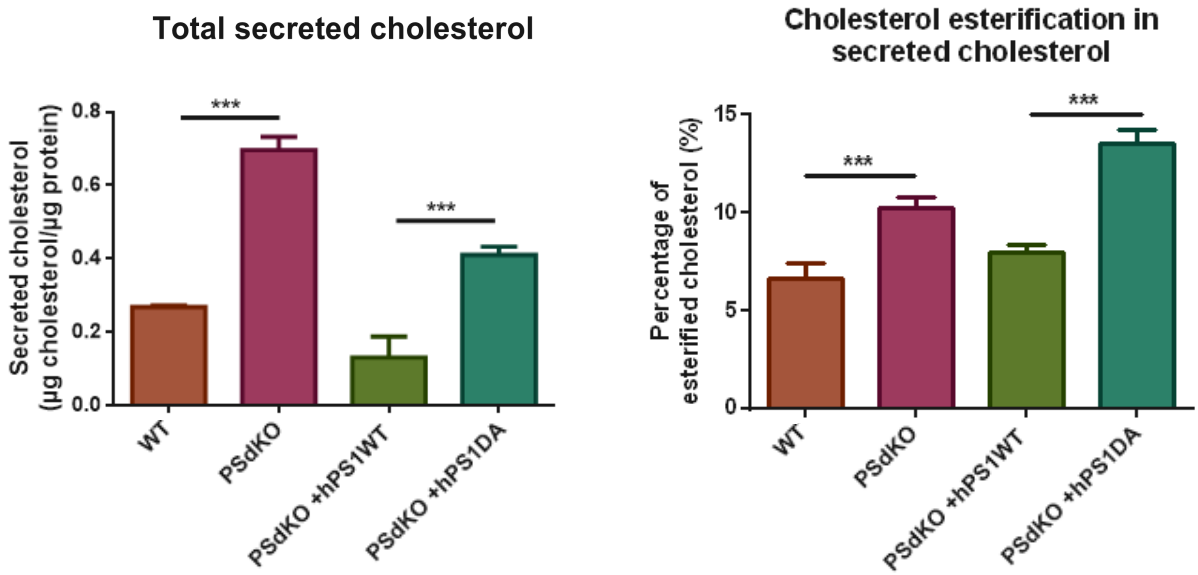

Figure 20: Secreted cholesterol levels in MEFs with different PS expression by GC-LC-MS*. Content analysis of total secreted cholesterol and cholesterol esterification in MEF culture media with different PS expression, determined by GC-LC-MS, normalized to protein concentration of the respective cell lysates. Significantly increased levels of secreted cholesterol, as well as increased esterification of secreted cholesterol, can be observed in cells lacking expression of functional PS. Data shown is average +/- SEM. N=4. Significance was analyzed by one-way Anova and Holms-Sidak multiple comparison test. Significance of compared groups shown with ***: P≤0.001.*

3.2 γ-secretase activity-dependent changes in LXR activation, and its relation to lipid metabolism

3.2.1 LXR activation in PS mutant cells

In light of our observations - revealing increased cholesterol metabolites, decreased cholesterol esterification and increased triglyceride levels on cells lacking PS activity - we were interested in uncovering a potential regulator involved in the mechanism associating PS activity with the effects described so far. The Liver-X receptor (LXR) was found to be a particularly suitable candidate. Indeed, this nuclear receptor is consistently described as a master regulator of lipid homeostasis, and its activation has been previously reported to lead to an increase in cholesterol efflux and triglyceride synthesis, both in the periphery and the brain[197,198].

3.2.1.1 Nuclear and cytoplasmic LXR levels are increased in MEFs lacking PS activity

In order to determine whether LXR might be regulated by PS activity, LXR protein levels in nuclear and cytoplasmic fractions were analyzed by Western-blotting (WB) on the MEF cell models. As LXR is a nuclear receptor, an increased nuclear translocation would be indicative of increased LXR activation. This analysis revealed substantially high levels of LXR, both in the nuclear and cytoplasmic fractions, on cells lacking functional PS activity (PSdKO and PSdKO +hPS1DA), and a partial recovery on PSdKO cells re-expressing functional human PS1 (Figure 21). It is important to note that an increased activation of LXR will lead to an upregulation of its own expression[199], and therefore to an overall increase in LXR protein levels, as is observed in PSKO cells. These observations are consistent with an increased activation of LXR upon loss of PS activity.

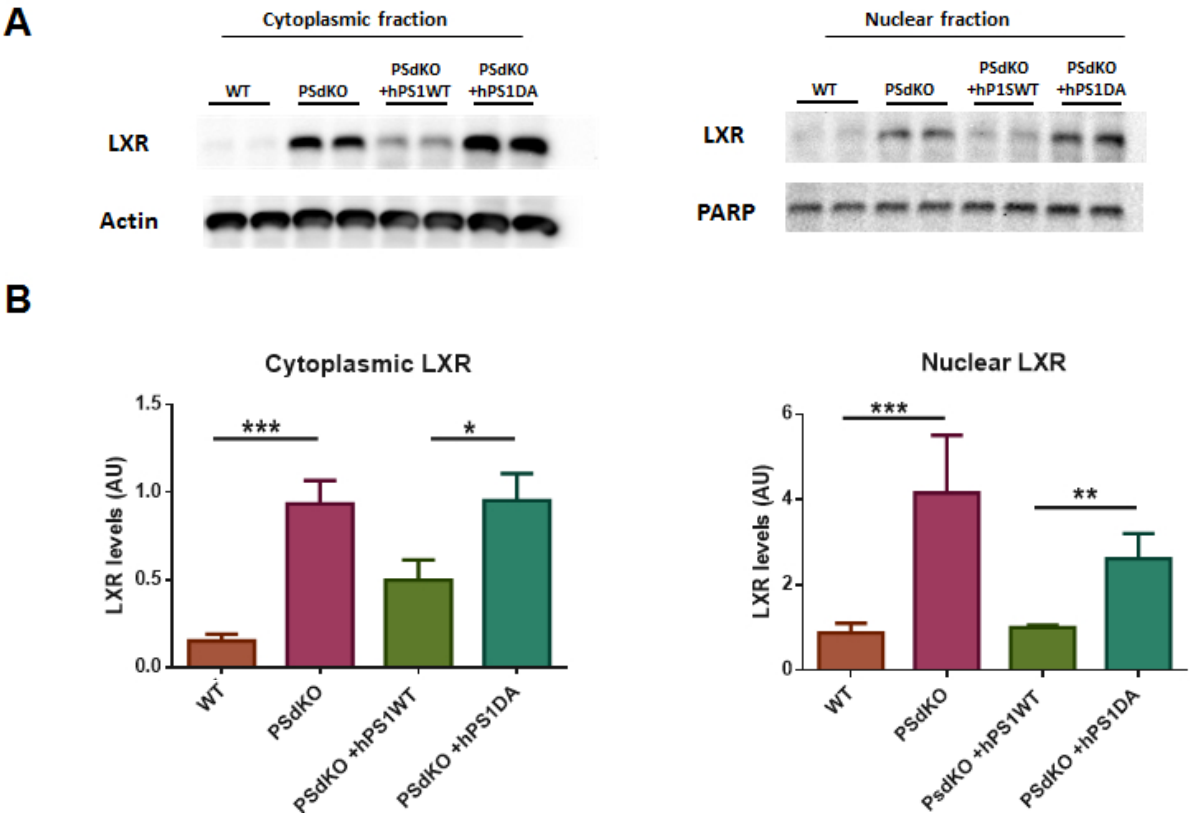

***Figure 21: Analysis of LXR activation in MEFs with different PS expression by Western-immunoblotting**. **A)** Cell fractionation and Western-blotting against LXRα/β. increased levels of LXR can be observed upon loss of γ-secretase activity, both on the nuclear and cytoplasmic fractions, which confirms an activation of LXR in backgrounds lacking functional PS. Actin and PARP are used as loading controls for the cytoplasmic and nuclear fractions respectively. **B)** Quantification of A. Data shown is average +/- SEM. N=9. Significance was analyzed by one-way Anova and Holms-Sidak multiple comparison test. Significance of compared groups shown with *: P≤0.05, **: P≤0.01, ***: P≤0.001.*

3.2.1.2 Elevated LXR gene target mRNA levels in MEFs lacking PS activity

To further evaluate the PS-dependent regulation of LXR activity, we chose to analyze transcription levels of known LXR target genes, by quantitative real-time PCR (q-rtPCR). We selected the following gene transcripts, which have functions corresponding to our previously described phenotypes: ATP-binding cassette, sub-family A, member 1 (ABCA1), known to be involved in cellular cholesterol efflux[200] ; Sterol regulatory element-binding transcription factor 1 (SREBF1), a transcription factor involved in triglyceride biosynthesis[201] ; and LXR-β itself, which, as indicated above, is transcriptionally upregulated by its own activation. For the analysis, RNA was isolated from the MEF cell models, and q-rtPCR analysis was performed. The findings from this analysis support an increased activation of LXR in cells lacking PS activity, with PSdKO and PSdKO +hPS1DA

MEFs displaying a substantial increase in transcript levels of the three studied genes (Figure 22) as compared to WT and PSdKO +hPS1WT. ABCA1 was of particular interest, with mRNA levels for this protein being consistently observed as more than 40-fold higher in cells lacking functional PS expression. Drastically altered levels of ABCA1 transcription in cells lacking functional PS expression could explain the observed increase in sterol secretion, as ABCA1 is known to play a pivotal role in cellular cholesterol efflux[200]. Our observations appeared to confirm a PS-dependent regulation of LXR activation, and it was of interest to verify if LXR activation alone would be sufficient to produce a comparable cellular phenotype as that described upon loss of functional PS.

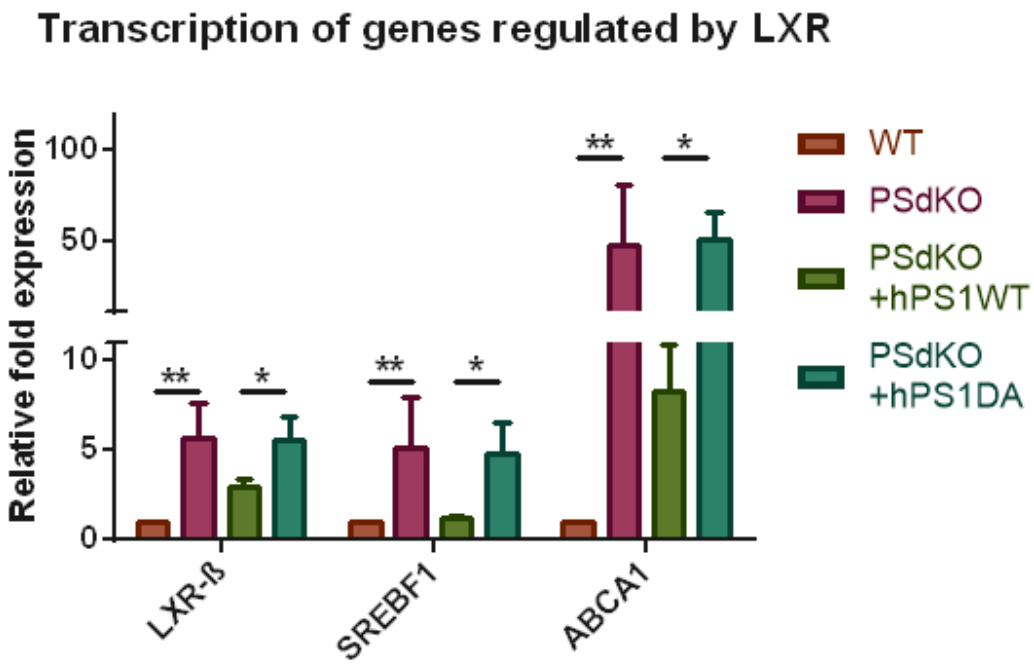

Figure 22: Analysis of LXR activation in MEFs with different PS expression by q-rtPCR of LXR gene targets*. Q-rtPCR analysis of transcript levels from LXR target genes. Higher mRNA transcript levels of AbcA1 (Lipoprotein and cholesterol efflux), SREBF1 (triglyceride synthesis), and LXR,ß detected on MEFs lacking PS activity. Data shown is Average +/- SEM. N=5. Significance was analyzed by Kruskal-Wallis non-parametric test and Dunn's multiple comparison test. Significance of compared groups shown with *: P≤0.05, **: P≤0.01.*

3.2.2 Pharmacological activation of LXR in WT cells leads to increased LD levels

To address the question of whether LXR activation alone could lead to a phenotype comparable to that observed in our PS deficient cell models, we inspected whether changes in lipid droplet levels could be observed upon treatment with GW3965, a known agonist of LXR[186], by fluorescence microscopy. Observations with H4 cells and primary human astrocytes showed significantly elevated LD levels upon treatment with GW3965 (Figure 23), suggesting that activation of LXR alone is sufficient to drive the described effects a lack of PS activity has on lipid metabolism.

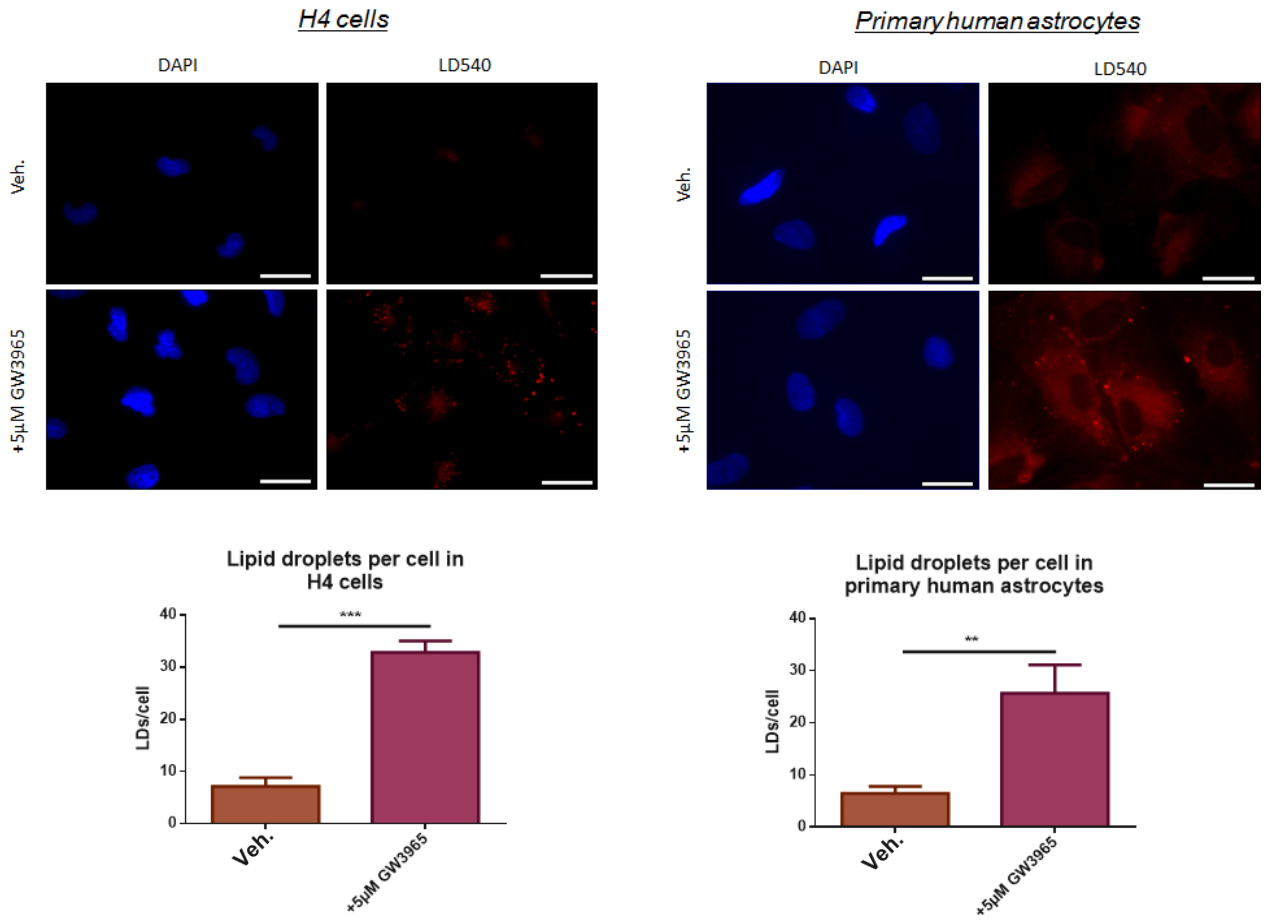

Figure 23: Lipid droplet staining of H4 cells and primary human astrocytes following treatment with LXR agonist GW3965. *Representative fluorescence microscopy images of H4 astroglioma cells and primary human astrocytes stained with the LD540 dye, specific for lipid droplets, and DAPI. A substantial increase in the number of lipid droplets can be observed with GW3965 treatment (5 µM). Scale bar = 20 µm. Quantification for the average amount of lipid droplets per cell in both cell types is shown below the respective microscopy images. Data shown is average +/- SEM. Significance was analyzed by unpaired t-test with Welch's correction, N=10 for H4 cells and N=11 for primary human astrocytes. Significance of compared groups shown with **: P≤0.01, ***: P≤0.001.*

3.2.3 Lipoprotein supplementation modulates LXR activation in MEFs

The previous findings by Tamboli et al.[64] indicated an impairment of lipoprotein endocytosis on PS-deficient cells, and implied a functional connection between reduced lipoprotein endocytosis and the reported alterations in cellular cholesterol homeostasis. LXR is known to function as cellular sterol sensor, and we therefore found it likely that the described impairment in lipoprotein endocytosis could be responsible for - or at least involved in - the observed upregulation of LXR activation. To clarify if this was the case in the PS-deficient models, the culture

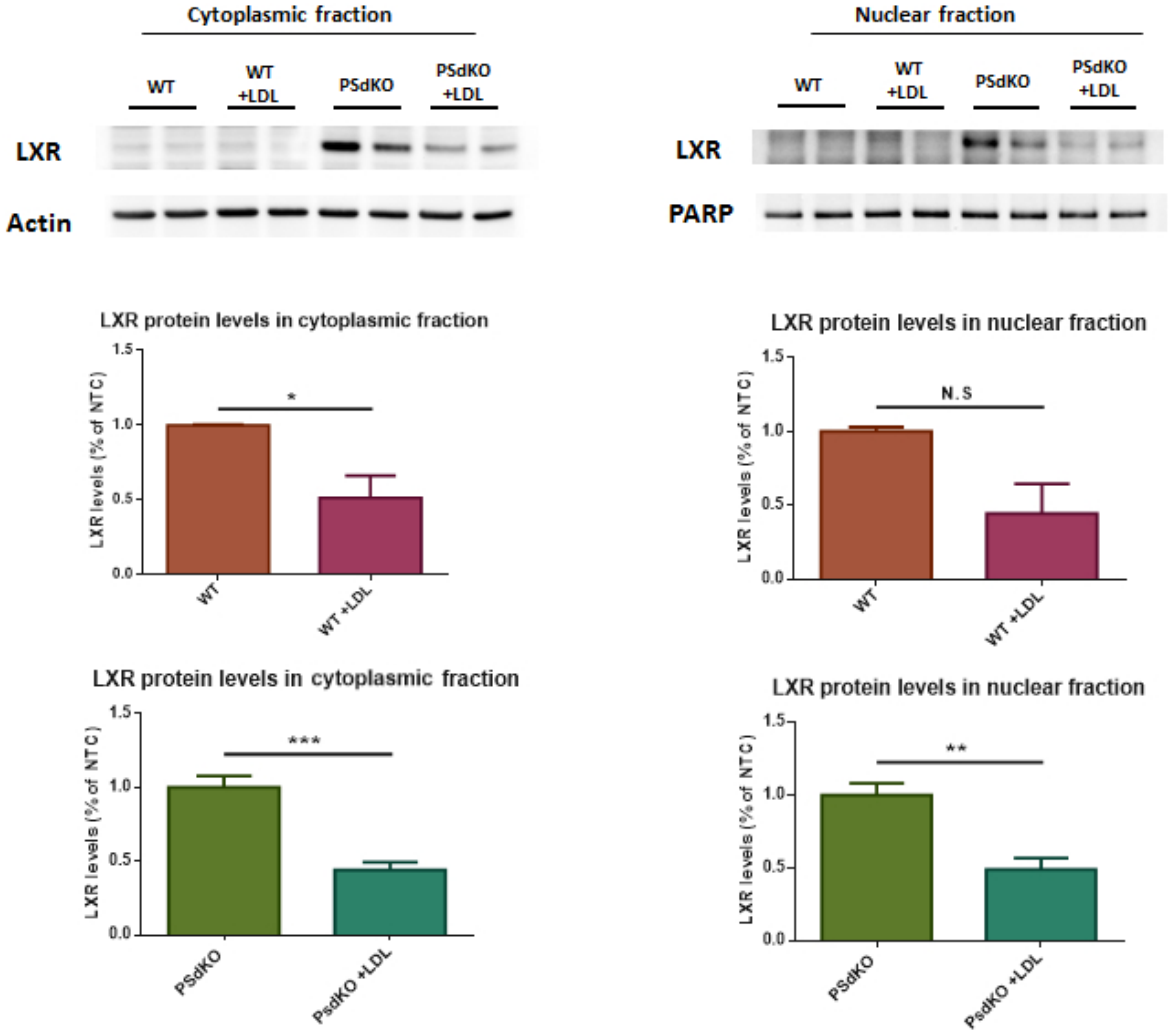

Figure 24: Analysis of the influence of LDL supplementation on LXR activation in MEFs with different PS expression by Western-blotting*. MEF culture medium was supplemented with a human LDL solution (final concentration: 10µM) or an aqueous NaCl vehicle solution for 16h, followed by harvesting and analysis. Samples were analyzed by cell fractionation and Western-blotting against LXRα/β. A partial but significant rescue of PSdKO background effect on LXR can be observed upon supplementation with LDL, both on the nuclear and cytoplasmic fractions. Actin and PARP are used as loading controls for the cytoplasmic and nuclear fractions respectively. Data shown is average +/- SEM. N=4. Significance was analyzed by the Student's t-test with Welch's correction. *: P≤0.05, **: P≤0.01, ***: P≤0.001.*

media of the MEF models was supplemented with low-density lipoprotein (10µM, 18h), the protein levels of LXR were analyzed by Western blot (Figure 24), and gene transcript levels of the aforementioned LXR gene targets was quantified by q-rtPCR (Figure 25). Both methods revealed a significant reduction in LXR protein levels and in LXR target gene transcript levels upon addition of LDL. These findings strongly support a mechanistic link between the described impairment of lipoprotein endocytosis in cells lacking functional γ-secretase and the observed increase in LXR activation on these models.

Taken together, these findings strongly suggest a critical involvement of LXR in the PS-dependent effect on cholesterol, lipid droplet and triglyceride metabolism.

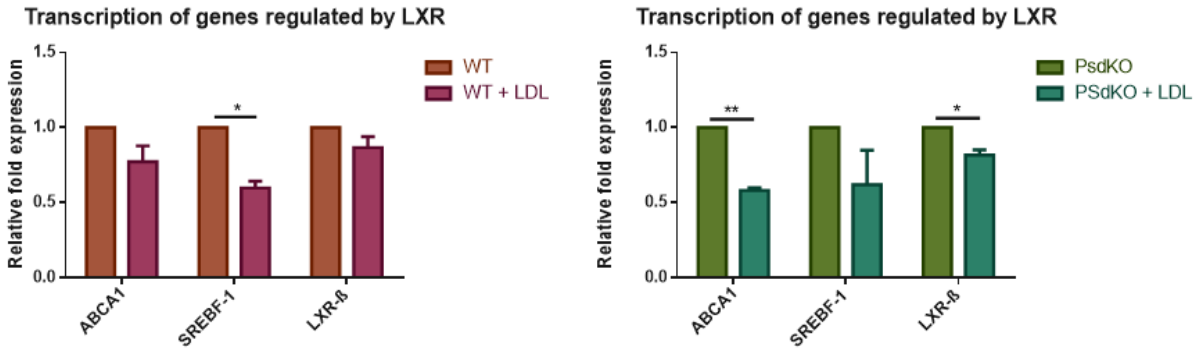

Figure 25: Analysis of the influence of LDL supplementation on LXR activation in MEFs with different PS expression by q-rtPCR. *MEF culture media was supplemented with a human LDL solution (final concentration: 10µM) or vehicle, followed by harvesting and analysis of the cell lysates by q-rtPCR. A partial but significant rescue of PSdKO background effect on LXR target genes can be observed upon supplementation with LDL, as well as a slight, non-significant effect on WT MEFs. Data shown is average +/- SEM. N=3. Significance was analyzed by unpaired t-test with Welch's correction. Significance shown as *: P≤0.05, **: P≤0.01. Non-marked pairs display P>0.05.*

3.3 Association of APP CTF C99 with cholesterol and lipid droplet levels

The amyloid precursor protein CTF C99 has been recently reported to be involved in AD pathogenesis[86,202], and has been recently described to strongly interact with cholesterol[92]. The physiological role of APP and its cleavage products remains enigmatic, and is a hotly debated topic in the AD field, but several publications have suggested APP, and in particular C99, may be involved in cellular sterol metabolism[10,203–206]. Moreover, C99 is a target of PS mediated γ-secretase cleavage, which makes C99 a promising candidate to study in relation to our observations on PS-dependent sterol and lipid homeostasis. Thus, the cholesterol-C99

interaction, and the effect of PS activity on said interaction, was investigated by using an H4 cell model carrying a GFP-tagged C99 overexpression construct (H4 C99-GFP) in fluorescence microscopy imaging.

3.3.1 The effects of γ-secretase inhibition on C99 distribution and accumulation

It has been previously reported[207] that, upon overexpression of C99, and following treatment with the γ-secretase inhibitor DAPT, the overexpressed CTFs will strongly accumulate in intracellular vesicular bodies and the cell membrane, whereas only minor perinuclear accumulation is

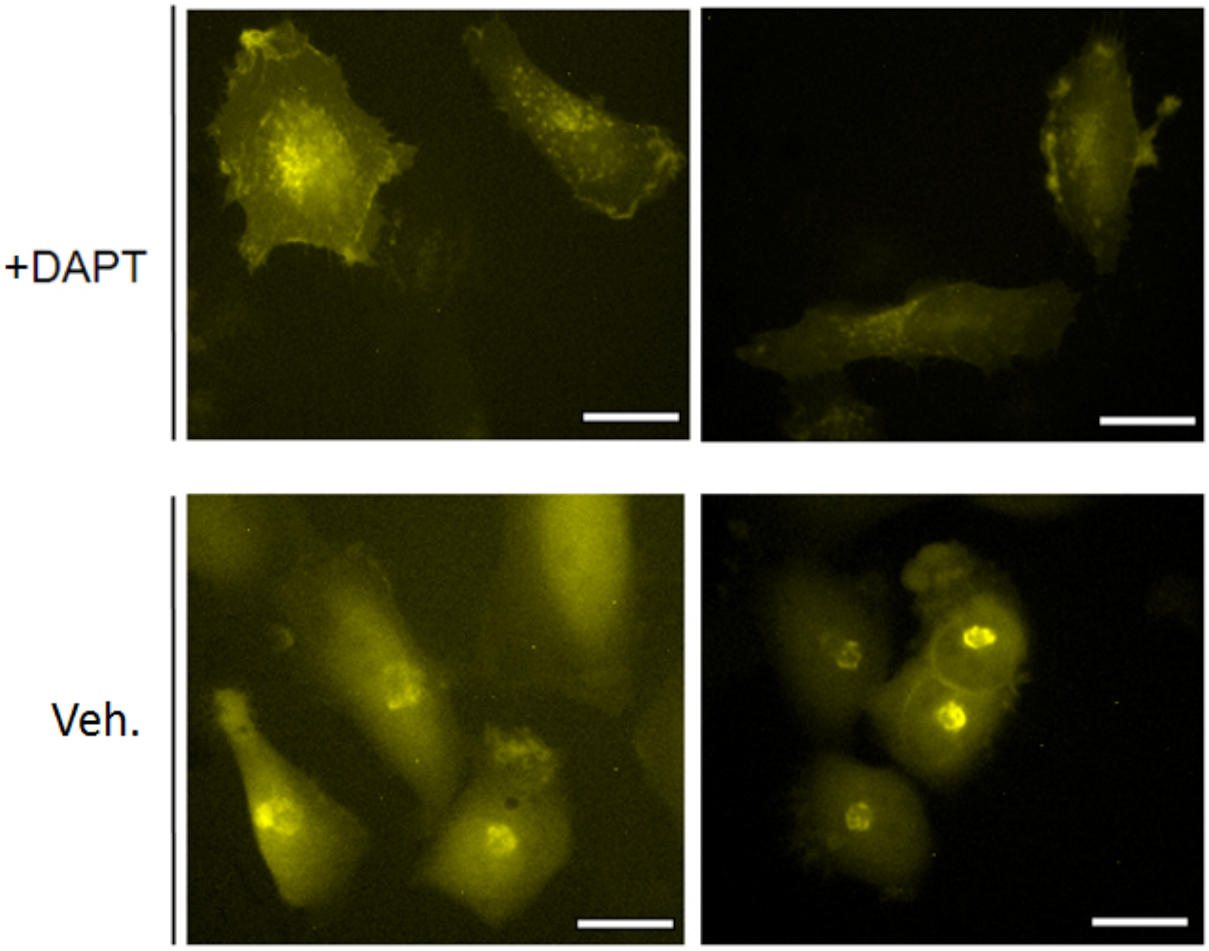

Figure 26: H4 cells expressing C99-GFP with pharmacological inhibition of γ-secretase activity. *Representative fluorescence microscopy images of C99-GFP overexpressing H4 cells with and without DAPT treatment for pharmacological inhibition of γ-secretase activity. C99-GFP can be observed to be mostly located perinuclear, Golgi-like compartments in absence of DAPT treatment, and shows no vesicular accumulation. Upon DAPT treatment, accumulated C99-GFP appears to accumulate in vesicular structures. Scale bar = 20 µm*

observed in absence of treatment by the inhibitor. With this in mind, H4 cells overexpressing GFP-tagged C99 were incubated with or without DAPT, and first analyzed by fluorescence microscopy (Figure 26). In absence of DAPT treatment, the overexpression model displayed primarily a polarized, diffuse, perinuclear localization of C99-GFP, indicative of a localization in Golgi compartments. In addition, a diffuse cytoplasmic staining could be observed, consistent with the localization of AICD-GFP upon cleavage of C99-GFP by γ-secretase. Upon DAPT treatment, however, the localization and distribution pattern of C99-GFP was notably altered, with substantial accumulation of C99-GFP in vesicular structures outside of Golgi-like compartments, as well as an accumulation on the plasma membrane. This indicates that upon inhibition of γ-secretase mediated cleavage of C99, this peptide accumulates on said vesicular structures and cell membrane domains.

3.3.2 C99-GFP and cholesterol colocalization upon γ-secretase inhibition by DAPT

In order to test for an association of C99 with cholesterol in a cellular environment, we took advantage of the properties of the polyene macrolide dye Filipin, which has been reported to bind cholesterol, and fluoresces in the UV range. The dye was used to stain fixed H4 C99-GFP after incubation of cells with or without DAPT, in order to look for colocalization patterns between cholesterol and C99 under both conditions (Figure 27). Under control conditions, C99-GFP overexpressing cells stained with Filipin showed some colocalization of C99 and cholesterol, restricted to Golgi-like structures. However, the DAPT treated cells showed a substantially higher degree of colocalization C99-GFP and Filipin. This colocalization was particularly pronounced in cytoplasmic vesicles, Golgi-like structures, and the plasma membrane. Of particular note were the C99-GFP positive intracellular vesicles formed upon DAPT treatment, which appear to be almost entirely cholesterol-rich vesicles. Similar cholesterol-rich vesicular structures could be observed in untreated cells but were C99-negative. This data suggests that the primary localization for intracellular C99 accumulation upon loss of γ-secretase is in cholesterol rich vesicles, highlighting the potential pathogenic role of the C99-cholesterol association, as it may sequester important pools of cholesterol and thereby intracellular cholesterol sensing.

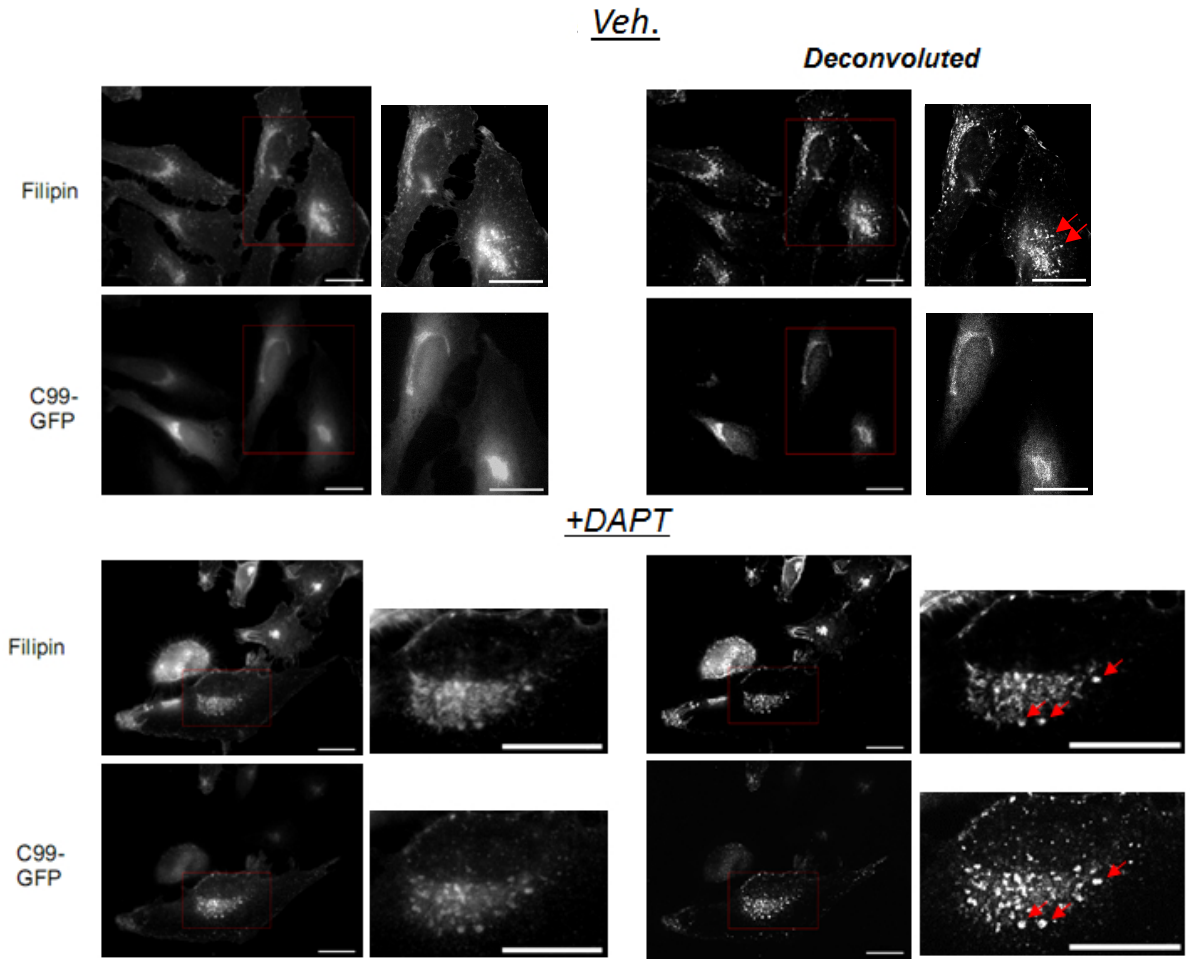

Figure 27: Free cholesterol staining of H4 cells expressing C99-GFP with pharmacological inhibition of γ-secretase activity. *Representative fluorescence microscopy images of C99-GFP overexpressing H4 cells with and without DAPT treatment for pharmacological inhibition of γ-secretase activity. Cells are stained with the cholesterol-binding dye Filipin-III. C99-GFP is observed in Golgi-like compartments in absence of DAPT treatment, with absence of vesicular accumulation. Upon DAPT treatment, the observed C99-GFP vesicular structures appear to colocalize with cholesterol-rich vesicular structures (red arrows). Scale bar = 20 µm, 40µm for Veh. magnification.*

3.3.3 Characterization of C99 localization within the Golgi compartments

A notable feature observed in the previous imaging of C99-GFP is the change in the distribution pattern of C99 upon DAPT treatment. While in the absence of treatment cells display what primarily resembles a Golgi stain, cells treated with DAPT show a distribution which partially remains peri-nuclear, although more vesicular and aggregated in nature, together with a limited plasma membrane distribution. This would suggest that either the Golgi-apparatus of DAPT treated-cells could change in its structure and distribution, or that the primary location of C99

changes following γ-secretase inhibition. In order to assess these possibilities, we employed H4 C99-GFP cells stained with antibodies targeting a protein of the *cis*-Golgi compartment (Giantin) and a protein of the *trans*-Golgi compartment (TGN46) in presence and absence of DAPT treatment, and analyzed the samples via fluorescence microscopy (Figure 28). Most C99-positive compartments were found to show colocalization with both the cis- and trans-Golgi compartments in absence of DAPT treatment. Upon DAPT treatment, however, C99 vesicular compartments appeared adjacent to Golgi compartments but not colocalizing with either *cis* or *trans*-Golgi markers, implying that the primary intracellular accumulation of C99 upon DAPT treatment is not taking place in the Golgi-compartment.

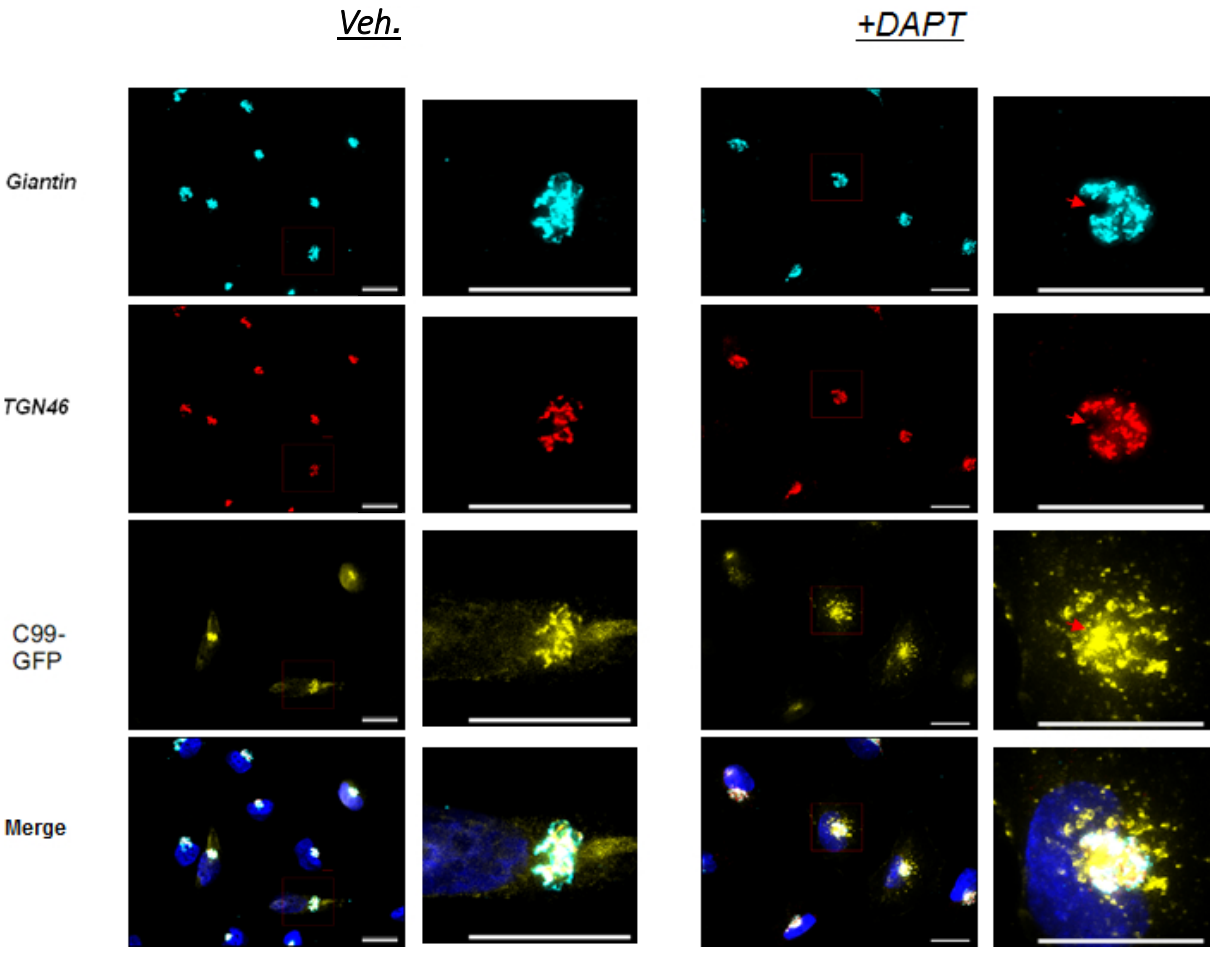

Figure 28: Cis and trans-Golgi staining of H4 cells expressing C99-GFP with and without pharmacological inhibition of γ-secretase activity. *Representative fluorescence microscopy images of C99-GFP overexpressing H4 cells with and without DAPT treatment for pharmacological inhibition of γ-secretase activity. Cells are stained with antibodies targeting the Cis-Golgi (Giantin) and the trans-Golgi (TGN-46) compartments. C99-GFP can be observed to be almost entirely colocalizing with the Golgi compartment markers in absence of DAPT treatment. Upon DAPT treatment, C99-GFP appear to lose this colocalization with cis and trans-Golgi structures, and accumulate in different compartments (red arrow). Scale bar = 20 µm.*

3.3.4 C99-GFP intracellular vesicles observed upon DAPT treatment colocalize with adaptor protein 1

To further characterize the compartments in which the C99-cholesterol interaction takes place upon DAPT treatment, we used a small panel of intracellular compartment markers for immunocytochemical analysis, including Calnexin (endoplasmic reticulum), Lamp-2 (Lysosomes), EEA-1 (early endosomes) and AP-1 (Golgi-network associated clathrin coated vesicles). Among these compartments, C99-GFP cytoplasmic compartments identified after DAPT treatment were

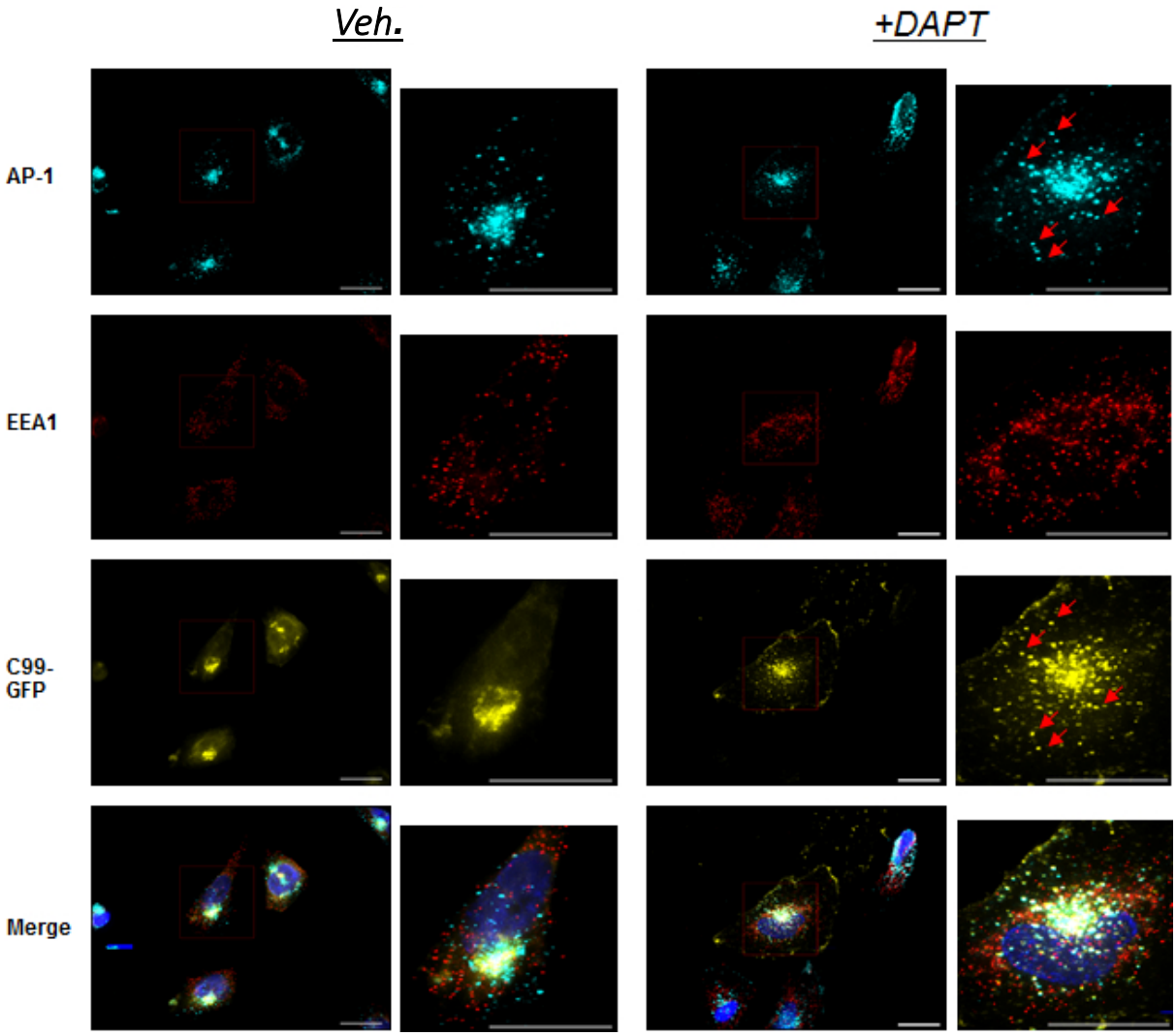

Figure 29: Early endosomes and Golgi forward trafficking vesicle staining on cells expressing C99-GFP with pharmacological inhibition of γ-secretase activity. *Representative fluorescence microscopy images of C99-GFP overexpressing H4 cells with and without DAPT treatment for pharmacological inhibition of γ-secretase activity. Cells are stained with antibodies targeting the early endosomes (EEA1) and forward trafficking vesicles from Golgi-compartments (AP1). The majority of C99-GFP-positive vesicles arising from γ-secretase inhibition display colocalization with AP1-possitive vesicles (red arrows). Scale bar = 20 µm.*

found to be primarily AP-1 positive compartments (Figure 29). AP-1 (adaptor protein 1), together with AP-2, are adaptor complexes found in clathrin coated membranes. While AP-2 is primarily found in the plasma membrane or in vesicles originating from the PM, AP-1 is predominantly found in clathrin coated membranes and vesicles derived from the trans-Golgi network[208–211]. This would indicate that, upon DAPT-mediated accumulation of C99, this CTF accumulates in cholesterol-rich, clathrin coated compartments issuing from the Golgi apparatus.

3.3.5 LD levels correlate with cellular C99 levels

In addition to studying the cholesterol-C99 association, we were interested in observing whether changes in lipid droplet levels are associated to intracellular C99 levels, both in the presence and absence of PS activity. To this aim, the cellular levels of both C99-GFP and LDs were analyzed in H4 C99-GFP cells in the presence and absence of DAPT by fluorescence microscopy. To do so, cells were individually analyzed for each condition (H4 WT ; H4 WT +DAPT ; H4 C99-GFP ; H4 C99-GFP +DAPT), with a quantification of both LDs per cell and average C99-GFP fluorescence per cell. Our findings revealed a link between C99-GFP levels and increased lipid droplet levels (Figure 30), where cells with low C99-GFP fluorescence displayed significantly and substantially reduced levels of LDs as compared to both mid and high C99-GFP levels. The effect could be observed more prevalently on cells treated with DAPT, but was also observable on vehicle-only treated cells. Additionally, the correlation between C99 levels and LD levels was analyzed by linear regression, and we could observe a significant correlation between both variables, both in presence or absence of DAPT treatment (P.value= <0.0001 ; R^2=29.65 and 27.20 respectively). These findings strongly suggest an involvement of C99 in the described lipoprotein and LXR-mediated alterations, of lipid metabolism, in cells with dysfunctional PS activity.

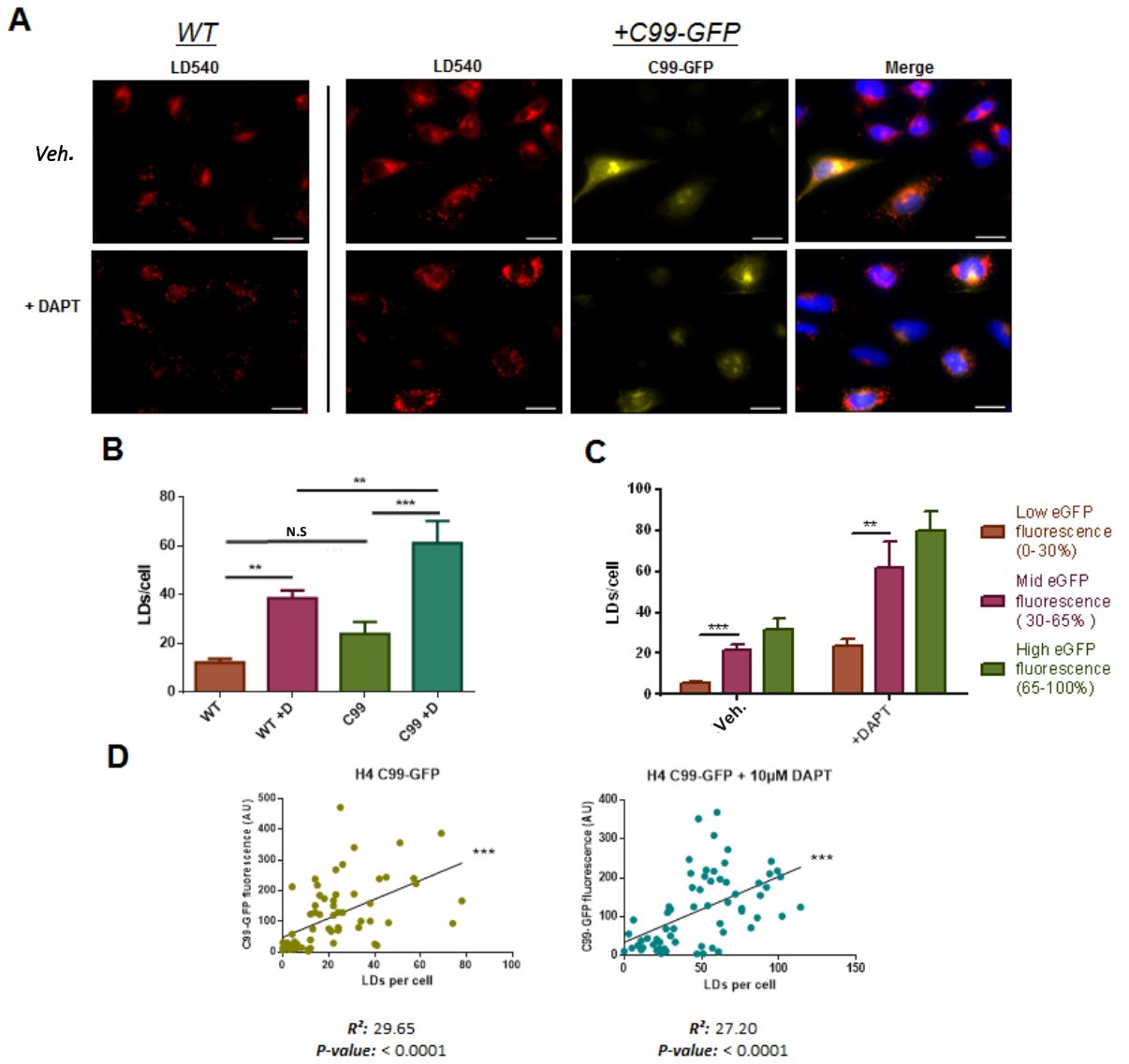

Figure 30: Lipid droplet staining of H4 C99-GFP cells with pharmacological inhibition γ-secretase activity. A) *Representative fluorescence microscopy images of WT and C99-GFP overexpressing H4 cells with and without DAPT treatment for pharmacological inhibition of γ-secretase activity. Cells are stained for lipid droplets with the LD540 dye. Higher levels of LDs can be observed in both WT and +C99-GFP cells following DAPT treatment, and C99-GFP overexpressing cells show higher lipid droplet levels than WT cells. Additionally, cells containing elevated levels of C99-GFP display a noticeably higher number of lipid droplets, both in the presence and absence of DAPT. Scalebar= 20µm.* ***B)*** *Quantification of LDs per cell in A. N =16. Significance was analyzed by one-way Anova and Holms-Sidak multiple comparison test.* ***C)*** *Quantification of lipid droplet levels as a function of cellular C99-GFP fluorescence. Cellular C99-GFP fluorescence levels were categorized in three different groups: Low (0-30% of max), Mid (30-70% of max) and High (70-100%). Higher lipid droplet levels observed in the groups with elevated C99-GFP fluorescence. N=23. Significance was analyzed by one-way Anova and Holms-Sidak multiple comparison test.* ***D)*** *Pearson linear correlation analysis of LDs and average cellular C99-GFP fluorescence in B. N=64. Significance of compared groups shown with **: P≤0.01, ***: P≤0.001, N.S: P>0.05.*

4 Discussion

The primary aim of this study was the characterization of the functional link between γ-secretase activity and lipid metabolism[64], in particular regarding cholesterol metabolism. Several biochemical and cellular factors which both supported and expanded previous observations were initially identified. In particular, we found that a lack of PS activity leads to an elevation in cellular levels of lipid droplets, triglycerides and cholesterol precursors as well as a decrease in cholesterol esterification and an increase in cholesterol secretion. Additionally, we could also show that observations which could seem conflicting at first sight - namely decreased cholesterol esterification together with increased LD levels - could also be observed in a cell model for Niemann-Pick Disease Type C [212]. This model displays comparable cellular cholesterol dysregulation, to the models lacking PS activity, with an entirely different underlying cause, thereby giving an additional level of robustness to these findings. The identified elevation of triglyceride levels in cells lacking PS activity further supported our findings on lipid droplet levels, as LDs are the primary organelle for the storage of excess cellular triglycerides.

The present data also revealed the involvement of LXR nuclear receptor activation in the observed phenotypes. We could show that, upon loss of PS activity, cells displayed increased levels of both nuclear and cytoplasmic levels of LXR protein. As a consequence, elevated transcription of LXR target genes responsible for triglyceride synthesis and cholesterol efflux could be observed, indicative of increased LXR activation. Additionally, we observed that pharmacological activation of LXR alone, by the use of LXR agonist GW3965, is sufficient to drive an increase in cellular LD levels, similar to those observed upon loss of PS activity. Furthermore, we described a link between lipoprotein availability and LXR activation in cells lacking PS activity. Specifically, PSdKO cell cultures in which the culture media was supplemented with LDL displayed significant attenuation in the activation of LXR, thereby supporting the hypothetical link between lipoprotein endocytosis, and PS-mediated LXR activation and lipid metabolism.

Finally, we studied the relation between the PS substrate APP-CTF C99 and cholesterol, and the potential role of C99 accumulation in lipid metabolism. By the use of an astroglial cell model overexpressing GFP-tagged C99, we observed a change in the cellular distribution of C99 upon

pharmacological inhibition of PS activity. Under control conditions, overexpressed C99 was primarily found in the Golgi compartment. In contrast, treatment with a PS inhibitor led to an accumulation of C99 primarily in cholesterol-rich vesicles outside of the Golgi compartment, as well as in the cell membrane. The vesicular compartments where C99 accumulated were shown to be positive for adaptor protein 1 (AP-1), a clathrin-associated protein found in forward transport vesicles of the trans-Golgi network and in recycling vesicles[211]. A positive correlation between cellular C99 levels and LD levels could additionally be observed, suggesting a functional link between C99 accumulation and lipid metabolism.

4.1 γ-secretase activity and APP processing are functionally linked to sterol metabolism

Tamboli et al. previously reported an effect of Presenilin (PS) function on sterol metabolism and lipoprotein uptake, which additionally implicated APP-CTF levels on the observed effects[64]. It was these findings which led us to further explore the effect PS deficiency has on lipid metabolism. In this article, several specific observations were described which are in line with and complement our findings. First, the article described an increase of cholesterol metabolism on cells lacking PS expression, not only through alterations in cholesterol and cholesterol metabolite levels, but also through an increase in the levels of enzymes involved in *de-novo* cholesterol synthesis, namely SREBP-2, CYP51, and HMG-CoA reductase. Both SREBP-2 and HMG-CoA reductase have been previously linked to LXR activation[213,214]. In addition, the internalization of lipoprotein receptors, and the corresponding cellular uptake of lipoproteins, was shown to be impaired on cells lacking PS activity, leading to an SREBP2-mediated upregulation of *de-novo* cholesterol synthesis. Finally, an accumulation of C99 was reported to enhance this effect, strongly suggesting that this accumulation contributes to the PS-LXR effect, and may be responsible for it. The participation of C99 was suggested to take place via C99 accumulation leading to a mistargeting of C99-binding adaptor proteins necessary for the internalization of cell surface receptors, including lipoprotein receptors. The effect of impaired lipoprotein uptake with subsequent upregulation of SREBP-2 expression is coherent with our own findings regarding lipoprotein feeding and its effects on suppressing LXR activation. Consistent with previous findings by Tamboli et al., the present study

strongly supports the hypothesis of an involvement of PS function in lipid metabolism, additionally involving APP processing and lipoprotein metabolism. Our initial findings strongly suggested that these effects were likely mediated by both LXR activation and C99 levels, and previous reports on the effects of LXR activation on lipid metabolism supported this hypothesis[171,197]. With this in mind, we propose a model (Figure 31), where the lack of PS activity initially leads to an accumulation of C99, followed by mistargeting of lipoprotein receptors. This, in turn decreases lipoprotein internalization, leading to an increase in *de-novo* lipid and cholesterol synthesis, followed by an increase in cholesterol efflux, triglyceride synthesis and lipid droplet formation, seemingly mediated by an increase in LXR activation. While understanding the precise role of this proposed mechanism and its relative contribution to AD pathogenesis - or disease progression – is something yet to be analyzed, we find it to have great explanatory potential, as both of the predominant proteins hosting FAD mutations (PS and APP), as well as the main risk factor for SAD (APOE) play a role in this mechanism. Moreover, numerous PS and APP FAD mutations have been reported to lead to impaired processing of APP by γ-secretase[59–61], thereby leading to an accumulation of C99[215]. An impairment of the functionality of any of these proteins would lead to a similar effect in our model: An LXR-mediated activation of cholesterol and triglyceride synthesis, and of cholesterol efflux (Figure 31). Together, these findings additionally suggest that one of the primary factors involved in the observed increase in lipid metabolism upon loss of PS activity is likely to be an impairment of internalization and transcytosis of cell surface proteins, including lipoprotein endocytosis. Indeed, an impairment of intracellular trafficking would properly explain both the accumulation of C99 in AP-1-positive forward transport vesicles, as well as the sequestering of cholesterol in such vesicles, leading to impaired cellular cholesterol sensing and elevated LXR activation. Such impairments in lipoprotein endocytosis and cholesterol sensing can have dire consequences for proper brain function, as the regulation of cholesterol levels and cholesterol transport is key for a wide array of essential neural processes, including axon and dendrite formation, synaptic transmission, and, ultimately, cognitive function[216–218].

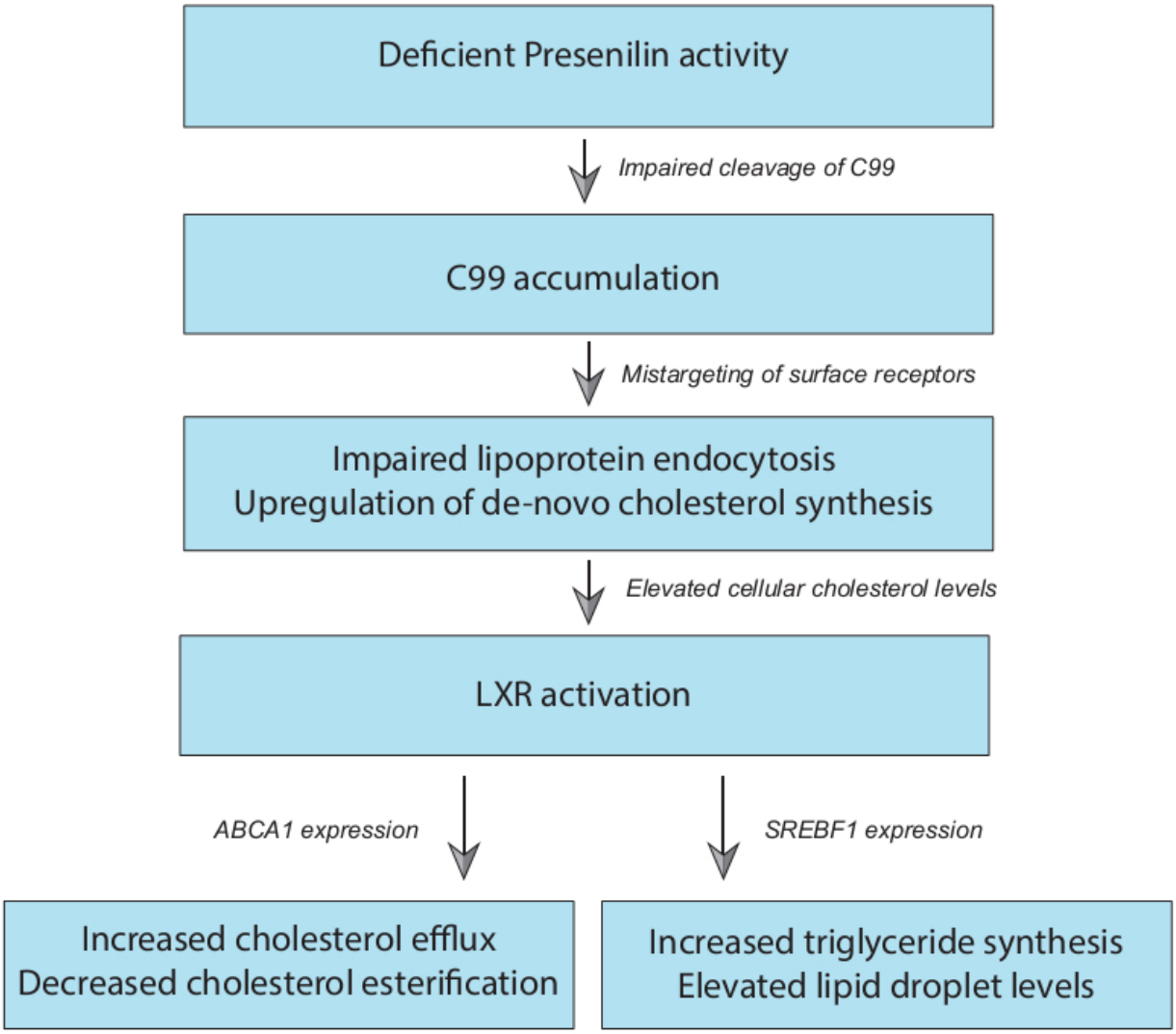

Figure 31: *Proposed mechanism functionally connecting PS activity, C99 processing and LXR activation to lipid metabolism.*

4.1.1 Participation of C99 and its processing in sterol metabolism

The peptide C99 is the APP-CTF produced by BACE cleavage, and a necessary intermediate in the production of Aβ[219,220]. C99 became of particular interest regarding the link between AD and sterol metabolism, as Barret et al. demonstrated an in-vitro interaction between this peptide and cholesterol[92]. Moreover, Kim et al. recently reported endosomal dysfunction as a consequence of C99 accumulation, which could be observed in models of both AD and Down syndrome (individuals with Down syndrome carry an extra copy of the APP gene)[221]. The suggested

involvement of C99 in AD pathology, through its effect on endosomal trafficking and sterol metabolism, is what led us to speculate that C99 accumulation may play a role on our lipid-related findings, as C99 accumulation is a direct consequence of deficient PS activity. In accord with this hypothesis, we could observe a significant increase in lipid droplet levels upon C99 overexpression, which is enhanced upon C99 accumulation caused by a pharmacological inhibition of PS. This, together with our previous findings, led us to conclude that C99 is indeed likely to play a role in the described alterations in lipid metabolism observed upon loss of PS activity.

Our findings on C99 offer a cursory glance into the potential involvement of C99 in the observed mechanism. However, a wealth of publications extensively support the proposed link between C99 and cholesterol metabolism, as partially illustrated by Beel et al.[206] (Figure 32), and provide insights into the potential mechanism by which this regulation could take place[205,206].

On the one hand, some sources have already reported a link between APP and sterol homeostasis. Neuronal overexpression of APP has been shown to lead to a reduction in HMG-CoA reductase and cholesterol 24-hydroxylase levels, both of which have notable effects on neural cholesterol turnover[222]. APP has also been reported to interact with SREBP-1 in Golgi compartments, thereby impairing SREBP-1 processing and leading to impaired transcriptional activation of its target genes[222]. Deletion of APP has additionally been shown to lead to increased expression of LRP1, an essential receptor for the endocytosis of lipoproteins and regulation of cholesterol levels in the central nervous system, and γ-secretase activity was shown to decrease LRP expression, ostensibly due to transcriptional suppression of the LRP1 gene by the AICD[223]. Furthermore, Aβ itself has been shown to promote the lipoprotein-mediated secretion of cholesterol[224], as well as to downregulate cholesterol biosynthesis[225]. On the other hand, cellular sterol metabolism has also been reported to regulate APP levels and processing, with pharmacological inhibition of *de-novo* cholesterol synthesis being shown to result in an impairment of γ-secretase processing of C99[226].

The effect of cellular sterol levels on APP metabolism has also been studied with overexpression models of ABCA and ABCG proteins, transporter proteins which mediate cellular cholesterol efflux. In these studies, overexpression of ABCA1[227] and ABCG1/4[228] lead to increased cellular

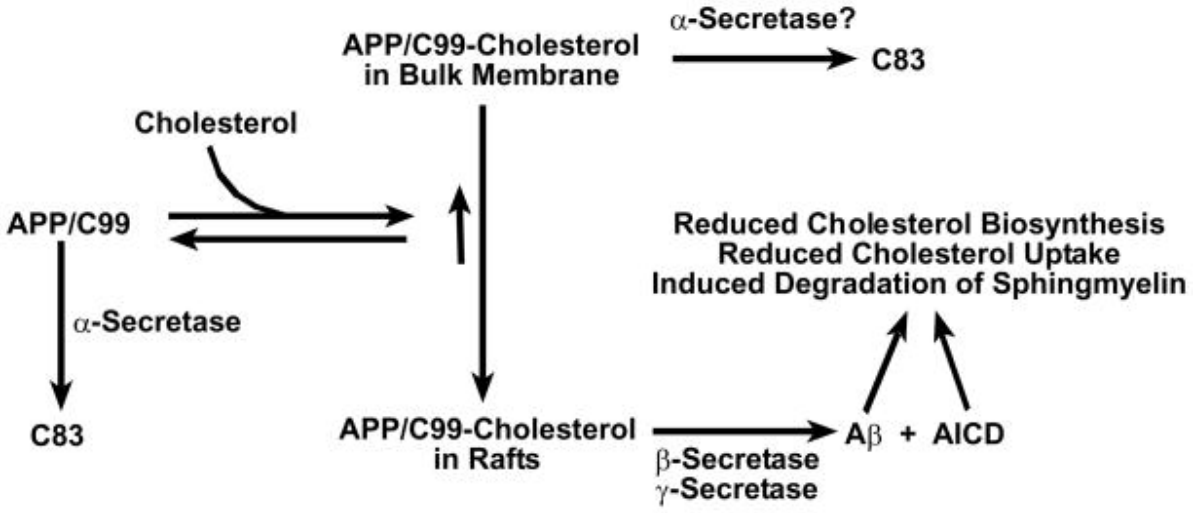

Figure 32: *Suggested role of APP processing and APP-cholesterol interaction in the regulation of cellular cholesterol metabolism, as presented by Beel et al.[206]. In the proposed model, a feedback loop can be observed, where cholesterol levels influence APP processing and vice-versa. Cholesterol binding to APP and C99 would influence its cellular distribution, and thereby dictate the processing pathway of APP and C99. Conversely, C99 processing would regulate the synthesis, uptake, and cellular availability of cholesterol.*

levels of C99 and decreased C99 processing, by an increase in α and β-secretase cleavage in parallel with decreased γ-secretase processing. Additionally, siRNA-mediated suppression of ABCG1/4 expression leads to increased Aβ secretion, concomitant with increased C99 processing by PS[228]. Findings on ABCA and ABCG proteins are relevant to our findings, as both of these cholesterol transporter classes are under transcriptional regulation by LXR[171,199,229], and ABCA1 is one of the main LXR genes reported as upregulated upon loss of PS activity in this thesis.

Interestingly, the C99-cholesterol interaction has also been reported to be modulated by the charge state of C99[230]. It was proposed that the charge-dependence of this interaction constitutes a sort of "pH switch", which spatially regulates where the interaction takes place, favoring the more acidic endosomal compartments. Moreover, the C99-cholesterol interaction has been shown to drive C99 localization to lipid-rich membrane microdomains, where γ-secretase cleavage is more prominent[206,231,232].

This reciprocal regulation of cellular cholesterol levels by APP processing, and vice versa, is highly indicative of a tightly regulated feedback mechanism. Therein, C99 accumulation and processing act as a mechanism for control of cholesterol homeostasis, with regulation of APP processing by cholesterol levels, and regulation of cholesterol synthesis and homeostasis genes by APP and its processing taking place simultaneously (Figure 32). The described literature reinforces the

hypothesis that C99 processing is central to the reported modulation of sterol metabolism by PS activity and LXR activation, although further experimental verification is necessary to validate this hypothesis.

4.1.2 The involvement of LXR

The LXR nuclear receptor is well known to play a role in cholesterol homeostasis[197], but it has been ascribed multiple other functions as well, including roles in the inflammatory response[233,234], triglyceride metabolism[171] and glucose metabolism[235]. The natural agonists of LXR are oxysterols[199], and activation of LXR is known to lead to an increase in triglyceride synthesis and cholesterol synthesis and efflux, as well as a decrease in cholesterol esterification[171,197]. This was concordant with our findings regarding triglyceride levels and cholesterol esterification and metabolism upon loss of PS activity, and led us to investigate whether LXR activation was altered in our models as well. Our study revealed that LXR protein levels, as well as transcript levels of genes activated by LXR, were significantly elevated in cells lacking PS activity, thus confirming our hypothesis that LXR activation is increased in these cell models. It should be noted, regarding our analysis of LXR protein levels, that LXR activation leads to the upregulation of its own expression[199], explaining why overall higher cytosolic levels of LXR protein can be observed in addition to increased LXR nuclear translocation. Furthermore, we could also show that pharmacologic activation of LX also leads to LD accumulation, and thereby, a similar phenotype to that of pharmacologic or genetic impairment of γ-secretase activity. The effects of LXR activation on triglyceride synthesis, as well as cholesterol synthesis, esterification and efflux are already well described[171,197]. Finally, we could observe that lipoprotein (LDL) supplementation on cells lacking PS activity significantly decreased nuclear and cytosolic LXR levels, strongly suggesting that the impaired lipoprotein endocytosis observed in these models is involved in, and may be responsible for, the elevated LXR activation. The observed effect of lipoprotein feeding in PS-defficient cells additionally implies that while lipoprotein endocytosis and sterol sensing may be impaired in such models, it is not fully blocked, and even cells lacking gamma-secretase activity can still respond to some degree, to environmental lipoprotein levels. Interestingly, LXR gene transcription has been reported to be indirectly regulated by LRP1 levels[236]. LRP1 is, as mentioned

above, an essential receptor for lipoprotein endocytosis in the brain, and has been shown to be upregulated upon deletion of the APP gene[223].

4.2 The use of astrocytic cell models for the study of sterol metabolism in the brain

This study initially focused on further developing our understanding of the previously described PS-related cholesterol and lipoprotein findings, and in identifying a general cellular mechanism involving several of the key AD players. For this purpose, mouse embryonic fibroblasts (MEFs) were found to be an appropriate initial cell model and constitutes the main body of this work. In addition to this, we elected to verify if the occurrence of the observed mechanism takes place in the context of a neural environment, and for this purpose we selected astrocytic cell models. While the majority of AD studies are preferentially done in neuronal cell models, our selection of astrocytic cell models is based on the fact that astrocytes have been recognized as the main neural cell responsible for the production and delivery of neuronal cholesterol[97]. As the blood-brain barrier (BBB) prevents dietary cholesterol from reaching the brain, neural cholesterol is generated exclusively by *de-novo* cholesterol synthesis within the brain, and around 80% of non-myelin neural cholesterol is produced by astrocytes[97]. With this in mind, we considered astrocytes to be the neural cell type where the observed mechanism was most likely to be relevant. Moreover, astrocytes play a wide variety of essential neuroprotective, metabolic, neurovascular, synaptic and structural roles in the functioning of the central nervous system[237,238]. Astrogliosis and astrocytic dysfunction have been linked to multiple neurodegenerative diseases, including AD[239,240], and the use of an astrocytic cell model can reveal key insights information which may not be accessible in neuronal cell models[241]. Nonetheless, the relevance of this mechanism in other neural cell types, namely neurons, oligodendrocytes and microglia, can be great interest and remains to be verified.

4.3 Potential relation to AD pathology

The joint participation of PS, APP-CTFs and lipoproteins in our findings would suggest that the described mechanism may play a role in AD pathology.

Several publications have already strongly suggested a link between AD pathology and sterol and lipid metabolism[10,11,106,159]. While there appears to be a primary focus on cholesterol, a link to AD pathology has been reported for a wide variety of biological lipids[106,156,159], as well as for sterol esterification[156,242] and lipid droplet levels[190]. Indeed, altering cholesterol metabolism was one of the first therapeutic approaches against AD since the identification of APOE4 as a risk factor for SAD. This was implemented by the use of HMG-CoA reductase inhibitors, collectively known as statins[243]. Their efficacy, however, is disputed, with early clinical studies showing little to no improvement on AD disease progression of patients under statin treatment[244–247], and two recent studies suggest treatment may be beneficial for AD patients[248,249]. The potential involvement of cholesterol homeostasis in AD has also been highlighted by the reported relation between ABC cholesterol transporters and AD pathology. ABCA7 gene variants which lead to impaired transporter activity have recently been reported as risk factors for the development of AD[28], and AD mice models lacking ABCA1 expression have been shown to have increased Aβ deposition and cognitive impairment[250,251]. The potential connection to our findings is noteworthy, as we see drastically elevated ABCA1 transcript levels on our PSdKO cell model. Additionally, the AD risk factor APOE4 has been linked to impaired cholesterol recycling[252,253]. While these findings reinforce the idea that sterol and lipid metabolism are key players in AD disease progression, a cellular mechanism which would link several of the main factors commonly recognized to play a role in AD, together with lipid or sterol metabolism, has yet to be comprehensively described.

A considerable number of publications have reported an effect of LXR activation on AD pathology[254]. The nuclear receptor has been reported to affect β and γ-secretase function[255,256], Aβ phagocytosis and Aβ secretion[257–259], as well as inflammatory response and cognitive performance in AD mouse models[254,260,261]. However, until now, most findings linking LXR to AD appear to be descriptive in nature, and the few proposed mechanisms linking it to AD are restricted to its role in immune response in the brain. Here, we propose a mechanism which

potentially provides a functional link between LXR, PS activity, and APP, via lipoprotein uptake impairment. Specifically, this model proposes that abnormal activation of LXR lies downstream of the impaired lipoprotein endocytosis caused by impaired γ-secretase cleavage of C99. A particularly interesting recent therapeutic development related to LXR and AD is the drug Bexarotene. This drug is an agonist of RXR, and has been reported to modulate gene expression of RXR/LXR heterodimer targets, including APOE and ABCA1[262,263]. The drug was initially developed for cancer treatment[264], but became relevant to AD when Cramer et al. reported that an AD mouse model treated with it displayed decreased amyloidogenesis and cognitive improvement[263]. Interestingly, early follow-up reports could not reproduce the effect on plaque burden, although one of them could observe an effect on cognitive improvement[265–268], and it was suggested that plaque reduction was unrelated to cognitive improvement[269]. Additionally, a single case study of Bexarotene treatment revealed that the drug substantially improved cognition in the patient without changes to Aβ deposition[270]. A link between ABCA1 and the therapeutic effect of Bexarotene in AD has also been reported. In that study, treatment of APP transgenic mice with Bexarotene lead to cognitive improvement and clearance of soluble Aβ (reported to foster the formation of small Aβ oligomers and leading to enhanced toxicity as compared to fibrillar Aβ), whereas AD models lacking ABCA1 expression did not respond favorably to the treatment[271]. These findings further highlight the potential role LXR and ABCA1 may have in AD pathology. Interestingly, the reported cognitive improvement together with an absence of plaque clearance would suggest a different pathogenic agent other than Aβ, possibly pointing to the Aβ precursor C99, as increased Aβ levels are likely to require increased cellular levels of C99.

The APP CTF C99 itself was shown to be potentially relevant in AD disease progression by Neve et al. in 1996, with mice overexpressing said CTF under a neural promoter[85,86]. This model had the surprising feature of simultaneously displaying no amyloidogenesis, together with drastic neuronal loss, indicating a potential role of the CTF in neurotoxicity, independent of amyloid toxicity. The mechanism by which neurotoxicity occurred in these models, however, remained unclear, and the absence of amyloid plaques displaced this model in most subsequent studies, in favor of models which displayed prominent amyloidogenesis[90,91,272,273]. Interestingly, FAD mutations, as well as the SAD risk factor APOE4, have been linked to an accumulation of C99. Indeed, C99 itself has recently been reported to aggregate and lead to impaired lysosomal

function in a transgenic AD mouse model[274]. A substantial number of studied FAD mutations, both in APP and PS, have been reported to have defective γ-secretase activity[58–61], which could lead to impaired C99 cleavage, and thereby to an increased rate of C99 accumulation in carriers of these mutations. Furthermore, APOE4 has been reported to lead to higher stimulation of APP expression when compared to APOE2 and APOE3[275], while non-APOE4 carriers were shown to display increased APP processing and Aβ production[276]. The described stimulation of APP expression together with reduced APP processing observed on APOE4 carriers is highly indicative of C99 accumulation. Our findings revealed that the accumulation of C99 upon γ-secretase inhibition primarily takes place in AP-1 positive, cholesterol-rich vesicles outside of the Golgi compartment. This link between C99 and AP-1 is of particular interest, as it relates to the impaired traffic and recycling of endosomes and vesicles associated to AD[260]. As highlighted above, Kim et al. have shown that C99 accumulation, in models of AD and Down syndrome, leads to Rab5 overactivation-mediated endosomal dysfunction, which manifests as an impairment of axonal transport of endosomes, altered endocytosis, and endosomal swelling[221]. In addition, human neurons which carry FAD mutations, both of PS and APP, were reported to show reduced uptake and transport of APP and lipoproteins, together with impaired recycling endosome transport, and these defects can be rescued by the use of β-secretase inhibitors, which prevent the production of C99[277]. The transport of APP has already been shown to be mediated by AP-1[278], and loss of AP-1 has been reported to impair both forward transport from the Golgi, as well as retrograde transport from recycling endosomes to the Golgi[279,280]. Furthermore, γ-secretase activity has been reported to be necessary for protein clearance from recycling endosomes, with an lack of γ-secretase activity leading to impaired transferrin clearance and APP-CTF accumulation in the endocytic recycling compartment[281]. The accumulation of C99-cholesterol in AP-1 compartments observed in our findings may lead to the dysfunction of these compartments, wherein AP-1 is essential for the sorting of cargo and endosomes originating from the TGN[282]. This dysfunction, in turn, could be responsible for the effect C99 accumulation has on vesicular trafficking and endocytosis, and thereby influence AD disease progression.

Beyond our findings, there appears to be a substantial amount of evidence implying that the proposed mechanism, linking PS activity to LXR activation and sterol metabolism, is likely to be involved in AD pathogenesis or disease progression[170,206,254,261,283]. The processing of APP and C99

by secretases, as well as the accumulation of C99, appear to play a central role, as they both influence and are influenced by sterol metabolism, are notably altered by FAD mutations and APOE4, and are associated to neurotoxicity and impaired cellular trafficking. Current therapeutic approaches against AD have focused primarily in targeting amyloidosis under the assumption of Aβ pathology as the main cause for AD[284]. Unfortunately, while clinical trials revealed that some of these therapeutic approaches have succeeded in reducing amyloidosis in AD patients[285], they have met little success in hindering AD disease progression so far[284,286]. In light of this, it is the opinion of this author that pursuing alternative leads, in this case namely the potential toxicity of C99 and the alteration of sterol and lipoprotein metabolism as principal factors in the development of AD pathogenesis, has the potential to provide a new avenue for the development of therapeutic approaches in AD.

5 Outlook

The role that Presenilins and APP processing play in AD pathogenesis remains a fundamental question to be answered, as does the functional role of APP. As shown above, the regulation of sterol metabolism, in this context, is a potentially promising area of study for answering both of these questions, and appears to provide a functional connection between AD factors involved in amyloidogenesis, and APOE4, the most prevalent genetic risk factor for SAD. The present study provides evidence of this, through a mechanism which involves PS, APP, lipoprotein function, and sterol metabolism. In addition, it emphasizes the potential role APP processing may play in sterol metabolism and cellular trafficking. Follow-up studies would be of great value to comprehensively characterize the described mechanism, and to assess its role in the etiology and disease progression of AD.

An essential next step is to further validate the participation of C99 in the proposed PS-LXR mechanism. We show a clear correlation between C99 accumulation and LD levels, and the presented literature on this topic reveals a substantial number of different links between C99 processing and sterol metabolism[92,205,206]. However, it would be of great value to assess the direct role C99 accumulation may have in our PSdKO models, regarding LXR activation and downstream effects on sterols and trigylcerides. This could be accomplished by the treatment of PSdKO cells with a β-secretase inhibitor, to verify if the treatment can rescue the observed alterations in LXR activation and lipid metabolism. An additional approach to verify this is through the use of the described C99-GFP overexpression cell models, in presence and absence of γ-secretase inhibition. Nonetheless, C99 overexpression in absence of γ-secretase inhibition may already be sufficient to saturate the effect on increased LXR activation. Due to this, the use of C99 overexpression under an inducible promoter is recommended as a more suitable approach. Additionally, it would be of interest to verify if the observed effects of C99 accumulation are unique to C99, or if these can be observed upon accumulation of other APP-CTFs such as C83 or even entirely different γ-secretase substrates, such as Notch-CTF. An interesting approach for this purpose would be the use of substrate-selective γ-secretase inhibitors, which specifically inhibit γ-secretase processing of APP CTFs without affecting Notch processing[287,288]. Assessing the effects of altered γ-secretase

processivity on LXR activation and lipid metabolism would also be of interest, specifically regarding the differential shedding of Aβ peptides following C99 γ-secretase cleavage, given how both γ-secretase inhibitors and FAD mutations have been reported to alter this processivity[287], leading to an increased ratio of Aβ42/Aβ40. γ-secretase modulators are ideal tools for this purpose, as they can alter the processivity of γ-secretase without affecting its activity, leading to altered Aβ42/Aβ40 ratios without noticeable changes to the levels of C99 or total Aβ[287].

Furthermore, it would be interesting to identify additional components which may participate in the described PS-LXR mechanism. While we have shown a substantially elevated transcription of ABCA1 in cells lacking PS activity, other ABC cholesterol transporters are interesting candidates for study in this context. ABCA7 is of particular interest, as certain allele variants have been reported to be risk factors for SAD[28]. With such drastic changes in ABCA1 transcription as observed, it would also be of interest to study the cellular distribution and functionality of ABC cholesterol transporters upon PS inhibition in our models.

Further assessing the direct role that cellular cholesterol levels have on the lipid dysregulation and the accumulation of C99 in AP-1 positive vesicles, described upon impaired γ-secretase activity, is also of interest. Analyzing this could be accomplished by altering the cellular cholesterol levels directly, through cholesterol feeding and depletion with β-methyl cyclodextrane[289], and test its impact on LXR activation, and C99 processing, in cells lacking PS activity. A similar cholesterol feeding and depletion approach could also be used on FAD mouse and neural cell models, which may yield important information regarding the connection between impairments in cholesterol homeostasis and AD-related neurodegeneration or cognitive decline.

An intriguing question arising from the work by Tamboli et al. is the mechanism by which C99 accumulation could lead to the mistargeting of surface receptors[64]. Studying the function and composition of the C99-cholesterol-AP-1 compartments, reported in the present study to accumulate upon loss of γ-secretase activity, is a promising approach to answer this question. Initially, it would be of interest to determine whether the accumulated vesicular structures are recycling endosomes or forward transport vesicles. For this purpose, the colocalization with recycling endosome marker RAB11 could be analyzed[290,291]. RAB11 is of particular interest, as it has been shown to colocalize with some AP-1 positive compartments[292], neurons carrying an FAD

PS mutation display impaired trafficking of RAB11 vesicles[277], and knockdown of RAB11 has been shown to lead to impaired transcytosis of APP and LDL[277]. Studying the presence of additional cargo proteins in these vesicles could also yield valuable information. Oxysterol-binding protein (OSBP1), for instance, is a Golgi-resident protein which binds one of the main agonist of LXR (25-hydroxycholesterol)[293], has been reported to modulate APP processing and transport[294], and could functionally link the accumulation of these vesicles to LXR activation. The presence of PS1 and PS2 in these compartments is similarly relevant, as the transport of γ-secretase complexes containing either PS1 or PS2, as well as their cellular localization, has been reported to differ from one another (with PS2 being restricted to endosomal and lysosomal compartments), and AP-1 is reported to play a role in this segregation[274,295]. In addition, PS has been shown to have an important role in protein clearance from recycling endosomes[281]. APOE and LRP1, as well, are interesting candidates as components of these vesicles, as they relate to both sterol homeostasis and AD. Furthermore, a central question regarding the described AP1-cholesterol-C99 vesicles is whether their trafficking is impaired upon γ-secretase inhibition. Live-cell microscopy would be suitable for this purpose, and a specially interesting approach, which could address this question and the previous one, would be the use of fluorolabeled LDL (Dil-LDL[296]). This approach could be used with both PSdKO cells and cells overexpressing C99-GFP, allowing us to study the effect of PS activity on LDL internalization, trafficking and degradation, as well as the presence or accumulation of LDL in AP1-cholesterol-C99 vesicles. The proposed experiments could yield valuable information to assess the role of this vesicular accumulation in both AD and sterol metabolism.

Finally, the use of FAD mutant models in place of knock-out or catalytically inactive PS models, as well as verifying the effect of the different APOE variants would yield valuable information on the relevance of our findings for AD. As previously noted, the pursuit of alternate therapeutic approaches against AD is likely to be of great value to the field[284,286], and some preliminary studies on LXR and RXR agonists have already proven successful in alleviating the biochemical and cognitive symptoms of AD in mouse models[263,297]. The characterization of the proposed LXR-C99-cholesterol mechanism in the frame of AD may lead to the identification of crucial drivers of AD pathogenesis to be used as therapeutic targets, and could ultimately lead to the development of

novel therapeutic and diagnostic approaches for AD, based on the targeting of LXR activation, APP-CTF accumulation, γ-secretase function, and altered sterol metabolism.

6 Bibliography

1. NIH Categorical Spending -NIH Research Portfolio Online Reporting Tools (RePORT). Available at: https://report.nih.gov/categorical_spending.aspx. (Accessed: 2nd June 2016)
2. Alzheimer's Association. 2015 Alzheimer's disease facts and figures. *Alzheimer's Dement. J. Alzheimer's Assoc.* **11,** 332–384 (2015).
3. Huang, Y. & Mucke, L. Alzheimer Mechanisms and Therapeutic Strategies. *Cell* **148,** 1204–1222 (2012).
4. Kumar, A., Singh, A. & Ekavali. A review on Alzheimer's disease pathophysiology and its management: an update. *Pharmacol. Rep.* **67,** 195–203 (2015).
5. Hardy, J. A Hundred Years of Alzheimer's Disease Research. *Neuron* **52,** 3–13 (2006).
6. Wolfe, M. S. *et al.* Two transmembrane aspartates in Presenilin-1 required for Presenilin endoproteolysis and γ-secretase activity. *Nature* **398,** 513–517 (1999).
7. Bekris, L. M., Yu, C.-E., Bird, T. D. & Tsuang, D. W. Genetics of Alzheimer disease. *J. Geriatr. Psychiatry Neurol.* **23,** 213–227 (2010).
8. Zhang, S., Zhang, M., Cai, F. & Song, W. Biological function of Presenilin and its role in AD pathogenesis. *Transl. Neurodegener.* **2,** 15 (2013).
9. Roses, A. D. On the discovery of the genetic association of Apolipoprotein E genotypes and common late-onset Alzheimer disease. *J. Alzheimer's Dis.* **9,** 361–366 (2006).
10. Walter, J. γ-Secretase, Apolipoprotein E and Cellular Cholesterol Metabolism. *Curr. Alzheimer Res.* **9,** 189–199 (2012).
11. Di Paolo, G. & Kim, T.-W. Linking lipids to Alzheimer's disease: cholesterol and beyond. *Nat. Rev. Neurosci.* **12,** 284–296 (2011).

12. O'Brien, R. J. & Wong, P. C. Amyloid precursor protein processing and Alzheimer's disease. *Annu. Rev. Neurosci.* **34,** 185–204 (2011).
13. Dawkins, E. & Small, D. H. Insights into the physiological function of the β-amyloid precursor protein: beyond Alzheimer's disease. *J. Neurochem.* **129,** 756–769 (2014).
14. Kaether, C., Haass, C. & Steiner, H. Assembly, trafficking and function of gamma-secretase. *Neurodegener. Dis.* **3,** 275–283 (2006).
15. Dementia Fact sheet N°362. *World Health Organ.*
16. Bonin-Guillaume, S., Zekry, D., Giacobini, E., Gold, G. & Michel, J.-P. [The economical impact of dementia]. *Presse Médicale Paris Fr. 1983* **34,** 35–41 (2005).
17. Meek, P. D., McKeithan, K. & Schumock, G. T. Economic considerations in Alzheimer's disease. *Pharmacotherapy* **18,** 68–73; discussion 79-82 (1998).
18. Alonso, A., Zaidi, T., Novak, M., Grundke-Iqbal, I. & Iqbal, K. Hyperphosphorylation induces self-assembly of tau into tangles of paired helical filaments/straight filaments. *Proc. Natl. Acad. Sci. U. S. A.* **98,** 6923–6928 (2001).
19. Braak, H., Braak, E. & Strothjohann, M. Abnormally phosphorylated tau protein related to the formation of neurofibrillary tangles and neuropil threads in the cerebral cortex of sheep and goat. *Neurosci. Lett.* **171,** 1–4 (1994).
20. Blacker, D. *et al.* Reliability and validity of NINCDS-ADRDA criteria for Alzheimer's disease. The National Institute of Mental Health Genetics Initiative. *Arch. Neurol.* **51,** 1198–1204 (1994).
21. McKhann, G. *et al.* Clinical diagnosis of Alzheimer's disease: report of the NINCDS-ADRDA Work Group under the auspices of Department of Health and Human Services Task Force on Alzheimer's Disease. *Neurology* **34,** 939–944 (1984).

22. Silbert, L. C. Does statin use decrease the amount of Alzheimer disease pathology in the brain? *Neurology* **69,** E8–E11 (2007).
23. Nixon, R. A. Autophagy, amyloidogenesis and Alzheimer disease. *J. Cell Sci.* **120,** 4081–4091 (2007).
24. Michaelson, D. M. APOE ε4: The most prevalent yet understudied risk factor for Alzheimer's disease. *Alzheimer's Dement. J. Alzheimer's Assoc.* **10,** 861–868 (2014).
25. Benjamin, R. *et al.* Protective effect of apoE epsilon 2 in Alzheimer's disease. *Lancet Lond. Engl.* **344,** 473 (1994).
26. Corder, E. H. *et al.* Protective effect of apolipoprotein E type 2 allele for late onset Alzheimer disease. *Nat. Genet.* **7,** 180–184 (1994).
27. Jones, L. *et al.* Genetic Evidence Implicates the Immune System and Cholesterol Metabolism in the Aetiology of Alzheimer's Disease. *PLOS ONE* **5,** e13950 (2010).
28. Steinberg, S. *et al.* Loss-of-function variants in ABCA7 confer risk of Alzheimer's disease. *Nat. Genet.* **47,** 445–447 (2015).
29. Harold, D. *et al.* Genome-wide association study identifies variants at CLU and PICALM associated with Alzheimer's disease. *Nat. Genet.* **41,** 1088–1093 (2009).
30. Lambert, J.-C. *et al.* Genome-wide association study identifies variants at CLU and CR1 associated with Alzheimer's disease. *Nat. Genet.* **41,** 1094–1099 (2009).
31. Atagi, Y. *et al.* Apolipoprotein E Is a Ligand for Triggering Receptor Expressed on Myeloid Cells 2 (TREM2). *J. Biol. Chem.* **290,** 26043–26050 (2015).
32. Bailey, C. C., DeVaux, L. B. & Farzan, M. The Triggering Receptor Expressed on Myeloid Cells 2 Binds Apolipoprotein E. *J. Biol. Chem.* **290,** 26033–26042 (2015).

33. Van Broeckhoven, C. *et al.* Amyloid beta protein precursor gene and hereditary cerebral hemorrhage with amyloidosis (Dutch). *Science* **248,** 1120–1122 (1990).
34. Levy, E. *et al.* Mutation of the Alzheimer's disease amyloid gene in hereditary cerebral hemorrhage, Dutch type. *Science* **248,** 1124–1126 (1990).
35. Goate, A. & Hardy, J. Twenty years of Alzheimer's disease-causing mutations. *J. Neurochem.* **120,** 3–8 (2012).
36. Citron, M. *et al.* Mutation of the beta-amyloid precursor protein in familial Alzheimer's disease increases beta-protein production. *Nature* **360,** 672–674 (1992).
37. Selkoe, D. J. The molecular pathology of Alzheimer's disease. *Neuron* **6,** 487–498 (1991).
38. Sherrington, R. *et al.* Cloning of a gene bearing missense mutations in early-onset familial Alzheimer's disease. *Nature* **375,** 754–760 (1995).
39. Levy-Lahad, E. *et al.* Candidate gene for the chromosome 1 familial Alzheimer's disease locus. *Science* **269,** 973–977 (1995).
40. Martin, J. J. *et al.* Early-onset Alzheimer's disease in 2 large Belgian families. *Neurology* **41,** 62–68 (1991).
41. Strittmatter, W. J. *et al.* Apolipoprotein E: high-avidity binding to beta-amyloid and increased frequency of type 4 allele in late-onset familial Alzheimer disease. *Proc. Natl. Acad. Sci. U. S. A.* **90,** 1977–1981 (1993).
42. Corder, E. H. *et al.* Gene dose of apolipoprotein E type 4 allele and the risk of Alzheimer's disease in late onset families. *Science* **261,** 921–923 (1993).
43. Wood, J. G., Mirra, S. S., Pollock, N. J. & Binder, L. I. Neurofibrillary tangles of Alzheimer disease share antigenic determinants with the axonal microtubule-associated protein tau (tau). *Proc. Natl. Acad. Sci. U. S. A.* **83,** 4040–4043 (1986).

44. Grundke-Iqbal, I. *et al.* Microtubule-associated protein tau. A component of Alzheimer paired helical filaments. *J. Biol. Chem.* **261,** 6084–6089 (1986).
45. Goedert, M., Wischik, C. M., Crowther, R. A., Walker, J. E. & Klug, A. Cloning and sequencing of the cDNA encoding a core protein of the paired helical filament of Alzheimer disease: identification as the microtubule-associated protein tau. *Proc. Natl. Acad. Sci. U. S. A.* **85,** 4051–4055 (1988).
46. AD&FTD Mutation Database. Available at: http://www.molgen.ua.ac.be/ADmutations/. (Accessed: 27th July 2016)
47. Jurisch-Yaksi, N., Sannerud, R. & Annaert, W. A fast growing spectrum of biological functions of γ-secretase in development and disease. *Biochim. Biophys. Acta BBA - Biomembr.* **1828,** 2815–2827 (2013).
48. Hutton, M. & Hutton, M. The Presenilins and Alzheimer's Disease. *Hum. Mol. Genet.* **6,** 1639–1646 (1997).
49. Duggan, S. P. & McCarthy, J. V. Beyond γ-secretase activity: The multifunctional nature of Presenilins in cell signalling pathways. *Cell. Signal.* **28,** 1–11 (2016).
50. Wolfe, M. S. Toward the structure of Presenilin/γ-secretase and homologs. *Biochim. Biophys. Acta* **1828,** 2886–2897 (2013).
51. Spasic, D. *et al.* Presenilin-1 Maintains a Nine-Transmembrane Topology throughout the Secretory Pathway. *J. Biol. Chem.* **281,** 26569–26577 (2006).
52. Dries, D. R. & Yu, G. Assembly, maturation, and trafficking of the gamma-secretase complex in Alzheimer's disease. *Curr. Alzheimer Res.* **5,** 132–146 (2008).

53. Kimberly, W. T., Xia, W., Rahmati, T., Wolfe, M. S. & Selkoe, D. J. The Transmembrane Aspartates in Presenilin 1 and 2 Are Obligatory for γ-Secretase Activity and Amyloid β-Protein Generation. *J. Biol. Chem.* **275,** 3173–3178 (2000).
54. Honarnejad, K. & Herms, J. Presenilins: role in calcium homeostasis. *Int. J. Biochem. Cell Biol.* **44,** 1983–1986 (2012).
55. Haapasalo, A. & Kovacs, D. M. The Many Substrates of Presenilin/γ-Secretase. *J. Alzheimer's Dis.* **25,** 3–28 (2011).
56. Walsh, D. M. & Selkoe, D. J. Deciphering the molecular basis of memory failure in Alzheimer's disease. *Neuron* **44,** 181–193 (2004).
57. Wolfe, M. S. When loss is gain: reduced Presenilin proteolytic function leads to increased Abeta42/Abeta40. Talking Point on the role of Presenilin mutations in Alzheimer disease. *EMBO Rep.* **8,** 136–140 (2007).
58. Kim, S. D. & Kim, J. Sequence analyses of Presenilin mutations linked to familial Alzheimer's disease. *Cell Stress Chaperones* **13,** 401–412 (2008).
59. Shen, J. & Kelleher, R. J. The Presenilin hypothesis of Alzheimer's disease: Evidence for a loss-of-function pathogenic mechanism. *Proc. Natl. Acad. Sci.* **104,** 403–409 (2007).
60. Xu, T.-H. *et al.* Alzheimer's disease-associated mutations increase amyloid precursor protein resistance to γ-secretase cleavage and the Aβ42/Aβ40 ratio. *Cell Discov.* **2,** 16026 (2016).
61. De Strooper, B. Loss-of-function Presenilin mutations in Alzheimer disease. Talking Point on the role of Presenilin mutations in Alzheimer disease. *EMBO Rep.* **8,** 141–146 (2007).
62. Szaruga, M. *et al.* Alzheimer's-Causing Mutations Shift Aβ Length by Destabilizing γ-Secretase-Aβn Interactions. *Cell* **170,** 443-456.e14 (2017).

63. Quintero-Monzon, O. *et al.* Dissociation between Processivity and Total Activity of γ-Secretase: Implications for the Mechanism of Alzheimer-Causing Presenilin Mutations. *Biochemistry (Mosc.)* **50,** 9023–9035 (2011).
64. Tamboli, I. Y. *et al.* Loss of gamma-secretase function impairs endocytosis of lipoprotein particles and membrane cholesterol homeostasis. *J. Neurosci. Off. J. Soc. Neurosci.* **28,** 12097–12106 (2008).
65. Kang, J. *et al.* The precursor of Alzheimer's disease amyloid A4 protein resembles a cell-surface receptor. *Nature* **325,** 733–736 (1987).
66. von Koch, C. S. *et al.* Generation of APLP2 KO mice and early postnatal lethality in APLP2/APP double KO mice. *Neurobiol. Aging* **18,** 661–669 (1997).
67. Wasco, W. *et al.* Identification of a mouse brain cDNA that encodes a protein related to the Alzheimer disease-associated amyloid beta protein precursor. *Proc. Natl. Acad. Sci. U. S. A.* **89,** 10758–10762 (1992).
68. Wasco, W. *et al.* Isolation and characterization of APLP2 encoding a homologue of the Alzheimer's associated amyloid beta protein precursor. *Nat. Genet.* **5,** 95–100 (1993).
69. Chow, V. W., Mattson, M. P., Wong, P. C. & Gleichmann, M. An Overview of APP Processing Enzymes and Products. *Neuromolecular Med.* **12,** 1–12 (2010).
70. Müller, U. C. & Zheng, H. Physiological Functions of APP Family Proteins. *Cold Spring Harb. Perspect. Med.* **2,** (2012).
71. Perez, R. G. *et al.* Mutagenesis identifies new signals for beta-amyloid precursor protein endocytosis, turnover, and the generation of secreted fragments, including Abeta42. *J. Biol. Chem.* **274,** 18851–18856 (1999).

72. Ring, S. *et al.* The secreted beta-amyloid precursor protein ectodomain APPs alpha is sufficient to rescue the anatomical, behavioral, and electrophysiological abnormalities of APP-deficient mice. *J. Neurosci. Off. J. Soc. Neurosci.* **27,** 7817–7826 (2007).
73. Aydin, D., Weyer, S. W. & Müller, U. C. Functions of the APP gene family in the nervous system: insights from mouse models. *Exp. Brain Res.* **217,** 423–434 (2012).
74. Slunt, H. H. *et al.* Expression of a ubiquitous, cross-reactive homologue of the mouse beta-amyloid precursor protein (APP). *J. Biol. Chem.* **269,** 2637–2644 (1994).
75. Lorent, K. *et al.* Expression in mouse embryos and in adult mouse brain of three members of the amyloid precursor protein family, of the alpha-2-macroglobulin receptor/low density lipoprotein receptor-related protein and of its ligands apolipoprotein E, lipoprotein lipase, alpha-2-macroglobulin and the 40,000 molecular weight receptor-associated protein. *Neuroscience* **65,** 1009–1025 (1995).
76. Bayer, T. A., Cappai, R., Masters, C. L., Beyreuther, K. & Multhaup, G. It all sticks together--the APP-related family of proteins and Alzheimer's disease. *Mol. Psychiatry* **4,** 524–528 (1999).
77. Perez, R. G., Zheng, H., Van der Ploeg, L. H. & Koo, E. H. The beta-amyloid precursor protein of Alzheimer's disease enhances neuron viability and modulates neuronal polarity. *J. Neurosci. Off. J. Soc. Neurosci.* **17,** 9407–9414 (1997).
78. Magara, F. *et al.* Genetic background changes the pattern of forebrain commissure defects in transgenic mice underexpressing the beta-amyloid-precursor protein. *Proc. Natl. Acad. Sci. U. S. A.* **96,** 4656–4661 (1999).
79. Hérard, A. S. *et al.* siRNA targeted against amyloid precursor protein impairs synaptic activity in vivo. *Neurobiol. Aging* **27,** 1740–1750 (2006).

80. Cai, X. D., Golde, T. E. & Younkin, S. G. Release of excess amyloid beta protein from a mutant amyloid beta protein precursor. *Science* **259,** 514–516 (1993).
81. Mullan, M. *et al.* A pathogenic mutation for probable Alzheimer's disease in the APP gene at the N-terminus of beta-amyloid. *Nat. Genet.* **1,** 345–347 (1992).
82. Suzuki, N. *et al.* An increased percentage of long amyloid beta protein secreted by familial amyloid beta protein precursor (beta APP717) mutants. *Science* **264,** 1336–1340 (1994).
83. Richardson, J. A. & Burns, D. K. Mouse Models of Alzheimer's Disease: A Quest for Plaques. *ILAR J.* **43,** 89–99 (2002).
84. Weggen, S. & Beher, D. Molecular consequences of amyloid precursor protein and Presenilin mutations causing autosomal-dominant Alzheimer's disease. *Alzheimer's Res. Ther.* **4,** 9 (2012).
85. Neve, R. L., Boyce, F. M., McPhie, D. L., Greenan, J. & Oster-Granite, M. L. Transgenic mice expressing APP-C100 in the brain. *Neurobiol. Aging* **17,** 191–203 (1996).
86. Oster-Granite, M. L., McPhie, D. L., Greenan, J. & Neve, R. L. Age-dependent neuronal and synaptic degeneration in mice transgenic for the C terminus of the amyloid precursor protein. *J. Neurosci. Off. J. Soc. Neurosci.* **16,** 6732–6741 (1996).
87. Kammesheidt, A. *et al.* Deposition of beta/A4 immunoreactivity and neuronal pathology in transgenic mice expressing the carboxyl-terminal fragment of the Alzheimer amyloid precursor in the brain. *Proc. Natl. Acad. Sci. U. S. A.* **89,** 10857 (1992).
88. Berger-Sweeney, J. *et al.* Impairments in learning and memory accompanied by neurodegeneration in mice transgenic for the carboxyl-terminus of the amyloid precursor protein. *Mol. Brain Res.* **66,** 150–162 (1999).

89. Lee, J.-H. *et al.* Lysosomal proteolysis and autophagy require Presenilin 1 and are disrupted by Alzheimer-related PS1 mutations. *Cell* **141,** 1146–1158 (2010).
90. Oddo, S. *et al.* Triple-transgenic model of Alzheimer's disease with plaques and tangles: intracellular Abeta and synaptic dysfunction. *Neuron* **39,** 409–421 (2003).
91. Oakley, H. *et al.* Intraneuronal β-Amyloid Aggregates, Neurodegeneration, and Neuron Loss in Transgenic Mice with Five Familial Alzheimer's Disease Mutations: Potential Factors in Amyloid Plaque Formation. *J. Neurosci.* **26,** 10129–10140 (2006).
92. Barrett, P. J. *et al.* The amyloid precursor protein has a flexible transmembrane domain and binds cholesterol. *Science* **336,** 1168–1171 (2012).
93. Fagan, A. M. *et al.* Unique lipoproteins secreted by primary astrocytes from wild type, apoE (-/-), and human apoE transgenic mice. *J. Biol. Chem.* **274,** 30001–30007 (1999).
94. Pitas, R. E., Boyles, J. K., Lee, S. H., Hui, D. & Weisgraber, K. H. Lipoproteins and their receptors in the central nervous system. Characterization of the lipoproteins in cerebrospinal fluid and identification of apolipoprotein B,E(LDL) receptors in the brain. *J. Biol. Chem.* **262,** 14352–14360 (1987).
95. Kim, J., Basak, J. M. & Holtzman, D. M. The Role of Apolipoprotein E in Alzheimer's Disease. *Neuron* **63,** 287–303 (2009).
96. Grehan, S., Tse, E. & Taylor, J. M. Two distal downstream enhancers direct expression of the human apolipoprotein E gene to astrocytes in the brain. *J. Neurosci. Off. J. Soc. Neurosci.* **21,** 812–822 (2001).
97. Pfrieger, F. W. & Ungerer, N. Cholesterol metabolism in neurons and astrocytes. *Prog. Lipid Res.* **50,** 357–371 (2011).

98. Xu, Q. *et al.* Profile and regulation of apolipoprotein E (ApoE) expression in the CNS in mice with targeting of green fluorescent protein gene to the ApoE locus. *J. Neurosci. Off. J. Soc. Neurosci.* **26,** 4985–4994 (2006).

99. Conejero-Goldberg, C. *et al.* APOE2 enhances neuroprotection against Alzheimer's disease through multiple molecular mechanisms. *Mol. Psychiatry* **19,** 1243–1250 (2014).

100. Wisniewski, T. & Frangione, B. Apolipoprotein E: a pathological chaperone protein in patients with cerebral and systemic amyloid. *Neurosci. Lett.* **135,** 235–238 (1992).

101. Jiang, Q. *et al.* ApoE promotes the proteolytic degradation of Aβ. *Neuron* **58,** 681–693 (2008).

102. Kline, A. Apolipoprotein E, amyloid-ß clearance and therapeutic opportunities in Alzheimer's disease. *Alzheimer's Res. Ther.* **4,** 32 (2012).

103. Deane, R. *et al.* apoE isoform–specific disruption of amyloid β peptide clearance from mouse brain. *J. Clin. Invest.* **118,** 4002–4013 (2008).

104. Verghese, P. B. *et al.* ApoE influences amyloid-β (Aβ) clearance despite minimal apoE/Aβ association in physiological conditions. *Proc. Natl. Acad. Sci.* **110,** E1807–E1816 (2013).

105. Kanekiyo, T., Xu, H. & Bu, G. ApoE and Aβ in Alzheimer's Disease: Accidental Encounters or Partners? *Neuron* **81,** 740–754 (2014).

106. Mielke, M. M. & Lyketsos, C. G. Alterations of the sphingolipid pathway in Alzheimer's disease: new biomarkers and treatment targets? *Neuromolecular Med.* **12,** 331–340 (2010).

107. Aqul, A. *et al.* Unesterified cholesterol accumulation in late endosomes/lysosomes causes neurodegeneration and is prevented by driving cholesterol export from this compartment. *J. Neurosci. Off. J. Soc. Neurosci.* **31,** 9404–9413 (2011).

108. Ricciarelli, R. *et al.* Cholesterol and Alzheimer's disease: a still poorly understood correlation. *IUBMB Life* **64,** 931–935 (2012).

109. Walter, J. & van Echten-Deckert, G. Cross-talk of membrane lipids and Alzheimer-related proteins. *Mol. Neurodegener.* **8,** 34 (2013).

110. van Echten-Deckert, G. & Walter, J. Sphingolipids: critical players in Alzheimer's disease. *Prog. Lipid Res.* **51,** 378–393 (2012).

111. Francis, P., Palmer, A., Snape, M. & Wilcock, G. The cholinergic hypothesis of Alzheimer's disease: a review of progress. *J. Neurol. Neurosurg. Psychiatry* **66,** 137–147 (1999).

112. Steele, L. S. & Glazier, R. H. Is donepezil effective for treating Alzheimer's disease? *Can. Fam. Physician* **45,** 917–919 (1999).

113. Qizilbash, N. *et al.* Cholinesterase inhibition for Alzheimer disease: a meta-analysis of the tacrine trials. Dementia Trialists' Collaboration. *JAMA* **280,** 1777–1782 (1998).

114. Gray, E. G., Paula-Barbosa, M. & Roher, A. Alzheimer's Disease: Paired Helical Filaments and Cytomembranes. *Neuropathol. Appl. Neurobiol.* **13,** 91–110 (1987).

115. Mudher, A. & Lovestone, S. Alzheimer's disease – do tauists and baptists finally shake hands? *Trends Neurosci.* **25,** 22–26 (2002).

116. Lorenzo, A. & Yankner, B. A. Amyloid fibril toxicity in Alzheimer's disease and diabetes. *Ann. N. Y. Acad. Sci.* **777,** 89–95 (1996).

117. DaRocha-Souto, B. *et al.* Brain Oligomeric β-Amyloid but Not Total Amyloid Plaque Burden Correlates With Neuronal Loss and Astrocyte Inflammatory Response in Amyloid Precursor Protein/Tau Transgenic Mice. *J. Neuropathol. Exp. Neurol.* **70,** 360–376 (2011).

118. Stefani, M. Biochemical and biophysical features of both oligomer/fibril and cell membrane in amyloid cytotoxicity. *FEBS J.* **277,** 4602–4613 (2010).

119. Caughey, B. & Lansbury, P. T. Protofibrils, pores, fibrils, and neurodegeneration: separating the responsible protein aggregates from the innocent bystanders. *Annu. Rev. Neurosci.* **26,** 267–298 (2003).

120. Wilcox, K. C., Lacor, P. N., Pitt, J. & Klein, W. L. Aβ oligomer-induced synapse degeneration in Alzheimer's disease. *Cell. Mol. Neurobiol.* **31,** 939–948 (2011).

121. Jin, M. *et al.* Soluble amyloid beta-protein dimers isolated from Alzheimer cortex directly induce Tau hyperphosphorylation and neuritic degeneration. *Proc. Natl. Acad. Sci. U. S. A.* **108,** 5819–5824 (2011).

122. Cleary, J. P. *et al.* Natural oligomers of the amyloid-beta protein specifically disrupt cognitive function. *Nat. Neurosci.* **8,** 79–84 (2005).

123. Reed, M. N. *et al.* Cognitive effects of cell-derived and synthetically derived Aβ oligomers. *Neurobiol. Aging* **32,** 1784–1794 (2011).

124. Sehlin, D. *et al.* Large aggregates are the major soluble Aβ species in AD brain fractionated with density gradient ultracentrifugation. *PloS One* **7,** e32014 (2012).

125. Esparza, T. J. *et al.* Amyloid-β oligomerization in Alzheimer dementia versus high-pathology controls. *Ann. Neurol.* **73,** 104–119 (2013).

126. Fukumoto, H. *et al.* High-molecular-weight beta-amyloid oligomers are elevated in cerebrospinal fluid of Alzheimer patients. *FASEB J. Off. Publ. Fed. Am. Soc. Exp. Biol.* **24,** 2716–2726 (2010).

127. Savage, M. J. *et al.* A sensitive aβ oligomer assay discriminates Alzheimer's and aged control cerebrospinal fluid. *J. Neurosci. Off. J. Soc. Neurosci.* **34,** 2884–2897 (2014).

128. Lacor, P. N. *et al.* Synaptic targeting by Alzheimer's-related amyloid beta oligomers. *J. Neurosci. Off. J. Soc. Neurosci.* **24,** 10191–10200 (2004).

129. Rammes, G., Hasenjäger, A., Sroka-Saidi, K., Deussing, J. M. & Parsons, C. G. Therapeutic significance of NR2B-containing NMDA receptors and mGluR5 metabotropic glutamate receptors in mediating the synaptotoxic effects of β-amyloid oligomers on long-term potentiation (LTP) in murine hippocampal slices. *Neuropharmacology* **60,** 982–990 (2011).

130. Benilova, I., Karran, E. & De Strooper, B. The toxic Aβ oligomer and Alzheimer's disease: an emperor in need of clothes. *Nat. Neurosci.* **15,** 349–357 (2012).

131. Peric, A. & Annaert, W. Early etiology of Alzheimer's disease: tipping the balance toward autophagy or endosomal dysfunction? *Acta Neuropathol. (Berl.)* **129,** 363–381 (2015).

132. Boland, B. *et al.* Autophagy induction and autophagosome clearance in neurons: relationship to autophagic pathology in Alzheimer's disease. *J. Neurosci. Off. J. Soc. Neurosci.* **28,** 6926–6937 (2008).

133. Nixon, R. A. & Yang, D.-S. Autophagy Failure in Alzheimer's Disease – Locating the Primary Defect. *Neurobiol. Dis.* **43,** 38–45 (2011).

134. Kroemer, G., Mariño, G. & Levine, B. Autophagy and the integrated stress response. *Mol. Cell* **40,** 280–293 (2010).

135. Damme, M., Suntio, T., Saftig, P. & Eskelinen, E.-L. Autophagy in neuronal cells: general principles and physiological and pathological functions. *Acta Neuropathol. (Berl.)* **129,** 337–362 (2015).

136. Morel, E. *et al.* Phosphatidylinositol-3-phosphate regulates sorting and processing of amyloid precursor protein through the endosomal system. *Nat. Commun.* **4,** 2250 (2013).

137. Pickford, F. *et al.* The autophagy-related protein beclin 1 shows reduced expression in early Alzheimer disease and regulates amyloid beta accumulation in mice. *J. Clin. Invest.* **118,** 2190–2199 (2008).

138. Caglayan, S. *et al.* Lysosomal sorting of amyloid-β by the SORLA receptor is impaired by a familial Alzheimer's disease mutation. *Sci. Transl. Med.* **6,** 223ra20 (2014).

139. Willnow, T. E. & Andersen, O. M. Sorting receptor SORLA--a trafficking path to avoid Alzheimer disease. *J. Cell Sci.* **126,** 2751–2760 (2013).

140. Coen, K. *et al.* Lysosomal calcium homeostasis defects, not proton pump defects, cause endo-lysosomal dysfunction in PSEN-deficient cells. *J. Cell Biol.* **198,** 23–35 (2012).

141. Mohamed, A., Saavedra, L., Di Pardo, A., Sipione, S. & Posse de Chaves, E. β-amyloid inhibits protein prenylation and induces cholesterol sequestration by impairing SREBP-2 cleavage. *J. Neurosci. Off. J. Soc. Neurosci.* **32,** 6490–6500 (2012).

142. Almeida, C. G., Takahashi, R. H. & Gouras, G. K. Beta-amyloid accumulation impairs multivesicular body sorting by inhibiting the ubiquitin-proteasome system. *J. Neurosci. Off. J. Soc. Neurosci.* **26,** 4277–4288 (2006).

143. Platt, F. M., Boland, B. & van der Spoel, A. C. Lysosomal storage disorders: The cellular impact of lysosomal dysfunction. *J. Cell Biol.* **199,** 723–734 (2012).

144. Vanier, M. T. & Millat, G. Niemann-Pick disease type C. *Clin. Genet.* **64,** 269–281 (2003).

145. Ohm, T. G. *et al.* Cholesterol and tau protein--findings in Alzheimer's and Niemann Pick C's disease. *Pharmacopsychiatry* **36 Suppl 2,** S120-126 (2003).

146. Jin, L.-W., Shie, F.-S., Maezawa, I., Vincent, I. & Bird, T. Intracellular accumulation of amyloidogenic fragments of amyloid-beta precursor protein in neurons with Niemann-Pick type C defects is associated with endosomal abnormalities. *Am. J. Pathol.* **164,** 975–985 (2004).

147. Kodam, A. *et al.* Altered levels and distribution of amyloid precursor protein and its processing enzymes in Niemann-Pick type C1-deficient mouse brains. *Glia* **58,** 1267–1281 (2010).

148. Swerdlow, R. H. & Khan, S. M. A 'mitochondrial cascade hypothesis' for sporadic Alzheimer's disease. *Med. Hypotheses* **63,** 8–20 (2004).

149. Swerdlow, R. H. Mitochondrial DNA--related mitochondrial dysfunction in neurodegenerative diseases. *Arch. Pathol. Lab. Med.* **126,** 271–280 (2002).

150. Yin, F., Sancheti, H., Patil, I. & Cadenas, E. Energy metabolism and inflammation in brain aging and Alzheimer's disease. *Free Radic. Biol. Med.* doi:10.1016/j.freeradbiomed.2016.04.200

151. Bratic, A. & Larsson, N.-G. The role of mitochondria in aging. *J. Clin. Invest.* **123,** 951–957 (2013).

152. Cui, H. *et al.* Oxidative Stress, Mitochondrial Dysfunction, and Aging, Oxidative Stress, Mitochondrial Dysfunction, and Aging. *J. Signal Transduct. J. Signal Transduct.* **2012, 2012,** e646354 (2011).

153. Vamecq, J. *et al.* Mitochondrial dysfunction and lipid homeostasis. *Curr. Drug Metab.* **13,** 1388–1400 (2012).

154. Zhao, L. *et al.* Evidence for association of mitochondrial metabolism alteration with lipid accumulation in aging rats. *Exp. Gerontol.* **56,** 3–12 (2014).

155. Navarro, A. & Boveris, A. The mitochondrial energy transduction system and the aging process. *Am. J. Physiol. Cell Physiol.* **292,** C670-686 (2007).

156. Chan, R. B. *et al.* Comparative lipidomic analysis of mouse and human brain with Alzheimer disease. *J. Biol. Chem.* **287,** 2678–2688 (2012).

157. Hutter-Paier, B. *et al.* The ACAT inhibitor CP-113,818 markedly reduces amyloid pathology in a mouse model of Alzheimer's disease. *Neuron* **44,** 227–238 (2004).

158. Puglielli, L., Ellis, B. C., Ingano, L. A. M. & Kovacs, D. M. Role of acyl-coenzyme a: cholesterol acyltransferase activity in the processing of the amyloid precursor protein. *J. Mol. Neurosci. MN* **24,** 93–96 (2004).

159. Lim, W. L. F., Martins, I. J. & Martins, R. N. The involvement of lipids in Alzheimer's disease. *J. Genet. Genomics Yi Chuan Xue Bao* **41,** 261–274 (2014).

160. Lütjohann, D., Meichsner, S. & Pettersson, H. Lipids in Alzheimer's disease and their potential for therapy. *Clin. Lipidol.* **7,** 65–78 (2012).

161. Janson, C. G. The importance of lipid for the Alzheimer's brain. *Sci. Transl. Med.* **7,** 306ec161-306ec161 (2015).

162. Hartmann, T., Kuchenbecker, J. & Grimm, M. O. W. Alzheimer's disease: the lipid connection. *J. Neurochem.* **103 Suppl 1,** 159–170 (2007).

163. Simons, K. & Ikonen, E. How Cells Handle Cholesterol. *Science* **290,** 1721–1726 (2000).

164. Ghayee, H. K. & Auchus, R. J. Basic concepts and recent developments in human steroid hormone biosynthesis. *Rev. Endocr. Metab. Disord.* **8,** 289–300 (2007).

165. Vitali, C., Wellington, C. L. & Calabresi, L. HDL and cholesterol handling in the brain. *Cardiovasc. Res.* **103,** 405–413 (2014).

166. Ikonen, E. Cellular cholesterol trafficking and compartmentalization. *Nat. Rev. Mol. Cell Biol.* **9,** 125–138 (2008).

167. Martin, S. & Parton, R. G. Lipid droplets: a unified view of a dynamic organelle. *Nat Rev Mol Cell Biol* **7,** 373–378 (2006).

168. Brown, M. S. & Goldstein, J. L. The SREBP pathway: regulation of cholesterol metabolism by proteolysis of a membrane-bound transcription factor. *Cell* **89,** 331–340 (1997).

169. Li, G., Gu, H.-M. & Zhang, D.-W. ATP-binding cassette transporters and cholesterol translocation. *IUBMB Life* **65,** 505–512 (2013).

170. Courtney, R. & Landreth, G. E. LXR Regulation of Brain Cholesterol: From Development to Disease. *Trends Endocrinol. Metab.* **27,** 404–414 (2016).

171. Schultz, J. R. *et al.* Role of LXRs in control of lipogenesis. *Genes Dev.* **14,** 2831–2838 (2000).

172. Zhang, L., Reue, K., Fong, L. G., Young, S. G. & Tontonoz, P. Feedback regulation of cholesterol uptake by the LXR-IDOL-LDLR axis. *Arterioscler. Thromb. Vasc. Biol.* **32,** 2541–2546 (2012).

173. Spann, N. J. & Glass, C. K. Sterols and oxysterols in immune cell function. *Nat. Immunol.* **14,** 893–900 (2013).

174. Hong, C. & Tontonoz, P. Liver X receptors in lipid metabolism: opportunities for drug discovery. *Nat. Rev. Drug Discov.* **13,** 433–444 (2014).

175. Calkin, A. C. & Tontonoz, P. Transcriptional integration of metabolism by the nuclear sterol-activated receptors LXR and FXR. *Nat. Rev. Mol. Cell Biol.* **13,** 213–224 (2012).

176. Skerrett, R., Malm, T. & Landreth, G. Nuclear receptors in neurodegenerative diseases. *Neurobiol. Dis.* **72,** 104–116 (2014).

177. Zelcer, N. *et al.* Attenuation of neuroinflammation and Alzheimer's disease pathology by liver x receptors. *Proc. Natl. Acad. Sci. U. S. A.* **104,** 10601–10606 (2007).

178. Vanmierlo, T. *et al.* Liver X receptor activation restores memory in aged AD mice without reducing amyloid. *Neurobiol. Aging* **32,** 1262–1272 (2011).

179. Riddell, D. R. *et al.* The LXR agonist TO901317 selectively lowers hippocampal Abeta42 and improves memory in the Tg2576 mouse model of Alzheimer's disease. *Mol. Cell. Neurosci.* **34,** 621–628 (2007).

180. Sandoval-Hernández, A. G. *et al.* Liver X Receptor Agonist Modifies the DNA Methylation Profile of Synapse and Neurogenesis-Related Genes in the Triple Transgenic Mouse Model of Alzheimer's Disease. *J. Mol. Neurosci. MN* **58,** 243–253 (2016).

181. Cui, W. *et al.* Liver X receptor activation attenuates inflammatory response and protects cholinergic neurons in APP/PS1 transgenic mice. *Neuroscience* **210,** 200–210 (2012).

182. Pol, A. *et al.* Dynamic and Regulated Association of Caveolin with Lipid Bodies: Modulation of Lipid Body Motility and Function by a Dominant Negative Mutant. *Mol. Biol. Cell* **15,** 99–110 (2004).

183. Nyabi, O. *et al.* No endogenous Aβ production in Presenilin-deficient fibroblasts. *Nat. Cell Biol.* **4,** E164–E164 (2002).

184. Capell, A. *et al.* Presenilin-1 differentially facilitates endoproteolysis of the beta-amyloid precursor protein and Notch. *Nat. Cell Biol.* **2,** 205–211 (2000).

185. Kaether, C., Schmitt, S., Willem, M. & Haass, C. Amyloid precursor protein and Notch intracellular domains are generated after transport of their precursors to the cell surface. *Traffic Cph. Den.* **7,** 408–415 (2006).

186. Collins, J. L. *et al.* Identification of a Nonsteroidal Liver X Receptor Agonist through Parallel Array Synthesis of Tertiary Amines. *J. Med. Chem.* **45,** 1963–1966 (2002).

187. Spandl, J., White, D. J., Peychl, J. & Thiele, C. Live cell multicolor imaging of lipid droplets with a new dye, LD540. *Traffic Cph. Den.* **10,** 1579–1584 (2009).

188. Kölsch, H. *et al.* Alterations of cholesterol precursor levels in Alzheimer's disease. *Biochim. Biophys. Acta* **1801,** 945–950 (2010).

189. Dovey, H. F. *et al.* Functional gamma-secretase inhibitors reduce beta-amyloid peptide levels in brain. *J. Neurochem.* **76,** 173–181 (2001).

190. Area-Gomez, E. del C. L. C., Maria Tambini, Marc D. Guardia-Laguarta, Cristina de Groof, Ad J. C. Madra, Moneek Ikenouchi, Junichi Umeda, Masato Bird, Thomas D. Sturley, Stephen L. Schon, Eric A. Upregulated function of mitochondria-associated ER membranes in Alzheimer disease. *EMBO J.* **31,** 4106–4123 (2012).

191. MacLachlan, J., Wotherspoon, A. T. L., Ansell, R. O. & Brooks, C. J. W. Cholesterol oxidase: sources, physical properties and analytical applications. *J. Steroid Biochem. Mol. Biol.* **72,** 169–195 (2000).

192. Slotte, J. P. Substrate specificity of cholesterol oxidase from Streptomyces cinnamomeus—A monolayer study. *J. Steroid Biochem. Mol. Biol.* **42,** 521–526 (1992).

193. Hofmann, K. *et al.* A novel alkyne cholesterol to trace cellular cholesterol metabolism and localization. *J. Lipid Res.* **55,** 583–591 (2014).

194. Chang, T.-Y. *et al.* Niemann-Pick Type C Disease and Intracellular Cholesterol Trafficking. *J. Biol. Chem.* **280,** 20917–20920 (2005).

195. Pentchev, P. G. *et al.* A defect in cholesterol esterification in Niemann-Pick disease (type C) patients. *Proc. Natl. Acad. Sci.* **82,** 8247–8251 (1985).

196. Gimpl, G. Cholesterol-protein interaction: methods and cholesterol reporter molecules. *Subcell. Biochem.* **51,** 1–45 (2010).

197. Zhao, C. & Dahlman-Wright, K. Liver X receptor in cholesterol metabolism. *J. Endocrinol.* **204,** 233–240 (2010).

198. Wang, L. *et al.* Liver X receptors in the central nervous system: From lipid homeostasis to neuronal degeneration. *Proc. Natl. Acad. Sci.* **99,** 13878–13883 (2002).

199. Edwards, P. A., Kennedy, M. A. & Mak, P. A. LXRs;: Oxysterol-activated nuclear receptors that regulate genes controlling lipid homeostasis. *Oxidized Lipids Potential Mediat. Atheroscler.* **38,** 249–256 (2002).

200. Chawla, A. *et al.* A PPARγ-LXR-ABCA1 Pathway in Macrophages Is Involved in Cholesterol Efflux and Atherogenesis. *Mol. Cell* **7,** 161–171

201. Eberlé, D., Hegarty, B., Bossard, P., Ferré, P. & Foufelle, F. SREBP transcription factors: master regulators of lipid homeostasis. *Recent Adv. Lipid Metab. Relat. Disord.* **86,** 839–848 (2004).

202. Schellenberg, G. D., Bird, T. D., Wijsman, E. M., Moore, D. K. & Martin, G. M. The genetics of Alzheimer's disease. *Biomed. Pharmacother. Bioméd. Pharmacothérapie* **43,** 463–468 (1989).

203. Maulik, M., Westaway, D., Jhamandas, J. H. & Kar, S. Role of cholesterol in APP metabolism and its significance in Alzheimer's disease pathogenesis. *Mol. Neurobiol.* **47,** 37–63 (2013).

204. Grimm, M. O. W., Rothhaar, T. L. & Hartmann, T. The role of APP proteolytic processing in lipid metabolism. *Exp. Brain Res.* **217,** 365–375 (2012).

205. Beel, A. J. *et al.* Structural studies of the transmembrane C-terminal domain of the amyloid precursor protein (APP): does APP function as a cholesterol sensor? *Biochemistry (Mosc.)* **47,** 9428–9446 (2008).

206. Beel, A. J., Sakakura, M., Barrett, P. J. & Sanders, C. R. Direct binding of cholesterol to the amyloid precursor protein: An important interaction in lipid-Alzheimer's disease relationships? *Biochim. Biophys. Acta* **1801,** 975–982 (2010).

207. Zhang, M. *et al.* Presenilin/γ-secretase activity regulates protein clearance from the endocytic recycling compartment. *FASEB J.* **20,** 1176–1178 (2006).

208. Boehm, M. & Bonifacino, J. S. Adaptins. *Mol. Biol. Cell* **12,** 2907–2920 (2001).

209. Touz, M. C., Kulakova, L. & Nash, T. E. Adaptor Protein Complex 1 Mediates the Transport of Lysosomal Proteins from a Golgi-like Organelle to Peripheral Vacuoles in the Primitive Eukaryote Giardia lamblia. *Mol. Biol. Cell* **15,** 3053–3060 (2004).

210. Conner, S. D. & Schmid, S. L. Differential requirements for AP-2 in clathrin-mediated endocytosis. *J. Cell Biol.* **162,** 773–780 (2003).

211. Bonifacino, J. S. Adaptor proteins involved in polarized sorting. *J. Cell Biol.* **204,** 7–17 (2014).

212. Cruz, J. C., Sugii, S., Yu, C. & Chang, T.-Y. Role of Niemann-Pick Type C1 Protein in Intracellular Trafficking of Low Density Lipoprotein-derived Cholesterol. *J. Biol. Chem.* **275,** 4013–4021 (2000).

213. DeBose-Boyd, R. A., Ou, J., Goldstein, J. L. & Brown, M. S. Expression of sterol regulatory element-binding protein 1c (SREBP-1c) mRNA in rat hepatoma cells requires endogenous LXR ligands. *Proc. Natl. Acad. Sci. U. S. A.* **98,** 1477–1482 (2001).

214. Wong, J., Quinn, C. M. & Brown, A. J. SREBP-2 positively regulates transcription of the cholesterol efflux gene, ABCA1, by generating oxysterol ligands for LXR. *Biochem. J.* **400,** 485–491 (2006).

215. McPhie, D. L. *et al.* Neuronal Expression of β-Amyloid Precursor Protein Alzheimer Mutations Causes Intracellular Accumulation of a C-terminal Fragment Containing Both the Amyloid β and Cytoplasmic Domains. *J. Biol. Chem.* **272,** 24743–24746 (1997).

216. Lane-Donovan, C., Philips, G. T. & Herz, J. More than cholesterol transporters: lipoprotein receptors in CNS function and neurodegeneration. *Neuron* **83,** 771–787 (2014).

217. Petrov, A. M., Kasimov, M. R. & Zefirov, A. L. Brain Cholesterol Metabolism and Its Defects: Linkage to Neurodegenerative Diseases and Synaptic Dysfunction. *Acta Naturae* **8,** 58–73 (2016).

218. Suzuki, R., Ferris, H. A., Chee, M. J., Maratos-Flier, E. & Kahn, C. R. Reduction of the Cholesterol Sensor SCAP in the Brains of Mice Causes Impaired Synaptic Transmission and Altered Cognitive Function. *PLOS Biol.* **11,** e1001532 (2013).

219. Sagi, S. A. *et al.* Substrate sequence influences γ-secretase modulator activity, role of the transmembrane domain of the amyloid precursor protein. *J. Biol. Chem.* **286,** 39794–39803 (2011).

220. Takami, M. *et al.* gamma-Secretase: successive tripeptide and tetrapeptide release from the transmembrane domain of beta-carboxyl terminal fragment. *J. Neurosci. Off. J. Soc. Neurosci.* **29,** 13042–13052 (2009).

221. Kim, S. *et al.* Evidence that the rab5 effector APPL1 mediates APP-βCTF-induced dysfunction of endosomes in Down syndrome and Alzheimer's disease. *Mol. Psychiatry* (2015). doi:10.1038/mp.2015.97

222. Pierrot, N. *et al.* Amyloid precursor protein controls cholesterol turnover needed for neuronal activity. *EMBO Mol. Med.* **5,** 608–625 (2013).

223. Liu, Q. *et al.* Amyloid Precursor Protein Regulates Brain Apolipoprotein E and Cholesterol Metabolism through Lipoprotein Receptor LRP1. *Neuron* **56,** 66–78 (2007).

224. Michikawa, M., Gong, J. S., Fan, Q. W., Sawamura, N. & Yanagisawa, K. A novel action of alzheimer's amyloid beta-protein (Abeta): oligomeric Abeta promotes lipid release. *J. Neurosci. Off. J. Soc. Neurosci.* **21,** 7226–7235 (2001).

225. Gong, J.-S. *et al.* Amyloid beta-protein affects cholesterol metabolism in cultured neurons: implications for pivotal role of cholesterol in the amyloid cascade. *J. Neurosci. Res.* **70,** 438–446 (2002).

226. Kim, Y., Kim, C., Jang, H. Y. & Mook-Jung, I. Inhibition of Cholesterol Biosynthesis Reduces γ-Secretase Activity and Amyloid-β Generation. *J. Alzheimer's Dis. JAD* **51,** 1057–1068 (2016).

227. Kim, W. S. *et al.* Role of ABCG1 and ABCA1 in regulation of neuronal cholesterol efflux to apolipoprotein E discs and suppression of amyloid-beta peptide generation. *J. Biol. Chem.* **282,** 2851–2861 (2007).

228. Sano, O. *et al.* ABCG1 and ABCG4 Suppress γ-Secretase Activity and Amyloid β Production. *PloS One* **11,** e0155400 (2016).

229. Kerr, I. D., Haider, A. J. & Gelissen, I. C. The ABCG family of membrane-associated transporters: you don't have to be big to be mighty. *Br. J. Pharmacol.* **164,** 1767–1779 (2011).

230. Panahi, A., Bandara, A., Pantelopulos, G. A., Dominguez, L. & Straub, J. E. Specific Binding of Cholesterol to C99 Domain of Amyloid Precursor Protein Depends Critically on Charge State of Protein. *J. Phys. Chem. Lett.* **7,** 3535–3541 (2016).

231. Hur, J.-Y. *et al.* Active gamma-secretase is localized to detergent-resistant membranes in human brain. *FEBS J.* **275,** 1174–1187 (2008).

232. Vetrivel, K. S. *et al.* Association of gamma-secretase with lipid rafts in post-Golgi and endosome membranes. *J. Biol. Chem.* **279,** 44945–44954 (2004).

233. Zelcer, N. & Tontonoz, P. Liver X receptors as integrators of metabolic and inflammatory signaling. *J. Clin. Invest.* **116,** 607–614 (2006).

234. A-González, N. & Castrillo, A. Liver X receptors as regulators of macrophage inflammatory and metabolic pathways. *Biochim. Biophys. Acta* **1812,** 982–994 (2011).

235. Mitro, N. *et al.* The nuclear receptor LXR is a glucose sensor. *Nature* **445,** 219–223 (2007).

236. Zhou, L., Choi, H. Y., Li, W.-P., Xu, F. & Herz, J. LRP1 Controls cPLA2 Phosphorylation, ABCA1 Expression and Cellular Cholesterol Export. *PLOS ONE* **4,** e6853 (2009).

237. Khakh, B. S. & Sofroniew, M. V. Diversity of astrocyte functions and phenotypes in neural circuits. *Nat. Neurosci.* **18,** 942–952 (2015).

238. Sofroniew, M. V. & Vinters, H. V. Astrocytes: biology and pathology. *Acta Neuropathol. (Berl.)* **119,** 7–35 (2010).

239. Osborn, L. M., Kamphuis, W., Wadman, W. J. & Hol, E. M. Astrogliosis: An integral player in the pathogenesis of Alzheimer's disease. *Prog. Neurobiol.* **144,** 121–141 (2016).

240. Phatnani, H. & Maniatis, T. Astrocytes in Neurodegenerative Disease. *Cold Spring Harb. Perspect. Biol.* **7,** a020628 (2015).

241. Kimelberg, H. K. & Nedergaard, M. Functions of astrocytes and their potential as therapeutic targets. *Neurotherapeutics* **7,** 338–353 (2010).

242. Bhattacharyya, R. & Kovacs, D. M. ACAT inhibition and amyloid beta reduction. *Biochim. Biophys. Acta* **1801,** 960–965 (2010).

243. Daneschvar, H. L., Aronson, M. D. & Smetana, G. W. Do statins prevent Alzheimer's disease? A narrative review. *Eur. J. Intern. Med.* **26,** 666–669 (2015).

244. Jick, H., Zornberg, G. L., Jick, S. S., Seshadri, S. & Drachman, D. A. Statins and the risk of dementia. *Lancet Lond. Engl.* **356,** 1627–1631 (2000).

245. Zandi, P. P. *et al.* Do statins reduce risk of incident dementia and Alzheimer disease? The Cache County Study. *Arch. Gen. Psychiatry* **62,** 217–224 (2005).

246. Feldman, H. H. *et al.* Randomized controlled trial of atorvastatin in mild to moderate Alzheimer disease: LEADe. *Neurology* **74,** 956–964 (2010).

247. Sano, M. *et al.* A randomized, double-blind, placebo-controlled trial of simvastatin to treat Alzheimer disease. *Neurology* **77,** 556–563 (2011).

248. Lin, F.-C. *et al.* Early Statin Use and the Progression of Alzheimer Disease: A Total Population-Based Case-Control Study. *Medicine (Baltimore)* **94,** e2143 (2015).

249. Zissimopoulos, J. M., Barthold, D., Brinton, R. D. & Joyce, G. Sex and Race Differences in the Association Between Statin Use and the Incidence of Alzheimer Disease. *JAMA Neurol.* (2016). doi:10.1001/jamaneurol.2016.3783

250. Wahrle, S. E. *et al.* Deletion of Abca1 increases Abeta deposition in the PDAPP transgenic mouse model of Alzheimer disease. *J. Biol. Chem.* **280,** 43236–43242 (2005).

251. Fitz, N. F. *et al.* ABCA1 Deficiency Affects Basal Cognitive Deficits and Dendritic Density in Mice. *J. Alzheimer's Dis. JAD* **56,** 1075–1085 (2017).

252. Heeren, J. *et al.* Impaired recycling of apolipoprotein E4 is associated with intracellular cholesterol accumulation. *J. Biol. Chem.* **279,** 55483–55492 (2004).

253. Gong, J.-S. *et al.* Novel action of apolipoprotein E (ApoE): ApoE isoform specifically inhibits lipid-particle-mediated cholesterol release from neurons. *Mol. Neurodegener.* **2,** 9 (2007).

254. Sodhi, R. K. & Singh, N. Liver X receptors: emerging therapeutic targets for Alzheimer's disease. *Pharmacol. Res. Off. J. Ital. Pharmacol. Soc.* **72,** 45–51 (2013).

255. Czech, C. *et al.* Cholesterol independent effect of LXR agonist TO-901317 on gamma-secretase. *J. Neurochem.* **101,** 929–936 (2007).

256. Cui, W. *et al.* Activation of liver X receptor decreases BACE1 expression and activity by reducing membrane cholesterol levels. *Neurochem. Res.* **36,** 1910–1921 (2011).

257. Koldamova, R. P. *et al.* 22R-Hydroxycholesterol and 9-cis-Retinoic Acid Induce ATP-binding Cassette Transporter A1 Expression and Cholesterol Efflux in Brain Cells and Decrease Amyloid β Secretion. *J. Biol. Chem.* **278,** 13244–13256 (2003).

258. Sun, Y., Yao, J., Kim, T.-W. & Tall, A. R. Expression of liver X receptor target genes decreases cellular amyloid beta peptide secretion. *J. Biol. Chem.* **278,** 27688–27694 (2003).

259. Terwel, D. *et al.* Critical role of astroglial apolipoprotein E and liver X receptor-α expression for microglial Aβ phagocytosis. *J. Neurosci. Off. J. Soc. Neurosci.* **31,** 7049–7059 (2011).

260. Lefterov, I. *et al.* Expression profiling in APP23 mouse brain: inhibition of Abeta amyloidosis and inflammation in response to LXR agonist treatment. *Mol. Neurodegener.* **2,** 20 (2007).

261. Kang, J. & Rivest, S. Lipid metabolism and neuroinflammation in Alzheimer's disease: a role for liver X receptors. *Endocr. Rev.* **33,** 715–746 (2012).

262. Lalloyer, F. *et al.* Rexinoid bexarotene modulates triglyceride but not cholesterol metabolism via gene-specific permissivity of the RXR/LXR heterodimer in the liver. *Arterioscler. Thromb. Vasc. Biol.* **29,** 1488–1495 (2009).

263. Cramer, P. E. *et al.* ApoE-directed therapeutics rapidly clear β-amyloid and reverse deficits in AD mouse models. *Science* **335,** 1503–1506 (2012).

264. Gniadecki, R. *et al.* The optimal use of bexarotene in cutaneous T-cell lymphoma. *Br. J. Dermatol.* **157,** 433–440 (2007).

265. Fitz, N. F., Cronican, A. A., Lefterov, I. & Koldamova, R. Comment on "ApoE-Directed Therapeutics Rapidly Clear β-Amyloid and Reverse Deficits in AD Mouse Models". *Science* **340,** 924–924 (2013).

266. Price, A. R. *et al.* Comment on "ApoE-Directed Therapeutics Rapidly Clear β-Amyloid and Reverse Deficits in AD Mouse Models". *Science* **340,** 924–924 (2013).

267. Tesseur, I. *et al.* Comment on "ApoE-Directed Therapeutics Rapidly Clear β-Amyloid and Reverse Deficits in AD Mouse Models". *Science* **340,** 924–924 (2013).

268. Veeraraghavalu, K. *et al.* Comment on "ApoE-Directed Therapeutics Rapidly Clear β-Amyloid and Reverse Deficits in AD Mouse Models". *Science* **340,** 924–924 (2013).

269. Landreth, G. E. *et al.* Response to Comments on "ApoE-Directed Therapeutics Rapidly Clear β-Amyloid and Reverse Deficits in AD Mouse Models". *Science* **340,** 924–92g (2013).

270. Pierrot, N. *et al.* Targretin Improves Cognitive and Biological Markers in a Patient with Alzheimer's Disease. *J. Alzheimer's Dis. JAD* **49,** 271–276 (2016).

271. Corona, A. W., Kodoma, N., Casali, B. T. & Landreth, G. E. ABCA1 is Necessary for Bexarotene-Mediated Clearance of Soluble Amyloid Beta from the Hippocampus of APP/PS1 Mice. *J. Neuroimmune Pharmacol. Off. J. Soc. NeuroImmune Pharmacol.* **11,** 61–72 (2016).

272. Onos, K. D., Sukoff Rizzo, S. J., Howell, G. R. & Sasner, M. Toward more predictive genetic mouse models of Alzheimer's disease. *Brain Res. Bull.* **122,** 1–11 (2016).

273. Esquerda-Canals, G., Montoliu-Gaya, L., Güell-Bosch, J. & Villegas, S. Mouse Models of Alzheimer's Disease. *J. Alzheimer's Dis. JAD* **57,** 1171–1183 (2017).

274. Lauritzen, I. *et al.* Intraneuronal aggregation of the β-CTF fragment of APP (C99) induces Aβ-independent lysosomal-autophagic pathology. *Acta Neuropathol. (Berl.)* **132,** 257–276 (2016).

275. Huang, Y.-W. A., Zhou, B., Wernig, M. & Südhof, T. C. ApoE2, ApoE3, and ApoE4 Differentially Stimulate APP Transcription and Aβ Secretion. *Cell* **168,** 427-441.e21 (2017).

276. Mattsson, N. *et al.* Increased amyloidogenic APP processing in APOE ε4-negative individuals with cerebral β-amyloidosis. *Nat. Commun.* **7,** 10918 (2016).

277. Woodruff, G. *et al.* Defective Transcytosis of APP and Lipoproteins in Human iPSC-Derived Neurons with Familial Alzheimer's Disease Mutations. *Cell Rep.* **17,** 759–773 (2016).

278. Icking, A., Amaddii, M., Ruonala, M., Höning, S. & Tikkanen, R. Polarized transport of Alzheimer amyloid precursor protein is mediated by adaptor protein complex AP1-1B. *Traffic Cph. Den.* **8,** 285–296 (2007).

279. Meyer, C. *et al.* μ1A-adaptin-deficient mice: lethality, loss of AP-1 binding and rerouting of mannose 6-phosphate receptors. *EMBO J.* **19,** 2193–2203 (2000).

280. Ishizaki, R., Shin, H.-W., Mitsuhashi, H. & Nakayama, K. Redundant Roles of BIG2 and BIG1, Guanine-Nucleotide Exchange Factors for ADP-Ribosylation Factors in Membrane Traffic between the trans-Golgi Network and Endosomes. *Mol. Biol. Cell* **19,** 2650–2660 (2008).

281. Zhang, M. *et al.* Presenilin/gamma-secretase activity regulates protein clearance from the endocytic recycling compartment. *FASEB J. Off. Publ. Fed. Am. Soc. Exp. Biol.* **20,** 1176–1178 (2006).

282. McMahon, H. T. & Mills, I. G. COP and clathrin-coated vesicle budding: different pathways, common approaches. *Curr. Opin. Cell Biol.* **16,** 379–391 (2004).

283. Koldamova, R. & Lefterov, I. Role of LXR and ABCA1 in the pathogenesis of Alzheimer's disease - implications for a new therapeutic approach. *Curr. Alzheimer Res.* **4,** 171–178 (2007).

284. Gold, M. Phase II clinical trials of anti–amyloid β antibodies: When is enough, enough? *Alzheimer's Dement. Transl. Res. Clin. Interv.* **3,** 402–409 (2017).

285. DeMattos, R. B. *et al.* A Plaque-Specific Antibody Clears Existing β-amyloid Plaques in Alzheimer's Disease Mice. *Neuron* **76,** 908–920 (2012).

286. Cummings, J. L., Morstorf, T. & Zhong, K. Alzheimer's disease drug-development pipeline: few candidates, frequent failures. *Alzheimer's Res. Ther.* **6,** 37 (2014).

287. Golde, T. E., Koo, E. H., Felsenstein, K. M., Osborne, B. A. & Miele, L. γ-Secretase inhibitors and modulators. *Biochim. Biophys. Acta BBA - Biomembr.* **1828,** 2898–2907 (2013).

288. Mayer, S. C. *et al.* Discovery of Begacestat, a Notch-1-Sparing γ-Secretase Inhibitor for the Treatment of Alzheimer's Disease. *J. Med. Chem.* **51,** 7348–7351 (2008).

289. Zidovetzki, R. & Levitan, I. Use of cyclodextrins to manipulate plasma membrane cholesterol content: evidence, misconceptions and control strategies. *Biochim. Biophys. Acta* **1768,** 1311–1324 (2007).

290. Sönnichsen, B., De Renzis, S., Nielsen, E., Rietdorf, J. & Zerial, M. Distinct Membrane Domains on Endosomes in the Recycling Pathway Visualized by Multicolor Imaging of Rab4, Rab5, and Rab11. *J. Cell Biol.* **149,** 901–914 (2000).

291. Lock, J. G. & Stow, J. L. Rab11 in Recycling Endosomes Regulates the Sorting and Basolateral Transport of E-Cadherin. *Mol. Biol. Cell* **16,** 1744–1755 (2005).

292. Matsudaira, T., Niki, T., Taguchi, T. & Arai, H. Transport of the cholera toxin B-subunit from recycling endosomes to the Golgi requires clathrin and AP-1. *J Cell Sci* **128,** 3131–3142 (2015).

293. Translocation of oxysterol binding protein to Golgi apparatus triggered by ligand binding. *J. Cell Biol.* **116,** 307–319 (1992).

294. Zerbinatti, C. V. *et al.* Oxysterol-binding protein-1 (OSBP1) modulates processing and trafficking of the amyloid precursor protein. *Mol. Neurodegener.* **3,** 5 (2008).

295. Sannerud, R. *et al.* Restricted Location of PSEN2/γ-Secretase Determines Substrate Specificity and Generates an Intracellular Aβ Pool. *Cell* **166,** 193–208 (2016).

296. Stephan, Z. F. & Yurachek, E. C. Rapid fluorometric assay of LDL receptor activity by DiI-labeled LDL. *J. Lipid Res.* **34,** 325–330 (1993).

297. Skerrett, R., Pellegrino, M. P., Casali, B. T., Taraboanta, L. & Landreth, G. E. Combined Liver X Receptor/Peroxisome Proliferator-activated Receptor γ Agonist Treatment Reduces Amyloid β Levels and Improves Behavior in Amyloid Precursor Protein/Presenilin 1 Mice. *J. Biol. Chem.* **290,** 21591–21602 (2015).

298. *'Lipoproteins.' Encyclopedia Britannica. 2007. Print.*

299. Mangravite, L. M., Thorn, C. F. & Krauss, R. M. Clinical implications of pharmacogenomics of statin treatment. *Pharmacogenomics J.* **6,** 360–374 (2006).

300. Ansari, A. Fat Storage and the Discovery of Lipid Droplets: How Understanding “Basic” Processes Can Lead to More Effective Medical Treatments. *Yale Scientific Magazine* (2013).

7 Acknowledments

Writing a doctoral thesis is, as it turns out, not quite a particularly simple challenge, and it is seldom, if ever, completed alone. There are indeed, in my case, a large number of people whose support, assistance, and encouragement were at the very least comforting, but, more likely, essential, for the completion of thesis, and who I very much want to thank. First and foremost among these is my supervising professor Jochen Walter. He had the rare quality of being consistently and frequently available and supportive, while simultaneously giving me a lot of freedom to explore and pursue what I found interesting or promising in our research, a balance which allowed me to develop scientifically while never feeling truly lost. His suggestions, insight and openness were essential, and made the progress and completion of this thesis possible. Furthermore, I'd like to thank Prof. Christoph Thiele and Dr. Lars Kuerschner for their assistance and advice regarding experimentation with lipids, in particular regarding alkyne cholesterol tracing, as well as Prof. Dieter Lütjohann and Anja Kerksiek for their experimental support with Gas-chromatography measurement of sterol species.

I was fortunate enough to have had a remarkably active and entertaining lab environment, and most of the Lab members I shared this experience with contributed in some way to the enjoyable and supportive atmosphere I experienced. Patrick Wünderlich is of special note, someone who seems to be helpful, supportive and selfless by instinct, and who helped me, and many others, navigate the maze of materials, protocols and literature which the lab environment can be to a new PhD candidate. Ilker Karaca is certainly also worthy of mention, whom I can only describe as a lovable jackass who developed into an undeniably competent scientist, and who helped me with the correction of this thesis. He, together with Nadja Kemmerling, shared and enhanced my PhD experience, inside and outside the lab. In addition, Marie, Janina, Sandra, Sathish, Constantin, and Ana Lena made up a dynamic and interesting workplace.

I'd also like to thank Michael Hons and Sybille Mitschka (Wait, where does the Y go again?), for their invaluable help in correcting this thesis, for our passionate scientific exchanges, and for making that period of my life rich, and fascinating. And, in that vein, I'd like to thank Felipe Aguirre, with whom I have had the privilege of sharing a friendship which has withstood the tests of time, distance, and women, a friend to discuss with, laugh, compete, and undoubtedly count on. A friend beyond friends, who helped me in more ways than one through this process.

Finally, I'd like to thank my parents, Leonardo Gutierrez and Lucia Cristina Ardila, who made all this possible, supported me through all of my academic road, in good times and bad, and lovingly encouraged me to pursue my aspirations, whatever they were.